Studies on deoxyribonucleic acid based photonic materials and their applications

PhD thesis submitted to

Cochin University of Science and Technology

in partial fulfillment to the requirements for the degree of

Doctor of Philosophy

Pradeep Chandran C

Reg. No. 3909

International School of Photonics
Cochin University of Science and Technology
Cochin 682022 | Kerala | India

January 2016

Studies on deoxyribonucleic acid based photonic materials and their applications

PhD thesis in the field of Photonics

Author

Pradeep Chandran C
Research Scholar
International School of Photonics
Cochin University of Science and Technology
Cochin 682022 | Kerala | India
chandran@cusat.ac.in

Research Advisors

V P N Nampoori
Professor (Emeritus Scientist)
International School of Photonics
Cochin University of Science and Technology
Cochin 682022 | Kerala | India
vpnnampoori@cusat.ac.in

P Radhakrishnan
Professor (Emeritus Scientist)
International School of Photonics
Cochin University of Science and Technology
Cochin 682022 | Kerala | India
radhak@cusat.ac.in

INTERNATIONAL SCHOOL OF PHOTONICS

COCHIN UNIVERSITY OF SCIENCE AND TECHNOLOGY

COCHIN 682022, KERALA, INDIA

Prof. V P N Nampoori
Emeritus Scientist

Certificate of Authenticity

Certified that the research work presented in this thesis entitled "Studies on deoxyribonucleic acid based photonic materials and their applications" is an authentic record of research work carried out by Mr. Pradeep Chandran C under my guidance at the International School of Photonics, Cochin University of Science and Technology, Cochin, India and has not been included in any other thesis submitted previously for the award of any degree.

Cochin 682022   P Radhakrishnan   Prof. V P N Nampoori
10.01.2016   (Co-guide)   (Supervising guide)

Phone: +91 0484 2575848   Fax: +91 0484 2576714
Email: vpnnampoori@cusat.ac.in; nampoori@gmail.com

INTERNATIONAL SCHOOL OF PHOTONICS

COCHIN UNIVERSITY OF SCIENCE AND TECHNOLOGY

COCHIN 682022, KERALA, INDIA

Prof. V P N Nampoori
Emeritus Scientist

Certificate of Completion

This is to certify that the thesis entitled "Studies on deoxyribonucleic acid based photonic materials and their applications" submitted by Mr. Pradeep Chandran C, has incorporated all the relevant corrections and modifications suggested by the audience during the pre-synopsis seminar and recommended by the Doctoral committee.

Cochin 682022   P Radhakrishnan   Prof. V P N Nampoori
10.01.2016   (Co-guide)   (Supervising guide)

Phone: +91 0484 2575848   Fax: +91 0484 2576714
Email: vpnnampoori@cusat.ac.in; nampoori@gmail.com

Declaration

I hereby declare that the work presented in this thesis entitled "Studies on deoxyribonucleic acid based photonic materials and their applications" is based on the original work done by me under the supervision of Prof. V P N Nampoori, Emeritus Scientist at International School of Photonics Cochin University of Science and Technology, Cochin, India and it has not been included in any other thesis submitted previously for the award of any degree.

Cochin 682022   Pradeep Chandran C
10.01.2016

Preface

We live in an Information age, which is marked by the onset of digital revolution during or after the latter half of the 20th century. In this era, we saw sweeping changes in digital computing and communication technology. We largely depend on electronics and photonics for hardware requirements to aid this technology. With the assistance of modern technology, electronic devices have become an indispensable tool in our everyday life.

Inorganic semiconductor materials like silicon and gallium arsenide have been exploited for the on-growing demands of digital revolution. Fifty years of continuous research and technological advancements have pushed these materials to their theoretical efficiency limit. On the other hand, the rapid advancement in technology has created a huge electronic waste which pose a threat to the environment. The scarcity of inorganic materials such as gallium and indium is an alarming factor and it is estimated that these will run out completely in the next 20 years. The availability of new suitable materials is crucial for the development of semiconductor technology. With much promise of delivering low-cost and energy efficient materials, organic semiconductors such as conjugated polymers and small molecules have opened up new avenues for research. Despite the intense effort by scientists and researchers, the performance and stability of organic devices have taken a back seat. Therefore an immediate large-scale replacement of inorganic components by organic counterparts are not foreseen in the near future. Although research is underway to improve the performance of organic materials, it is important to constantly search for new materials.

Nature is a big treasure-trove of successfully conducted experiments by natural selection. Inspired by its apparent simplicity and actual complexity, researchers look out for natural materials or synthetic materials mimicked from natural models, systems or elements. Bio-inspired photonics use natural design as their inspiration to solve human problems and channel these solutions in new directions. It is promising that natural and nature-inspired materials can achieve the ambitious goal of 'green' technology for sustainable future.

CHAPTER 1

Introduction to DNA Photonics

We press the need for 'Green' for sustainable development and to save non-renewable resources for the future generation. Biomaterials have become exotic materials for electronics due to their biocompatible and biodegradable nature. For long, DNA has been thought as a biomaterial that carry genetic information in all living organisms and has led research in DNA oriented towards life science, molecular biology and biomedicine. In the past decade, DNA has made tremendous advancements in the field of optical science and technology and has emerged as new field 'DNA Photonics'. DNA for applications in photonics is available from salmon testes and calf thymus, which are abundant, inexpensive, readily available, renewable resource, environment and human friendly. Recently, new avenues for research have opened in nanobiotechnology (as structuring and templating agent for nanoparticles), DNA origami, optoelectronic devices (OLED, OFET, light emitting FET, nonlinear opto-electric modulators), photonic devices (nonlinear optical devices, optical waveguides, and lasers), organic catalysis and organic memory devices.

CHAPTER 2

DNA as an optical material

Here we review the DNA as an optical/photonic material rather than a biomaterial carrying genetic information. The natural fibrous DNA extracted from salmon testes is soluble only in water. However, to fabricate the DNA thin films in aqueous form pose an adverse problem, when using simple techniques such as spin coating. We refer to the modification of

DNA by attaching a cationic surfactant with the phosphate-sugar chain of DNA which makes it insoluble in water, but soluble in most of organic solvents. The optical and electrical properties of DNA-surfactant lipid complex are discussed to reveal the fact that DNA could be used in photonic and optoelectronic applications.

CHAPTER 3

Experimental techniques

This chapter describes the experimental techniques used in the following three chapters. The chapter is divided into three sections, first - focusing on the Z-scan techniques used for measurement of nonlinear absorption coefficient and third order nonlinear susceptibility of dyes; second – detailing the techniques used for casting thin films and measurement of amplified spontaneous emission; and third – describing the fabrication of light emitting diodes by spin coating and thermal evaporation techniques, and characterization of LEDs by measuring their jV and LV curves.

CHAPTER 4

Effect of DNA on nonlinear optical properties of dyes

The nonlinear property of DNA has been investigated earlier and observed reverse saturable absorption (RSA) due to two photon absorption property in DNA-poly vinyl alcohol system. Earlier reports from our laboratory shows addition of DNA flips the saturable absorption (SA) curve of Rhodamine 6G to RSA. We were interested to extend this investigation in other dyes with different nonlinear properties. Therefore we chose two dyes, one that exhibits RSA and the other with RSA-SA curves. This chapter presents the results of optical nonlinear properties of these two dyes, namely PicoGreen (PG) and Triazatriangulenium (TATA) salt. Through this chapter we also show the effect of DNA on nonlinear properties of PG and TATA. We observed that the two photon absorption coefficient decreased in both dyes as the concentration of DNA was increased.

a system could not find relevance as a light emitting polymer/dye due to the high lowest unoccupied molecular orbital (LUMO) level of the DNA that restrict itself as a host material for light emitting dyes. By the use of DNA as an electron blocking layer, we fabricated an all solution processable polymer LED with improved performance. We further propose possible future advancements in DNA Photonics.

Acknowledgments

I would like to express my sincere gratitude to Professor Ganesan Singaravelu, whose encouragement led me to pursue research, to whom I dedicate this achievement.

I feel very much honored to have had the opportunity to work with and learn from my advisor Professor Vadakedathu Parusurama Narayana Nampoori. He is truly a rare breed, a physicist jack-of-all-trades from whom one can draw inspiration. Thank you Sir. I profusely thank my co-advisor Professor Radhakrishnan Padbhanabhan and Professor C P Girijavallabhan for their guidance and pain-staking effort to review my thesis and manuscripts; and my supervisors Dr. Manoj A G Namboothiry and Professor Martti Kauranen.

I owe a lot of gratitude to all my friends at ISP, to whom I share a bond of fraternal love, for being with me as a family. No words would suffice the kindness and nurturing from my dear friend and brother, Mathew. A special thanks to Sony for his timely advises. I would like to extend my gratitude to my seniors Nithyaja, Linesh, Thomas, Misha, Libish, Bobby, Sreeja, Tintu and Sreelekha for educating me the nuts and bolts of our laboratory. The company of Bejoy would remain cherished, especially when finding trails during trekking along the strip of Western Ghats running into Kerala. It was a wonderful experience to share lab space with my colleagues Vishnu, Roseleena, Rejeena, Divya, Retheesh, Indu, Linslal, Suneetha, Aparna, Bini, Jaison, Sabitha, Nideep and Musfir. I owe a great deal to my junior colleagues and project assistants, Roopa, Keerthi, Jessy, Mintu, Anju, Manju, Alina, Ajina, Anand, Adrine, Boni, Sony, Vijesh, Ramya, Anupama and Vineetha for providing me an opportunity to assist them. It was in their presence could I lose my depression and insanity that plagued me during the

I am so happy to have my family – achan, amma, chetan, chechi and kunjoos – beside me at all times while pursuing this endeavor. My best and sincere gratitude to all my respectful teachers and loving friends who have helped me to walk through this journey. Their pain-staking efforts in shaping me up instills me to be a gentleman.

Pradeep

Publications

A. Related to this thesis

1. C Pradeep, C P G Vallabhan, P Radhakrishnan, V P N Nampoori, Amplified spontaneous emission from PicoGreen dye intercalated in deoxyribonucleic acid lipid complex, **Laser Phys. Lett.**, 12, 125802, (2015) [online]

2. C Pradeep, S Mathew, B Nithyaja, P Radhakrishnan, V P N Nampoori, Studies of nonlinear optical properties of PicoGreen dye using Z-scan technique, **Appl. Phys. A**, 115, 291, (2014) [online]

3. C Pradeep, S Mathew, B Nithyaja, P Radhakrishnan, V P N Nampoori, Effect of marine derived deoxyribonucleic acid on nonlinear optical properties of PicoGreen dye, **Appl. Phys. B**, 111, 611, (2013) [online]

B. Other works

4. C Pradeep, S Mathew, M A G Namboothiry, C P G Vallabhan, P Radhakrishnan, V P N Nampoori, Performance of polymer/cadmium sulphide hybrid light-emitting diodes, **Optoelectron. Lett.**, (accepted, 2015) [online]

5. Jolly V A, Pradeep C, Philip K, Nampoori P N V, George E K, Surface effects on photoluminescence and optical nonlinearity of CdS quantum dots stabilized by sulfonated polystyrene in water, **J. Phys. Chem. C**, 119, 8280, (2015) [online]

6. T M Libish, M C Bobby, J Linesh, S Mathew, C Pradeep, V P N Nampoori, P Biswas, S Bandyopadhyay, K Dasgupta, P Radhakrishnan, Detection of adulteration in virgin

olive oil using a fiber optic long period grating based sensor, **Laser Phys.**, 23, 045112, (2013) [online]

7. Libish T M, Bobby M C, Linesh J, Mathew S, Pradeep C, Nampoori V P N Radhakrishnan P, Refractive index and temperature dependent displacements of resonant peaks of long period grating inscribed in hydrogen loaded SMF-28 fiber, **Optoelectron. Lett.**, 8, 101, (2012) [online]

8. Libish T M, Linesh J, Bobby M C, Nithyaja B, Mathew S, Pradeep C, Radhakrishnan P, Glucose concentration sensor based on long period grating fabricated from hydrogen loaded photosensitive fiber, Sensors & Transducers Journal, 129, 142, (2011) [online]

9. Vishnu K, Nithyaja B, Pradeep C, Sujith R, Mohanan P, Nampoori V P N, Studies on the effect of mobile phone radiation on DNA using laser induced fluorescence technique, **Laser Phys.**, 21, 1945, (2011) [online]

C. International conference papers

1. Pradeep Chandran. C, Mani Rahulan. K, Ganesan. S, Synthesis and study of photodynamic activity of silver nanoparticles, Photonics 2010, 10th International Conference on Fiber optics & Photonics, December 11-15, 2010, Indian Institute of Technology Guwahati, AS, India.

2. T.M. Libish, J. Linesh, Bobby Mathews, C. Pradeep, P. Radhakrishnan, Fiber optic sensor for the adulteration detection of edible oils, XXXV OSI Symposium, International Conference on Contemporary Trends in Optics and Optoelectronics, January 17-19, 2011, Indian Institute of Space Science and Technology, Thiruvananthapuram, KL, India.

3. C. Pradeep, S. Mathew, B. Nithyaja, P. Radhakrishnan, V. P. N. Nampoori, PicoGreen - A new optical nonlinear material, IONS CHENNAI, December 7-8, 2012, Indian Institute of Technology Madras, TN, India.

4. C. Pradeep, S. Mathew, B. Nithyaja, P. Radhakrishnan, V. P. N. Nampoori, Investigation of optical nonlinear properties of cyanine dye, Photonics 2012, 11th International Conference on Fiber optics and Photonics, December 9-12, 2012, Indian Institute of Technology Madras, TN, India. (paper TPo.38) [online]

5. Vineetha Ram, Vishnu. K, Pradeep. C, V. P. N. Nampoori, Silver nanoparticles as radiation absorbers to reduce the effect of mobile phone radiation on DNA, Photonics 2012, 11th International Conference on Fiber optics and Photonics, December 9-12, 2012, Indian Institute of Technology Madras, TN, India. (paper W3B.3) [online]

6. A Slablab, K Koskinen, R Czaplicki, N T Karunakaran, I Sebastian, C P Chandran, M Kailasnath, P Radhakrishnan and M Kauranen, Multipolar second-harmonic generation from films of chalcogenide glasses, Nanophotonics V, SPIE Photonics Europe 2014, April 14, 2014, Brussels, Belgium, Proc. SPIE 9126, 912621 (May 2, 2014); doi: 10.1117/12.2051477 [online]

7. Pradeep Chandran, Ramkumar Sekar, Manoj A G Namboothiry, C P G Vallabhan, P Radhakrishnan, V P N Nampoori, Effect of gold nanoparticles doped PEDOT:PSS in polymer light emitting diodes, Photonics 2014, 12th International Conference on Fiber optics & Photonics, December 13-16, 2014, Indian Institute of Technology Kharagpur, WB, India. (post-deadline paper, T3A.84) [online]

8. S Mathew, K Koskinen, R Czaplicki, M Kailasnath, C Pradeep, Vallabhan C P G, M Kauranen, P Radhakrishnan, Study of second-harmonic generation from CdS nanostructured thin film, Photonics 2014, 12th International Conference on Fiber optics & Photonics, December 13-16, 2014, Indian Institute of Technology Kharagpur, WB, India. (paper M4A.46) [online]

9. C Pradeep, S Mathew, Manoj A G Namboothiry, C P G Vallabhan, P Radhakrishnan, V P N Nampoori, Effect of cadmium sulphide on polymer light emitting diodes, International Conference on Optics and Photonics, February 20-22, 2015, University of Calcutta, WB, India.

10. Pradeep Chandran, Manoj A G Namboothiry, C P G Vallabhan, P Radhakrishnan, V P N Nampoori, Enhanced brightness from all solution processable biopolymer LED, Nanobiosystems: Processing, Characterization and Applications VIII, SPIE Optics + Photonics 2015, August 9-13, 2015, San Diego, CA, United States of America, Proc. SPIE 9557, 95570O (August 26, 2015); doi: 10.1117/12.2190836 [online]

11. Pradeep Chandran, P Radhakrishnan, V P N Nampoori, Picogreen dye as an active medium for plastic lasers, Nanobiosystems: Processing, Characterization and Applications VIII, SPIE Optics + Photonics 2015, August 9-13, 2015, San Diego, CA, United States of America. Proc. SPIE 9557, 95570N (August 26, 2015); doi: 10.1117/12.2190946 [online]

12. Pradeep Chandran, Mathew Sebastian, Manoj A G Namboothiry, C P G Vallabhan, P Radhakrishnan, V P N Nampoori, Study on cadmium sulphide nanoparticles on blue and green light emitting polymers, Organic Light Emitting Materials and Devices XIX, SPIE Optics + Photonics 2015, August 9-13, 2015, San Diego, CA, United States of America, Proc. SPIE 9566, 95661Z (September 22, 2015); doi: 10.1117/12.2188369 [online]

D. National conference papers

13. K. Vishnu, B. Nithyaja, C. Pradeep, V. P. N. Nampoori, Studies on the effect of mobile phone radiation on DNA using laser induced fluorescence technique, 21st Swadeshi Science Congress, November 7-8, 2011, Kollam, KL, India.

14. Vineetha Ram, K. Vishnu, D. Laila, C. Pradeep, V. P. N. Nampoori, Effect of mobile phone radiation on DNA, its harmful effects and possible solution, XXIV Kerala Science Congress, January 29-31, 2012, Rubber Research Institute of India, Kottayam, KL, India.

15. I. Rejeena, B. Lillibai, C. Pradeep Chandran, S. Mathew, V. P. N. Nampoori P. Radhakrishnan, Sol gel derived lead chloride crystals for optical limiting applications, XXIV Kerala Science Congress, January 29-31, 2012, Rubber Research Institute of India, Kottayam, KL, India.

16. C. Pradeep, S. Mathew, B. Nithyaja, P. Radhakrishnan, V. P. N. Nampoori, Nonlinear optical response of PicoGreen dye on interaction with deoxyribonucleic acid, Indian Association of Physics Teachers Convention and Seminar, November 2-4, 2012, International School of Photonics, CUSAT, Kochi, KL, India.

17. Keerthi G. Nair, Kamal P. Mani, Vimal George, Pradeep Chandran, Cyriac Joseph, V. P. N. Nampoori, Effect of samarium on NLO properties of nano zinc oxide, Indian Association of Physics Teachers Convention and Seminar, November 2-4, 2012, International School of Photonics, CUSAT, Kochi, KL, India.

18. C. Pradeep, S. Mathew, B. Nithyaja, P. Radhakrishnan, V. P. N. Nampoori, Nonlinear optical properties of PicoGreen dye : DNA system, National Laser Symposium, NLS - 21, Feburary 6-8, 2013, Bhabha Atomic Research Centre, Trombay, Mumbai, MH, India.

19. Keerthi G. Nair, Kamal P. Mani, Vimal George, Pradeep Chandran, Cyriac Joseph, V. P. N Nampoori, Nonlinear optical characterization of samarium doped zinc oxide nanoparticles, National Laser Symposium, NLS - 21, Feburary 6-8, 2013, Bhabha Atomic Research Centre, Trombay, Mumbai, MH, India.

20. Vineetha Ram, Vishnu. K, Pradeep. C, V. P. N. Nampoori, Silver nanoparticles to reduce the effect of mobile phone radiation on DNA using thermal lens spectroscopy, National Laser Symposium, NLS - 21, Feburary 6-8, 2013, Bhabha Atomic Research Centre, Trombay, Mumbai, MH, India.

21. Pradeep C, Gopidas K R, Radhakrishnan P, Nampoori V P N, Investigation of optical nonlinear properties in Triazatriangulenium salt by Z scan technique, National Laser Symposium, NLS - 22, January 8-11, 2014, Manipal University, Manipal, KA, India.

22. A. Slablab, K. Koskinen, R. Czaplicki, M. Kailasnath, I. Sebastian, P. Chandran, P. Radakrishhnan, M. Kauranen, Second-harmonic generation from Ge-Se-Sb chalcogenide films, Physics Days, 48th Annual Meeting of the Finnish Physical Society, March 11-13, 2014, Tampere, Finland. [online]

23. Pradeep Chandran, Manoj A G Namboothiry, C P G Vallabhan, P Radhakrishnan, V P N Nampoori, Effect of DNA as electron blocking layer for efficient biopolymer LED, 24th Swadeshi Science Congress, November 6-8, 2014, Thunchath Ezhuthachan Malayalam University, Tirur, KL, India

24. Pradeep Chandran, Mathew Sebastian, C P G Vallabhan, P Radhakrishnan, V P N Nampoori, Light amplification and lasing in fluorene based copolymer, National Laser Symposium, NLS - 23, December 3-6, 2014, Sri Venkateswara University, Tirupati, AP, India.

25. Pradeep C, Gopidas K R, Radhakrishnan, Nampoori V P N, Z scan studies in triazatriangulenium salt to determine its nonlinear refractive index, National Seminar on Advanced Materials and their Applications, September 10-11, 2015, Aquinas College, Cochin, KL, India.

26. Mathew S, Pradeep C, Kailasnath M, Radhakrishnan P, Nampoori V P N, Vallabhan C P G, Nonlinear optical properties of CdS nanostructured thin film under the excitation of 355 nm nanosecond laser pulses, National Seminar on Advanced Materials and their Applications, September 10-11, 2015, Aquinas College, Cochin, KL, India.

27. Jessy Simon, Mathew S, Pradeep C, Nideep T K, Kailasnath M, Synthesis of copper nanoparticles by pulsed laser ablation and its optical characterization, National Seminar on Advanced Materials and their Applications, September 10-11, 2015, Aquinas College, Cochin, KL, India.

28. Pradeep C, Vallabhan C P G, Radhakrishnan P, Nampoori V P N, Amplified spontaneous emission of PicoGreen dye embedded in DNA matrix, National Laser Symposium, NLS - 24, December 2-5, 2015, Raja Ramanna Centre for Advanced Technology, Indore, MP, India.

29. Pradeep C, Mathew S, Nithyaja B, Gopidas K R, Manoj A G Namboothiry, Vallabhan C P G, Radhakrishnan P and Nampoori V P N, DNA based materials for photonic applications, 25th Swadeshi Science Congress, November 5-8, 2015, Sree Sankaracharya University of Sanskrit, Kalady, KL, India.

Contents

1

Introduction to DNA Photonics

Abstract

We press the need for 'Green' for sustainable development and to save natural resources for the future generation. Green materials have become exotic materials for electronics due to their biocompatible and biodegradable nature. For long, DNA has been thought as a biomaterial that carry genetic information in all living organisms and has led research in DNA oriented towards life science, molecular biology and biomedicine. In the past decade, DNA has made tremendous advancements in the field of optical science and technology and has emerged as a new field 'DNA Photonics'. DNA for applications in photonics is available from salmon testes and calf thymus, which are abundant, inexpensive, readily available, renewable resource, environment and human-friendly. Recently, new avenues for research have opened in nanobiotechnology (structuring and templating agent for nanoparticles), DNA origami, optoelectronic devices (OLED, OFET, light emitting FET, nonlinear electro-optic modulators), photonic devices (nonlinear optics, optical waveguides, lasers and light emission), organic catalysis and organic memory devices.

1.1 GREEN FOR SUSTAINABLE FUTURE

'Green' signifies life, prosperity and environment. In scientific term, as defined by United Nations World Commission on Environment and Development[1], it is to "establish sustainable development", i.e. meeting our present needs without destroying or depleting the natural resources for the future generation. The word 'green' carry a lot of importance and became a fashionable tag to any advancement directed towards achieving sustainability. The ultimate goal of green technology is to identify the materials of natural origin or of nature inspired synthetic materials that are environment-friendly and find solutions to our problems. Green technology has been applied to various fields such as green energy, green building, agriculture, organic electronics, green chemistry, photonics, green computing, biomedical engineering and biomimetics.

The boom in the electronic industries has accumulated the toxic heavy metals in plants and animals that are otherwise scattered around in trace quantities. Today we live in this world with a pile of electronic garbage because our parent generation did not foresee the dangers they have set by incorporating inorganic semiconductors. Therefore, it is our responsibility to set up an environment that is safe for our future generations to live in. Our society must address this problem by choosing environmentally sustainable pathways for the design, production, and disposal of such electronic devices. It is not only (i) the danger that pose to the environment, but (ii) complete energy imbalance embodied in them. The energy consumed by these inorganic semiconductors or nanomaterials in their processing or production phase is much more than the energy consumed by them as a product. To achieve sustainability, materials that have low embodied energy have to be used. (iii) Depletion rate of scarce natural materials such as gallium and indium estimates that these materials will be exhausted completely in the next 20 years. These three problems present a negative impact on the present and future generation.

It is best hoped that the answer to the problem lies in the 'green technology'. In 1987, the Brundtland Commission formally known as United Nations World Commission on Environment and Development was set up by Gro Harlem Brundtland, a pioneer and international leader in sustainable development. The Commission released its report

"Our Common Future"[1] coining and defining the term Sustainable Development as the process that "meets the needs of the present without compromising the ability of future generations to meet their own needs". This Commission gave the momentum to host the first conference on sustainable development, 'Earth Summit' held at Rio de Janeiro in 1992, recognized that sustainable development could be achieved by encompassing economic development, social development and environmental protection. It also acknowledged the right to development to the developing countries and declared policies and principles to guide the developing countries as well as developed countries to sustainable development. Influenced by the 2008 Financial Crisis and 2009 Copenhagen Summit on climate change, 'green' stimulus packages were considered to overcome the crisis along with environmental protection. With the developing countries anguished by the risky green initiatives that might limit their development due to the new trade restrictions imposed by the developed countries, the United Nations Department of Economic and Social Affairs released World Economic and Social Survey (WESS) in 2011. The survey entitled 'The Great Green Technological Transformation'[2] not only discusses the need and importance of green technology but also the policies and recommendations to develop green technology to safeguard earth's ecosystem. The survey insisted the use of biodegradable, renewable and green resources along with waste reduction to protect biodiversity and ecosystem.

1.2 GREEN MATERIALS

With the dangers posed by inorganic materials cited in the last section, there is an urgent need to identify new materials that are natural, abundant, economical and renewable resource which could be easily processed without consuming or producing toxic wastes. Organic (carbon-based) materials came with many of these features along with the promise of low-cost energy efficient materials and increased lifetime. But they were jolted down by the performance and stability their inorganic counterparts offered. However, they require intense research to overcome these hurdles. With no immediate replacement of inorganic materials in the near future, we turn to nature for help. Nature is a continuous researching engine whose successful experiments survive time from which we profit. It would be beneficial if we could learn to mimic nature that would

provide environmental safe technologies. The idea of green materials is to study the systems in nature and re-engineer them with synthetic materials or use those natural materials to solve our complex problems. Such studies are already in the research table providing a plethora of unexplored phenomena.

Researchers have been working on recreating photosynthesis process[3], fabricating artificial compound eyes[4], replicating natural photonic fibers[5], designing hydrophobic surface inspired from the lotus petals[6], crafting super-adhesive surface motivated by gecko effect in tree frogs[7], reproducing natural infrared camouflage coatings from cephalopod proteins[8] and exploiting spermatozoid motion for micro-bio-motor[9]. Biodegradable, biocompatible and bioresorbable allows integration of electronics into biological systems for achieving real-time monitoring, diagnosis and trigger instant drug delivery. Such materials has stimulated wearable and implantable devices[10-14] such as bioresorbable stents, cochlear implants, flexible biosensors on brain (neural interfaces), heart (pacemaker/defibrillators), beneath the skin (glucose monitoring), and smart electronic tattoos that comes with data or power transfer through wireless communication[15-18]. Such devices are not only biocompatible but also absorbed and broken down by the body that avoids extraction of those devices via surgery.

These interesting problems require contributions from various fields viz. physics, chemistry, material science, biology, electrical and mechanical engineering and have now emerged as 'organic bioelectronics'. This emerging new field may prove to be the suitable host for welcoming natural and nature-inspired organic materials and for achieving the ambitious goal of 'green' and sustainable electronics.

In their quest to achieve sustainable development in electronics, highly unusual natural materials are being investigated. Some natural materials and their applications that are reviewed recently[19-22] are presented here. In the context of organic electronics, the basic building blocks are the substrates, smoothening agents, encapsulate layers, contact electrodes, dielectrics and semiconductors.

Researchers have moved towards the use of flexible and stretchable substrates from conventional glass substrates. Cotton cellulose-fiber paper[23] coated with natural mineral pigments has been employed as cheap substrates. However, the mineral pigments make them non-biodegradable. Apart from paper, various synthetic polymers

(degradable plastics) like polydimethylsiloxane (PDMS)[24], low density polyethylene (LDPE), polyhydroxy alkanoates (PHA), parylene, polylactic acid (PLA)[25], polylactic-*co*-glycolic acid (PLGA), polyethylene glycol (PEG), poly(2-hydroxyethyl methacrylate) (pHEMA), polyurethane (PU)[26,27], polyvinyl alcohol (PVA)[28,29], are currently investigated in fabrication of flexible, deformable and implantable devices. Polycaprolactone (PCL), polybutylene succinate (PBS), polyhydroxybutyrate-co-valerate (PHBV), polyhydroxybutyrate-co-hexanoate (PHBH), polybutylene adipate-co-terephthalate (PBAT) have established themselves as potential biodegradable substrates. Fully biodegradable and biocompatible substrates from natural materials such as silk[30,31], shellac[32], hard gelatin, collagen, chitin, chitosan, alginate and dextran are remarkably attractive substrates for organic electronics applications.

The surface roughness and porosity nature of paper necessitate the use of smoothening agents. The rosolic acid from the roots of *Plantago Asiatical L.*[33] and PDMS act as a very good smoothening layers to aid the inherent rough surface of the above-mentioned biodegradable substrates.

Novel conductive electrodes were investigated that could aid the interface between electronics and biological matter[34]. Contact electrodes have been tested on living organisms using different approaches as mentioned below. One is by using conformable metal electrodes, such as gold electrode arrays on brain tissue[31], and another by using soft conducting polymers, where a common polymer PEDOT:PSS poly-(3,4-ethylenedioxythiophene):poly(styrene sulfonate) was either directly polymerized[35] or by growing it on a biocompatible substrates by photolithography technique[36] and transplanting it - on a living neural tissue of a mouse brain to realize implantable devices.

The dielectric nature of nucleic acid, especially deoxyribonucleic acid (DNA)[37,38], and its nucleobases - adenine, guanine, thymine, cytosine and uracil[39], and various sugar molecules (glucose, sucrose, lactose) have been identified with good insulating properties. The unique properties of DNA that make it a photonic material are discussed in the next chapter and throughout this thesis. Silk[40], shellac[41], hard gelatin, peptide sequence and even edible caramelized sugar (glucose)[33] have been explored as biodegradable dielectrics. Innovative use of irreversible denaturation of natural

proteins from chicken albumen[42] as a dielectric material in high-performance field effect transistor has been recently demonstrated.

The performance and stability of organic semiconductors were limited due to the weak van der Waal forces that are linked to each other as against strong intramolecular covalent bonds in inorganic semiconductors. It has been reviewed that organic molecules such as DNA, cellulose and various pigments with strong intermolecular hydrogen bonding shall pose as a good organic semiconductor[19]. The hydrogen bonded semiconductors exhibit good electric charge transporting properties despite the lack of π-conjugated system. A list of synthetic organic semiconductors are reviewed elsewhere[43], however, some biodegradable and green semiconductors are mentioned here. Natural materials such as chlorophyll, cellulose, melanin[44,45], hemin, phenazine, terpenoid molecules (beta-carotene[46,47], bixin, retinal), and indigo[32], Tyrian purple (6-60-Br-indigo)[48,49] have been investigated for their semiconducting properties and their applicability in various devices. Nature inspired synthetic materials also provide cheap, non-toxic and biodegradable semiconductors such as colorants used in textile, food and cosmetics such as, Indanthrene yellow G, Indanthrene brilliant orange RF, perylene diimide, naphthalene diimide and anthraquinone derivatives, commonly known as vat dyes.

1.3 DNA AS AN EXOTIC MATERIAL

DNA was first identified and isolated from leucocytes by Miescher[50] in 1869. With the confirmation of DNA as a genetic material by Hershey and Chase[51] in 1952 and the subsequent discovery of the molecular structure of DNA by Watson and Crick[52] in 1953 using Franklin and Gosling's X-ray analyses and finally cracking the genetic code by Holley in 1960 led to the understanding of the function of DNA that ushered a whole new era of molecular genetics. Research in DNA followed in various fields such as molecular biology, genetic engineering, DNA profiling, life science, and biomedicine.

While the DNA was vigorously investigated by biologists and chemists, the physicochemical and electronic properties and its material applications were being explored by physicists and engineers. A decade of research in this line has led DNA

being applied to nanotechnology, nano-motors, bio-sensors[53], bioinformatics, DNA origami, organic catalysis, optoelectronic devices, organic memory devices, lasers, and more recently in digital data storage[54]. An exhaustive list of applications of DNA in various fields is discussed in the next chapter.

One of the important argument in favor of DNA being used as an exotic green material is its natural availability from plant and animal sources. This makes them biodegradable i.e. they decompose easily without causing any environmental hazards. DNA that is available in the market, for investigations in photonics, are extracted from calf thymus, herring sperm or salmon roe sacs. Salmon roe sacs being a waste product of fishing industries combined with the easy extraction process makes it cheaper than DNA available from other sources. The use of such renewable resource also suffices the present scientific policy as discussed in section 1.1, to create sustainable development and minimize environmental pollution. Besides these eco-friendly beneficial features, DNA also possesses unique electronic and optical properties (elaborated in chapter 2) which make them a good optical material for their use in photonic and optoelectronic applications.

1.4 ORGANIZATION OF THIS THESIS

This thesis is organized, with each core chapter (4,5 and 6) investigating an applicability of DNA incorporated with various dyes and polymers along with strenuous analysis.

Understanding the need for green materials and with this brief introduction on DNA Photonics, we shall move to the second chapter where the structure and basic functions of DNA are stated. For DNA to be applicable to thin film fabrication, certain processing and tailoring techniques are elaborated. The electrical and optical properties of functionalized DNA are discussed. The application of DNA in various photonic and optoelectronic devices are reviewed from literature.

The experimental techniques that are used in this thesis are detailed in chapter 3. The techniques include Z-scan techniques and analysis for measuring nonlinear optical properties, experimental setup to measure amplified spontaneous emission from thin

film samples and setup to measure luminance – current density – voltage characteristics and electroluminescence from the fabricated light emitting diodes. This chapter also discusses various thin film fabrication techniques such as drop casting, spin coating and thermal deposition techniques.

Chapter 4 deals with the effect of DNA on nonlinear optical properties of various dyes. This is an extension of an earlier work from our lab. Nithyaja et al.[55,56] has reported the nonlinear optical properties of DNA – Rhodamine 6G – PVA complex. This work was extended to various other dyes with nonlinear optical properties different from that of Rhodamine 6G.

Chapter 5 exploits the property of DNA to enhance the photoluminescence of dyes. This chapter presents the enhancement of fluorescence from PicoGreen dye on intercalation with DNA on otherwise fluorescence quenched pristine dye. The enhanced emission is amplified by providing a planar microcavity and its amplified spontaneous emission properties are presented. The gain and photo-stability of the dye:DNA complex is also measured and compared with other organic dyes.

The electron blocking property of DNA is featured in chapter 6 using fluorene-based polymer light emitting diode. We have used two fluorenes based polymer blend as active emissive material and observed an eight-fold increase in the brightness of the LED when DNA is used as an electron blocking layer.

Finally, this thesis is concluded in chapter 7 by presenting the summary of the work discussed in the previous chapters. The novel findings that add to the scientific knowledge are listed out for further investigations and discussions.

1.5 CONCLUSIONS

We bring the reader's attention to the need for green materials for sustainable development. Inspired by nature, natural and nature inspired synthetic materials shall be used to protect our environment and help thrive biodiversity and ecosystem. We chose naturally occurring biomaterial, deoxyribonucleic acid for developing photonic

and optoelectronic devices. This interesting natural material with unique properties and earlier work on DNA Photonics generated interest to work on this field.

REFERENCES

[1.] United Nations, Report of the World Commission on Environment and Development, "Our common future", Oxford University Press, (1987)

[2.] United Nations Department of Economic and Social Affairs, World Economic and Social Survey, "The great green technological transformation", (2011)

[3.] S Y Reece, J A Hamel, K Sung, T D Jarvi, A J Esswein, J J H Pijpers, D G Nocera, Wireless solar water splitting using silicon-based semiconductors and earth abundant catalysts, Science, 334, 645, (2011)

[4.] K H Jeong, J Kim, L P Lee, Biologically inspired artificial compound eyes, Science, 312, 557, (2006).

[5.] M Kolle, A Lethbridge, M Kreysing, J J Baumberg, J Aizenberg, P Vukusic, Bio-inspired band-gap tunable elastic optical multilayer fibers, Adv. Mater., 25, 2239, (2013)

[6.] A Ressine, G M Varga, T Laurell, Porous silicon protein microarray technology and ultra-superhydrophobic states for improved bioanalytical readout, Biotechnol. Annu. Rev., 13, 149, (2007)

[7.] T Endlein, A Ji, D Samuel, N Yao, Z Wang, W J P Barnes, W Federle, M Kappl, Z Dai, Sticking like sticky tape: Tree frogs use friction forces to enhance attachment on overhanging surfaces, J. R. Soc. Interface, 10, 20120838, (2013)

[8.] L Phan, W G Walkup IV, D D Ordinario, E Karshalev, J M Jocson, A M Burke, A A Gorodetsky, Reconfigurable infrared camouflage coatings from a cephalopod protein, Adv. Mater., DOI: 10.1002/adma.201301472, (2013)

[9.] V Magdanz, S Sanchez, O G Schmidt, Development of a sperm-flagella driven micro-bio-robot, Adv. Mater., DOI: 10.1002/adma.201302544, (2013)

[10.] J Rivnay, R M Owens, G G Malliaras, The rise of organic bioelectronics, Chem. Mater., 26, 679, (2014)

[11.] G G Malliaras, Organic bioelectronics: A new era for organic electronics, Biochim. Biophys. Acta., 1830, 4286, (2013)

[12.] K Svennersten, K C Larsson, M Berggren, A R Dahlfors, Organic bioelectronics in nanomedicine, Biochim. Biophys. Acta., 1810, 276, (2011)

[13.] M Berggren, A R Dahlfors, Organic bioelectronics, Adv. Mater., 19, 3201, (2007)

[14.] G Lanzani, Materials for bioelectronics: Organic electronics meets biology, Nature Mater., 13, 775, (2014)

15. K Y Yazdandoost, R Kohno, Wireless communication for body implanted medical device, Microwave Conference, APMC 2007, Asia-Pacific, doi. 10.1109/APMC.2007.4554534

16. J E Ferguson, A D Redish, Wireless communication with implanted medical devices using the conductive properties of the body, Expert. Rev. Med. Devices., 8, 427, (2011)

17. C M Boutry, H Chandrahamil, P Streit, M Schinhammer, A C Hanzi, C Hierold, Towards biodegradable wireless implants, Phil. Trans. R. Soc. A, 370, 2418, (2011)

18. A Yakovlev, S Kim, A Poon, Implantable biomedical devices: Wireless powering and vommunication, Communications Magazine, IEEE, 50, 152, (2012)

19. M I Vladu, ''Green'' electronics: biodegradable and biocompatible materials and devices for sustainable future, Chem. Soc. Rev., 43, 588, (2014)

20. M I Vladu, N S Sariciftci, S Bauer, Exotic materials for bio-organic electronics, J. Mater. Chem., 21, 1350, (2011)

21. S Mühl, B Beyer, Bio-organic electronics – Overview and prospects for the future, Electronics, 3, 444, (2014)

22. R P Babu, K O'Connor, R Seeram, Current progress on bio-based polymers and their future trends, Prog. Biomater., 2:8, 1, (2013)

23. D Tobjörk, R Österbacka, Paper electronics, Adv. Mater., 23, 1935, (2011)

24. E Delivopoulos, D J Chew, I R Minev, J W Fawcett, S P Lacour, Concurrent recordings of bladder afferents from multiple nerves using a microfabricated PDMS microchannel electrode array, Lab Chip, 12, 2540, (2012)

25. Y Fukuhira, E Kitazonoa, T Hayashia, H Kanekoa, M Tanakab, M Shimomurac, Y Sumi, Biodegradable honeycomb-patterned film composed of poly(lactic acid) and dioleoylphosphatidylethanolamine. Biomaterials, 27, 1797, (2006)

26. Y Onuki, U Bhardwaj, F Papadimitrakopoulos, D J Burgess, A review of the biocompatibility of implantable devices: Current challenges to overcome foreign body response, J. Diabetes Sci. Technol., 2, 1003, (2008)

27. M C Serrano, E J Chung, G A Ameer, Advances and applications of biodegradable elastomers in regenerative medicine, Adv. Funct. Mater., 20, 192, (2010)

28. C J Bettinger, Z Bao, Organic thin-film transistors fabricated on resorbable biomaterial substrates, Adv. Mater., 22, 651, (2010)

29. D H Kim, N Lu, R Ma, Y S Kim, R H Kim, S Wang, J Wu, S M Won, H Tao, A Islam, K J Yu, T Kim, R Chowdhury, M Ying, L Xu, M Li, H J Chung, H Keum, M McCormick, P Liu, Y W Zhang, F G Omenetto, Y Huang, T Coleman, J A Rogers, Epidermal electronics, Science, 333, 838, (2011)

30. F G Omenetto, D Kaplan, New opportunities for an ancient material, Science, 329, 528, (2010)

31. D H Kim, J Viventi, J J Amsden, J Xiao, L Vigeland, Y S Kim, J A Blanco, B Panilaitis, E S Frechette, D Contreras, D L Kaplan, F G Omenetto, Y Huang, K C Hwang, M R Zakin, B Litt, J A Rogers, Dissolvable films of silk fibroin for ultrathin conformal bio-integrated electronics, Nat. Mater., 9, 511, (2010)

32. M I Vladu, E D Glowacki, P A Troshin, G Schwabegger, L Leonat, D K Susarova, O Krystal, M Ullah, Y Kanbur, M A Bodea, V F Razumov, H Sitter, S Bauer, N S Saricifci, Indigo - a natural pigment for high performance ambipolar organic field effect transistors and circuits, Adv. Mater., 24, 375, (2012)

33. M I Vladu, P A Troshin, M Reisinger, L Shmygleva, Y Kanbur, G Schwabegger, M Bodea, R Schwödiauer, A Mumyatov, J W Fergus, V Razumov, H Sitter, N S Sariciftci, S Bauer, Biocompatible and biodegradable materials for organic field-effect transistors, Adv. Funct. Mater., 20, 4069, (2010)

34. R M Owens, G G Malliaras, Organic electronics at the interface with biology, Mater. Today, 35, 449, (2010)

35. S M R Burns, J L Hendricks, D C Martin, Electrochemical polymerization of conducting polymers in living neural tissue, J. Neural Eng., 4, L6, (2007)

36. D Khodagholy, T Doublet, M Gurfinkel, P Quilichini, E Ismailova, P Leleux, T Herve, S Sanaur, C Bernard, G G Malliaras, Highly conformable conducting polymer electrodes for *in vivo* recordings, Adv. Mater., 23, H268, (2011)

37. Y W Kwon, C H Lee, D H Choi, J I Jin, Material science of DNA, J. Mater. Chem., 19, 1353, (2009)

38. Y W Kwon, D H Choi, J I Jin, Optical, electro-optic and optoelectronic properties of natural and chemically modified DNAs, Polym. J., 44, 1191, (2012)

39. E F Gomez, V Venkatraman, J G Grote, A J Steckl, Exploring the potential of nucleic acid bases in organic light emitting diodes, Adv. Mater., 2014, 1, (2014)

40. V Benfenati, S Toffanin, R Capelli, L M A Camassa, S Ferroni, D L Kaplan, F G Omenetto, M Muccini, R Zamboni, A silk platform that enables electrophysiology and targeted drug delivery in brain astroglial cells, Biomaterials, 31, 7883, (2010)

41. M I Vladu, E D Głowacki, G Schwabegger, L Leonat, H Z Akpinar, H Sitter, S Bauer, N S Sariciftci, Natural resin shellac as a substrate and a dielectric layer for organic field-effect transistors, Green Chem., 15, 1473, (2013)

42. J W Chang, C G Wang, C Y Huang, T D Tsai, T F Guo, T C Wen, Chicken albumen dielectrics in organic field-effect-transistors, Adv. Mater., 23, 4077, (2011)

43. J Mei, Y Diao, A L Appleton, L Fang, Z Bao, Integrated materials design of organic semiconductors for field-effect transistors, J. Am. Chem. Soc., 135, 6724, (2013)

44. C J Bettinger, J P Bruggeman, A Misra, J T Borenstein, R Langer, Biocompatibility of biodegradable semiconducting melanin films for nerve tissue engineering, Biomaterials, 30, 3050, (2009)

45. A B Mostert, B J Powell, F L Pratt, G R Hanson, T Sarnad, I R Gentle, P Meredith, Role of semiconductivity and ion transport in the electrical conduction of melanin, Proc. Natl. Acad. Sci., 109, 8943, (2012)

46. R R Burch, Y H Dong, C Fincher, M Goldfinger, P E Rouviere, Electrical properties of polyunsaturated natural products: field effect mobility of carotenoid polyenes, Synt. Met., 146, 43, (2004)

47. I V Fisher, K Dale, Y Terazono, C Herrero, F Fungo, L Otero, E Durantini, J J Silber, L Sereno, D Gust, T A Moore, A L Moore, S M Lindsay, Conductance of a biomolecular wire, Proc. Natl. Acad. Sci. U.S.A, 103, 8686, (2006)

48. E D Glowacki, L N Leonat, G Voss, M Badea, Z Bozkurt, M I Vladu, S Bauer, N S Sariciftci, Ambipolar organic field effect transistors and inverters with the natural material tyrian purple, AIP Adv., 1, 042132, (2011)

49. Y Kanbur, M I Vladu, E D Glowacki, G Voss, M Baumgartner, G Schwabegger, L Leonat, M Ullah, H Sarica, S E Ela, R Schwodiauer, H Sitter, Z Kucukyavuz, S Bauer, N S Saricifci, Vacuum-processed polyethylene as a dielectric for low operating voltage organic field effect transistors, Org. Electron., 13, 919, (2012)

50. F Miescher, Ueber die chemische Zusammensetzung der Eiterzellen, Med. Chem. Unters., 4, 441, (1871)

51. A D Hershey, M Chase, Independent functions of viral proteins and nucleic acid in growth of bacteriophage, J. Gen. Physiol., 36, 39, (1952)

52. J D Watson, F H C Crick, A structure for deoxyribose nucleic acid, Nature 171, 737, (1953)

53. Y C Hung, D M Bauer, I Ahmed, L Fruk, DNA from natural sources in design of functional devices, Methods, 67, 105, (2014)

54. N Goldman, P Bertone, S Chen, C Dessimoz, E M LeProust, B Sipos, E Birney, Toward practical high-capacity low-maintenance storage of digital information in synthesised DNA, Nature, 494, 77, (2013)

55. B Nithyaja, H Misha, P Radhakrishnan, V P N Nampoori, Effect of deoxyribonucleic acid on nonlinear optical properties of rhodamine 6G-polyvinyl alcohol system, J. Appl. Phys., 109, 023110, (2011)

56. S Sreeja, B Nithyaja, D Swain, V P N Nampoori, P Radhakrishnan, S V Rao, Nonlinear optical studies of DNA doped rhodamine 6G-PVA films using picosecond pulses, Optics and Photonics Journal, 2, 135, (2012)

2

DNA as an optical material

Abstract

In this chapter we review the DNA as an optical/photonic material rather than a biomaterial carrying genetic information. The natural fibrous DNA extracted from salmon testes is soluble only in water. However, to fabricate the DNA thin films in aqueous form pose an adverse problem, when using simple techniques such as spin coating. We refer to the modification of DNA by attaching a cationic surfactant with the phosphate-sugar chain of DNA which makes it insoluble in water, but soluble in most of the organic solvents. The optical and electrical properties of DNA-surfactant lipid complex are discussed to reveal the fact that DNA could be used in photonic and optoelectronic applications.

2.1 INTRODUCTION – the 'molecule of life'

Probably everyone had heard about DNA either in their high school or visualized them in sci-fi movies such as Jurassic Park, The Amazing Spider-Man or Prometheus. DNA or deoxyribonucleic acid is the hereditary material in humans and almost all other living organism that carry the blueprint of genetic information. DNA is wound and coiled along with proteins into supercoiled structures called chromosomes which either floats in the cytoplasm of the cell in the case of prokaryotic organism such as bacteria or resides inside the nucleus of the cell in eukaryotic organism such as plants and animals. If one could stretch out DNA from a cell, it could span to the height of an average human and from all the cells would extend to the sun and half way back. The iconic structure of DNA as a spiraling ladder that is credited to Watson and Crick (1953)[1] has attracted interests from biologists, chemists and recently from physicists.

DNA resembles a right handed twisted ladder, famously known as the 'double helix'[2] structure. It consists of base pairs namely Adenine – Thymine pair and Guanine – Cytosine pair which are linked by hydrogen bonds; and sugar-phosphate backbone internally linked by phosphodiester bonds. The adenine and guanine are similar in structure and are known as purines while thymine and cytosine which are similar are known as pyrimidines. The phosphate group gives negative charge to DNA which are neutralized by positively charged sodium ions, which can move freely along the backbone chain. The structure of DNA is depicted in figure 2.1. The diameter of the helix is about 2.2 nm and the distance between each base pair is around 0.34 nm. The two helical chains coiled around same axis produces two groves, a wider known as the major grove and narrow known as minor grove. These groves expose the bases and are more accessible at those sites. The pitch of the major grove is about 3.4 nm. The size of the DNA strands is usually expressed in base pairs and molecular mass in dalton.

DNA is important in terms of hereditary as it stores the genetic information and passes it to the next generation. The biological functions of DNA are beyond the scope of this thesis, for which the readers may be referred elsewhere[3] and hence shall not be discussed here.
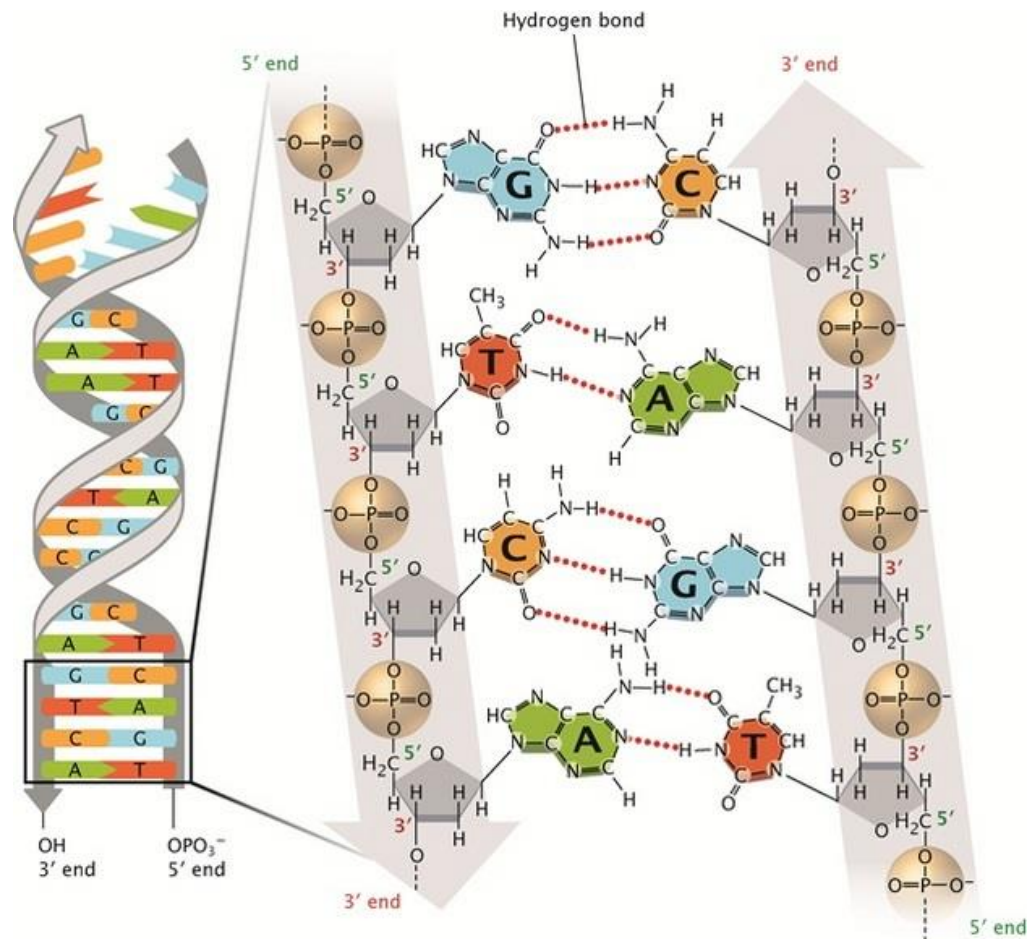
Figure 2.1: The double helical structure of DNA showing the sugar-phosphate backbone with nucleobases: Guanine (G), Cytosine (C), Thymine (T) and Adenine (A) [Courtesy. Nature Education, 2013]

2.2 NATURAL DNA FROM SALMON TESTES

Biomaterials such as DNA has been an area of interest in photonics community working in the fields of organic electronics and photonic devices. Such materials are highly preferred over conventional polymer materials, due to their natural availability,

renewable and biodegradable property. DNA, for their use in photonic applications has been extracted from herring sperm[4], calf thymus[5] and salmon roe sacs[6-10].

The DNA used in the present work is deoxyribonucleic acid sodium salt extracted from salmon testes. It is available in a white fibrous form which is soluble in water. This DNA procured from Sigma Aldrich, USA (Product No. D1626) is a double stranded molecule extracted from sperm cells of salmon fish. Being a marine waste product of fishing industry and easy extraction and purification methods makes it cheapest available DNA in the market. The extraction and purification method is reported briefly by Ogata et al.[11]

However, pure DNA has limited performance[12,13] for applications in photonics. Being a water soluble polymer, it is not preferred in device fabrication techniques. However, such water soluble polymers such as PEDOT:PSS are extensively used in electronic device fabrication. Another limitation arises from its weak π electron conjugation that provides limited hyper-polarizabilities. Therefore, it is necessary to functionalize DNA for practical application in photonics and optoelectronics. Functionalization of DNA can be done either by electrostatic interaction, intercalation or doping.

2.3 MODIFIED DNA-SURFACTANT COMPLEX

As discussed in the above section, natural DNA from salmon testes is soluble in water. But it is not suitable for thin film fabrication as it is susceptible to water absorption. Hence a cationic surfactant such as hexadecetyltrimethylammonium bromide (CTAB) is used to transform hydrophilic DNA to hydrophobic DNA, which is soluble in organic solvents. The negatively charged DNA binds with cationic nitrogen atom in CTMA leaving the bromine anion to ionically bind with sodium.

The protocol for modifying the water soluble DNA to organic-soluble compositions is reported by Heckman et al.[14] The procedure for preparing DNA:CTMA lipid complex is detailed here. All the chemicals and solvents were procured from Sigma Aldrich. The molecular weight of the as received DNA was not reported by the manufacturer. However a report by Tanaka et al states the molecular weight of the DNA to be 2000 bp. The as received DNA was used without any further purification. DNA solution is

prepared in ultra-pure (Milli-Q) water at a concentration of 4 g/L. To reduce the molecular weight of DNA, the solution is subjected to sonication using a probe type ultrasonic processor. This processor uses an ultrasonic generator, a transducer and a probe. The generator uses AC power supply to generate high frequency signal which is fed to a transducer. The transducer converts the electrical signal to mechanical vibrations which are amplified and transmitted down the length of the probe. The probe is immersed in the solution and during operation produces compression and rarefaction. In the liquid, rarefaction causes cavitation or microscopic vacuum bubbles which implodes at enormous temperature and pressure during compression. This tremendous energy causes hydrodynamic shear on the DNA causing it to tear randomly. Since sonication causes localized temperature to raise which may rupture DNA, it is done with brief resting periods while the sample is placed in an ice bath. The ultrasonicator used is a Branson 250 analog ultrasonic processor. DNA aqueous solution was sonicated in ice bath for 50 cycles, with each containing 10 sec sonication - at 50% of
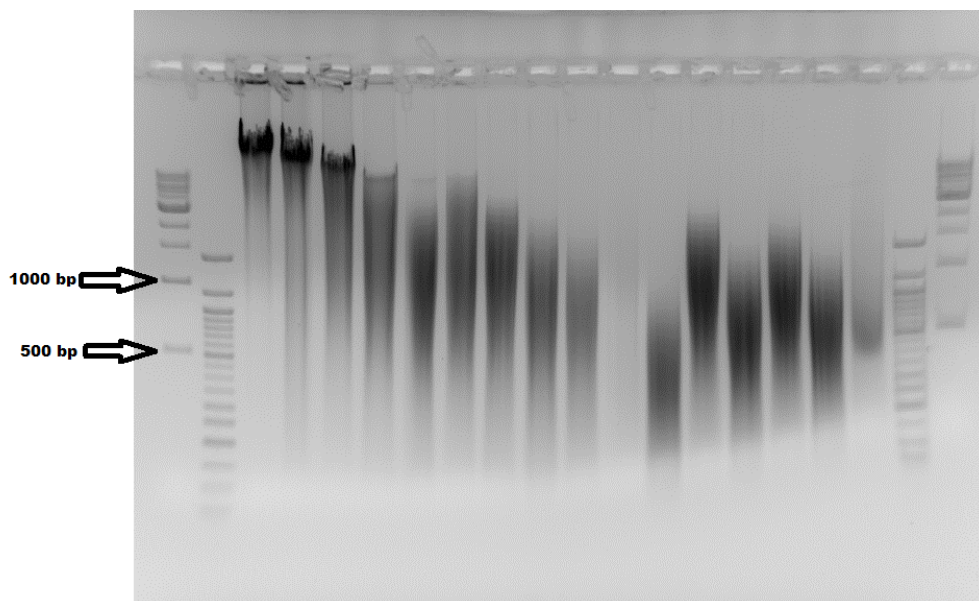
Figure 2.2: Determination of molecular weight of sonicated DNA by gel electrophoresis method

the output power and 50% duty cycle - and 20 sec rest period. The molecular weight of the sonicated sample was measured by gel electrophoresis method and was estimated to be around 500-200 bp (see 13th well in Figure 2.2).

CTAB aqueous solution was also prepared at same concentration (4 g/L). The CTAB solution was added to DNA solution drop by drop while stirring. The DNA-CTAB solution was additionally stirred for 2 more hours at room temperature. The DNA:CTMA precipitates through ionic bonding leaving NaBr with the solvent. The precipitate was filtered using 0.45 μm nylon membrane to remove any impurities and then dried in vacuum at 40°C overnight. The precipitate collected as a white powder is stored in a cool dry place. The DNA:CTMA lipid complex was dissolved in butanol at the desired concentration which is now suitable for fabrication into thin films. Recently, other groups have shown an alternative method[15] to modify natural DNA. In the following sections we shall discuss the properties of DNA:CTMA complex that makes it an excellent optical and photonic material.

2.4 ELECTRICAL PROPERTIES OF DNA:CTMA COMPLEX

For long, the idea of DNA as a molecular wire[16] that can efficiently conduct charge carriers has spurred hot debates[17]. Reports of electron transfer rates in π-stacking polymers such as proteins through electron tunneling has inspired the study of charge transport in DNA. Eley et al was the first to propose the use DNA as electrical conductor[18]. Experiments that followed by various groups held varying views on conduction in DNA due to the contradictory theoretical predictions. Results have revealed to be controversial as the data showed all ranges of conductivities from insulator to superconductivity.[19] By the beginning of 21st century, the chemists and physicists have reached a consensus view[20] on charge migration in DNA. Barton's group[21,22] had demonstrated the use of DNA as a molecular wire by transferring electron from donor to acceptor molecules through DNA over a distance of 34 nm. Fink et al.[23] and Porath et al.[24] has revealed the semiconducting behavior of DNA using

current-voltage measurements. The resistivity of DNA was found to be comparable with those of the conducting polymers. However, the mechanism of charge conduction is still an unsolved problem. Electrical conductivity in DNA–lipid complex fabricated into thin films[25,26] have been studied. The results suggested that the stacked base-pairs of the DNA strands were responsible for electrical conduction.

The conductivity of DNA depends on many factors, such as its molecular weight, base pair sequence, structure (single/double stranded), environment (presence of water or counter ions), shape (stretched/combed), assembly (free standing or attached to surface), contact electrodes.

The electrical properties of DNA:CTMA thin films were studied by Hagen et al.[11] It was observed that the resistivity was dependent on molecular weight of DNA. The resistivity varied from 10^{15} Ω-cm for higher molecular weight to 10^9 Ω-cm for lower molecular weight of DNA. It was also presented that the doping with suitable conductive polymers or organic small molecules can bring down the resistivity. The dielectric constant for DNA:CTMA[27] was found to be around 7. The charge transport in a material is controlled by its energy level, defined in eV. The energy levels for organic semiconductors are known as Highest Occupied Molecular Orbital (HOMO) and Lowest Unoccupied Molecular Orbital (LUMO). The DNA:CTMA[11] has a HOMO of 5.6 eV and LUMO of 0.9 eV. Another study by Lin et al.[28] (Lin, 2011) reports HOMO of 5.7 eV and LUMO of 1.634 eV. The HOMO/LUMO levels of nucleobases A, G, C, T and Uracil have been reported by Ouchen at al.[29] The hole mobility of DNA:CTMA has been found to be 1.14 x 10^{-6} cm^2/Vs.

The charge transport in DNA has attracted much interest due to its potential in molecular electronics. This has opened new avenues for research in DNA-based electronic devices.

2.5 OPTICAL PROPERTIES OF DNA:CTMA COMPLEX

The optical properties of DNA:CTMA have well been studied[30], as these properties define the applicability of this material in optoelectronic devices. The optical absorption/transmission, optical loss and refractive index has been examined by Grote

et al. The DNA:CTMA thin film showed its characteristic peak in the UV-Vis spectrum at 260 nm, corresponding to each of the four base bridging the two backbone. Above 300 nm extending to near infra-red region, the nucleic acid exhibit excellent transmissivity.[27] This feature is highly attractive in photonic and optoelectronic devices. The refractive index is found to vary from 1.535 at 300 nm to 1.480 at 1600 nm[6]. This, along with low optical loss makes it a good optical cladding material for nonlinear electro-optic modulators and waveguides.

Apart from electrical and optical properties, other useful measurements such as thermogravimetric analysis, microwave insertion loss and gamma ray irradiation tolerance have been studied.[31]

2.6 APPLICATION OF DNA IN PHOTONICS AND OPTOELECTRONIC SYSTEMS

The applicability of DNA in various photonic devices has been on the rise for about a decade[32,33]. DNA has been used as a template and a structuring agent for synthesis of nanoparticles[4], as DNA origami for self-assembly of pre-defined structures[34-36], as fluorescence enhancer in fluorescent and phosphorescent dyes (refer section 5.1), as a cladding material for optical waveguides[27], cladding and host matrix for nonlinear optical devices[8], as a low optical loss host material for electro-optic modulators, as a hole transporting layer in polymer solar cells[37], as electron blocking layer in organic light emitting diodes (refer section 6.1), as an insulating gate dielectric material in field effect transistors and high energy capacitors[38-40], electro-fluidic fluorescent biosensor[41-43], sensing toxic gases and glucose for biomedical application[44], microfluidic switches, organic memory devices and as organic catalysts. DNA based nanocomposite materials are also developed as a non-conductive, optically transparent systems for shielding electromagnetic interference and radio frequency[7]. DNA films have proven effective for cell culture and wound healing of skin[45] in medical applications.

2.7 CONCLUSIONS

From the above discussion, we perceive how DNA has transformed itself from a biomolecule to an attractive optical material. Marine derived DNA, extracted from salmon roe sacs is found to be a novel material for use in photonic and optoelectronic devices, due to its unique electrical and optical properties. In the course of this thesis, one may find flourishing reports on the successful use of DNA in various devices. It is necessary to identify suitable organic materials that intercalate with DNA to yield high performance devices. Such environmental safe devices and materials are the way forward to achieve sustainable electronics.

REFERENCES

1. L Pray, Discovery of DNA structure and foundation: Watson and Crick, Nature Education, 1, 100, (2008)

2. J D Watson, The double helix: A personal account of the discovery of the structure of DNA, Simon and Schuster, (2011)

3. M Amos, Chapter 1: DNA: The molecule of life, in 'Theoretical and experimental DNA computation', Springer-Verlag Berlin Heidelberg, (2005)

4. B Nithyaja, H Misha, V P N Nampoori, Synthesis of silver nanoparticles in DNA template and its influence on nonlinear optical properties, J. Nanosci. Nanotechnol., 2, 99, (2012)

5. V G Bregadze, T G Giorgadze, Z G Melikishvili, DNA and nanophotonics: original methodological approach, Nanotechnol. Rev., 3, 445, (2014)

6. J G Grote, D E Diggs, R L Nelson, J S Zetts, F K Hopkins, N Ogata, J A Hagen, E Heckman, P P Yaney, M O Stone, L R Dalton, DNA Photonics [Deoxyribonucleic acid], Mol. Cryst. Liq. Cryst., 426, 3, (2005)

7. J G Grote, D Y Zang, F Ouchen, G Subramanyam, P P Yaney, C Bartsch, E Heckman, R Naik, Progress of DNA photonics, Nanobiosuystems: Processing, Characterization, and Applications III, edited by N Kobayashi, F Ouchen, I Rau, Proc. of SPIE, 7765, 776502, (2010)

8. J A Hagen, J G Grote, N Ogata, J S Zetts, R L Nelson, D E Diggs, F K Hopkins, P P Yaney, L R Dalton, S J Clarson, DNA Photonics, Organic Photonic Materials and Devices VI, edited by J G Grote, T Kaino, Proc. of SPIE, 5351, (2004)

9. Y W Kwon, C H Lee, D H Choi, J I Jin, Material science of DNA, J. Mater. Chem., 19, 1353, (2009)

10. T B Singh, N S Sariciftci, J G Grote, Bio-organic optoelectronic devices using DNA, Adv. Polym. Sci., 223, 189, (2010)

11. J A Hagen, Enhanced luminous efficiency and brightness using DNA electron blocking layers in bio-organic light emitting diodes, PhD thesis, University of Cincinnati, (2006)

12. I Rau, A Szukalski, L Sznitko, A Miniewicz, S Bartkiewicz, F Kajzar, B Sahraoui, J Mysliwiec, Amplified spontaneous emission of Rhodamine 6G embedded in pure deoxyribonucleic acid, Appl. Phys. Lett., 101, 171113, (2012)

13. R Grykien, B Luszczynska, I Glowacki, F Kajzar, I Rau, Pure DNA as an efficient electron blocking layer, Mol. Cryst. Liq. Cryst., 604, 213, (2014)

14. E M Heckman, J A Hagen, P P Yaney, J G Grote, F K Hopkins, Processing techniques for deoxyribonucleic acid: Biopolymer for photonics applications, Appl. Phys. Lett., 87, 211115, (2005)

15. F Ouchen, G A Sotzing, T L Miller, K M Singh, B A Telek, A C Lesko, R Aga, E M Fehrman-Cory, P P Yaney, J G Grote, C M Bartsch, E M Heckman, Modified processing techniques of a DNA biopolymer for enhanced performance in photonics applications, Appl. Phys. Lett., 101, 153702, (2012)

16. R G Endres, D L Cox, R R P Singh, Colloquium: The quest for high-conductance DNA, Rv. Mod. Phys., 76, 195, (2004)

17. D N Beratan, S Priyadarshy, S M Risser, DNA: insulator or wire?, Chem. Biol. 4,3, (1997)

18. D D Eley, D I Spivey, Semiconductivity of organic substances. Part 9. – Nucleic acid in the dry state, Trans. Faraday Soc., 58, 411, (1962)

19. S Abdalla, Electrical conduction through DNA molecule, Prog. Biophys. Mol. Bio., 106, 485, (2011)

20. E Wilson, DNA charge migration: No longer issue, Chem. Eng. News, 79, 29, (2001)

21. E M Boon, J K Barton, Charge transport in DNA, Curr. Opin. Struct. Biol., 12, 320, (2002)

22. J D Slinker, N B Muren, S E Renfrew, J K Barton, DNA charge transport over 34 nm, Nat. Chem., 3, 228, (2011)

23. H W Fink, C Schönenberger, Electrical conduction through DNA molecules, Nature, 398, 407, (1999)

24. D Porath, A Bezryadin, S de Vries, C Dekker, Direct measurement of electrical transport through DNA molecules, Nature, 403, 635, (2000)

25. Y Okahata, T Kobayashi, K Tanaka, M Shimomura, Anisotropic electric conductivity in an aligned DNA cast film, J. Am. Chem. Soc., 120, 6165, (1998)

26. P P Yaney, T Gorman, F Ouchen, J G Grote, Studies of charge transport in DNA films using the time-of-flight (TOF) technique, Nanobiosystems: Processing, Characterization and Applications IV, edited by, N Kobayashi, F Ouchen, I Rau, Proc. of SPIE., 8103, 81030H, (2011)

27. J G Grote, J A Hagen, J S Zetts, R L Nelson, D E Diggs, M O Stone, P P Yaney, E M Heckman, C Zhang, W H Steier, A K Y Jen, L R Dalton, N Ogata, M J Curley, S J Clarson, F K Hopkins, Investigation of polymers and marine derived DNA in optoelectronics, J. Phys. Chem. B, 108, 8584, (2004)

28. T Y Lin, C Y Chang, C H Lien, Y W Chiu, W T Hsu, C H Su, Y S Wang, Y C Hung, Preparation and characterization of DNA-aromatic surfactant complexes for optoelectronic applications, Organic Photonic Materials and Devices XIII, edited by R L Nelson, F Kajzar, T Kaino, Y Koike, Proc. of SPIE, 7935, 79350E, (2011)

29. F Ouchen, E Gomez, D Joyce, A Williams, S Kim, E M Keckman, L Johnson, P Yaney, N Venkat, A Steckl, F Kajzar, I Rau, A Pawlicka, P Prasad, J Grote, Latest advances in bio materials: From deoxyribonucleic acid to nucleobases, Organic Photonic Materials and Devices XVI, edited by C E Tabor, F Kajzar, T Kaino, Y Koike, Proc. of SPIE, 8983, 89831A, (2014)

30. Y W Kwon, D H Choi, J I Jin, Optical, electro-optic and optoelectronic properties of natural and chemically modified DNAs, Polym. J., 44, 1191, (2012)

31. J A Hagen, J G Grote, N Ogata, E Heckman, P P Yaney, D E Diggs, G Subramanyam, R L Nelson, J S Zetts, F K Hopkins, E W Taylor, Deoxyribonucleic acid (DNA) photonics for space environments, Photonics for Space Environments IX, edited by E W Taylor, Proc. of SPIE, 5554, 28, (2004)

32. I Rau, J G Grote, F Kajzar, A Pawlicka, DNA – novel nanomaterial for applications in photonics and in electronics, C. R. Physique, 13, 853, (2012)

33. Y C Hung, D M Bauer, I Ahmed, L Fruk, DNA from natural sources in design of functional devices, Methods, 67, 105, (2014)

34. K Sanderson, What to make with DNA origami, Nature, 464, 158, (2010)

35. K E Dunn, F Dannenberg, T E Ouldridge, M Kwiatkowska, A J Turberfield, J Bath, Guiding the folding pathway of DNA origami, Nature, 525, 52, (2015)

36. P W K Rothemund, Design of DNA origami, ICCAD '05, Proceedings of the 2005 IEEE/ACM International conference on Computer-aided design, 471, (2005)

37. V Kolachure, DNA based thin film as hole transport layer in bulk heterojunction polymer solar cells, MSc Thesis, University of Texas, (2007)

38. C M Bartsch, Development of a field-effect transistor using DNA biopolymer as the semiconductor layer, PhD Dissertation, University of Dayton, (2007)

39. C M Bartsch, G Subramanyam, J G Grote, K M Singh, R R Naik, B Singh, N S Sariciftci, Bio-organic field-effect transistors, Nanobiotronics, edited by, E M Heckman, T B Singh, J Yoshida, Proc. of SPIE, 6646, 66460K, (2007)

40. D M Joyce, N Venkat, F Ouchen, K M Singh, S R Smith, C A Grabowski, P T Murray, J G Grote, Deoxyribonucleic acid-based hybrid thin films for potential application as high energy density capacitors, J. Appl. Phys., 115, 114108, (2014)

41. A J Steckl, J A Hagen, Z Yu, R A Jones, W Li, D Han, D Y Kim, H Spaeth, Challenges and opportunities for biophotonic devices in the liquid state and the solid state, IEEE Nanotechnology Conference, 1, 159, (2006)

42. F Lucarelli, S Tombelli, M Minunni, G Marrazza, M Mascini, Electrochemical and piezoelectric DNA biosensors for hybridization detection, Anal. Chim. Acta., 609, 139, (2008)

43. J Wang, Electrochemical biosensors: Towards point-of-care cancer diagnostics, Biosens. Bioelectron., 21,1887, (2006)

44. N Ogata, Developments of highly sensitive DNA sensors, Nanobiosystems: Processing, Characterization, and Applications IV, edited by N Kobayashi, F Ouchen, I Rau, Proc. of SPIE, 8103, 810302, (2011)

45. N Ogata, K Yamaoka, J Yoshida, Progress of DNA biotronics and other applications, Nanobiosystems: Processing, Characterization, and Applications III, edited by N Kobayashi, F Ouchen, I Rau, Proc. of SPIE, 7765, 776508, (2010)

3

Experimental techniques

Abstract

This chapter describes the experimental techniques used in the following three chapters. The chapter is divided into three sections, first - focusing on the Z-scan techniques used for measurement of nonlinear optical (NLO) properties such as nonlinear absorption coefficient and third order nonlinear susceptibility of dyes; second – detailing the techniques used for casting thin films and measurement of amplified spontaneous emission; and third – describing the fabrication of light emitting diodes by spin coating and thermal evaporation techniques, and characterization of LEDs measuring its J-V (current density vs voltage characteristics), L-V (luminance vs voltage characteristics) curves and electroluminescence spectra.

3.1 TECHNIQUES USED IN NONLINEAR OPTICAL MEASUREMENT

The invention of laser in 1960 has ushered various new fields, one being 'nonlinear optics'. Unlike linear optics, when the intensity of light is sufficiently intense, it can modify the optical properties of the material it pass through. These modifications respond nonlinearly to the intensity of light. In this thesis we limit our study to third-order nonlinear optical process, where the processes involve third-order polarization. One of the results of third-order optical nonlinearity is the intensity dependent refractive index. The intensity dependent refractive index manifests as intensity dependent optical transmission and absorption. These can be studied using Z-Scan technique, detail of which are given in the following section.

3.1.1 Z-SCAN EXPERIMENTAL SETUP

Z-Scan (ZS) technique is a simple and commonly used experimental configuration to measure nonlinear optical properties. This technique, proposed by Bahae et al.[1-5] requires simple optical arrangements unlike interferometry and wave-mixing techniques. This single beam ZS technique has two configurations viz. open aperture (OA) and closed aperture (CA) to measure nonlinear absorption coefficient and nonlinear refractive index respectively. The ease of this technique lies in the direct and simultaneous measurement of the sign and magnitude of the nonlinear parameters. The sign of the nonlinear parameters can be known by simply observing the ZS curve. While nonlinear absorption directly affects the amplitude of the propagating electric field, nonlinear refraction directly affects the phase of the propagating electric field, which propagate to give spatial and temporal amplitude changes.

This technique involves measuring the transmittance of the test material as a function of 'Z' position which in turn is a function of fluence realized by a focusing lens. A typical ZS experimental arrangement is shown in figure 3.1. A thin sample of thickness less than the diffraction length (z_0) of a focused laser beam is scanned across the focal point with a scan range extending from $\pm z_0$. This sample thickness condition is required to satisfy the 'thin sample approximation'[4]. The scan range depends on beam parameters and thickness of the sample and is typically of $\pm 5z_0$ considering the experimental imperfections. The sample is scanned through the focal profile using a

motorized translation stage. The laser intensity fluctuations were considered by using a reference detector (A, in figure 3.1) to stabilize the transmittance from the sample.
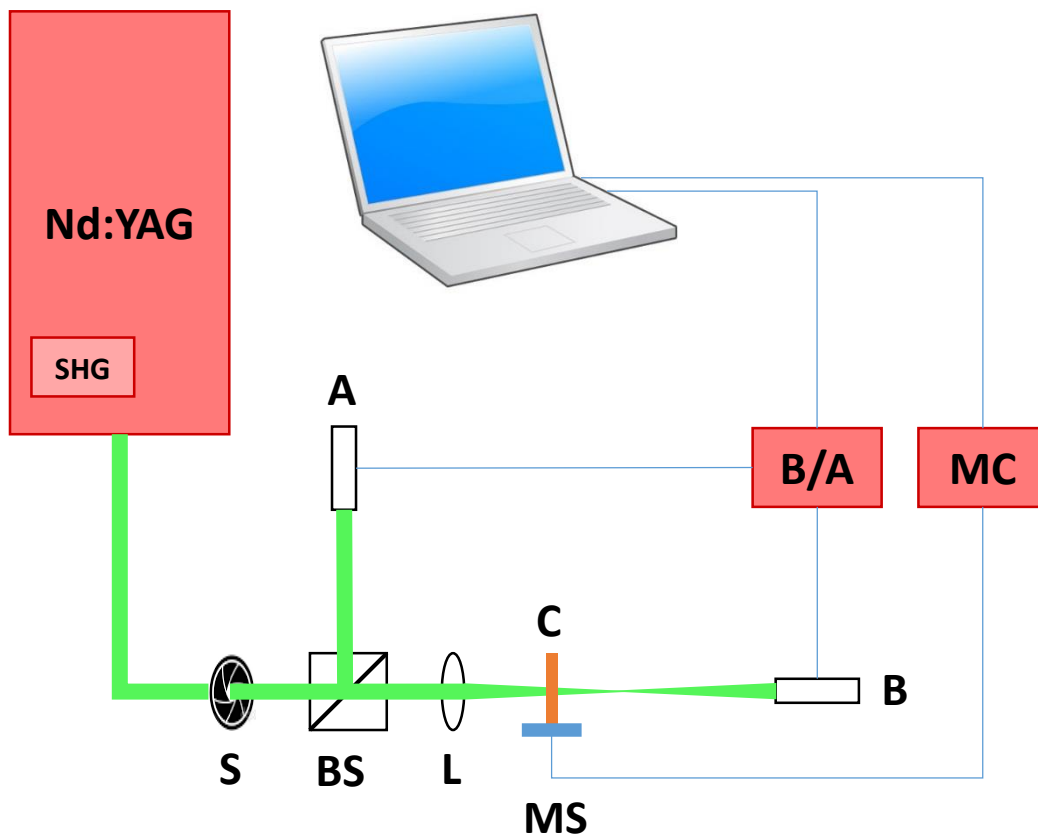
Figure 3.1: ZS experimental setup to measure third order nonlinear optical properties [SHG: Second Harmonic Generator; S: Aperture; BS: Beam Splitter; L: Lens; C: Cuvette Cell; A & B: Detectors; B/A: Energy Ratiometer; MS: Motor Stage; MC: Motor Controller]

The laser source used in this study is a frequency doubled Nd:YAG laser with a pulse duration of 7 ns and a repetition rate of 10 Hz. A 20 cm lens was used to produce a beam waist of 42.56 µm with a Rayleigh length of 10.7 mm at 532 nm. A cuvette of 1

mm optical path is used that satisfies the thin sample approximation. The make and model of the energy ratio meter are Laser Probes Inc. (Rj-7620) with two identical pyroelectric detectors (RjP-735 probes). The ratio meter and the motor controller connected to a computer and the experimental procedure were automated using a LabView program.

3.1.2 OPEN APERTURE Z-SCAN

At low intensity, the light absorption property in an absorbing medium behaves linearly with the intensity. However at high intensities, the medium shows nonlinear response due to population redistribution, energy transitions in complex molecular systems and generation of free carriers. These characteristics results in increase or decrease in absorption known as reverse saturable absorption (RSA) and saturable absorption (SA) respectively. The typical ZS curves for RSA and SA, which depicts a positive and negative nonlinear absorption coefficient, respectively are shown in figure 3.2.
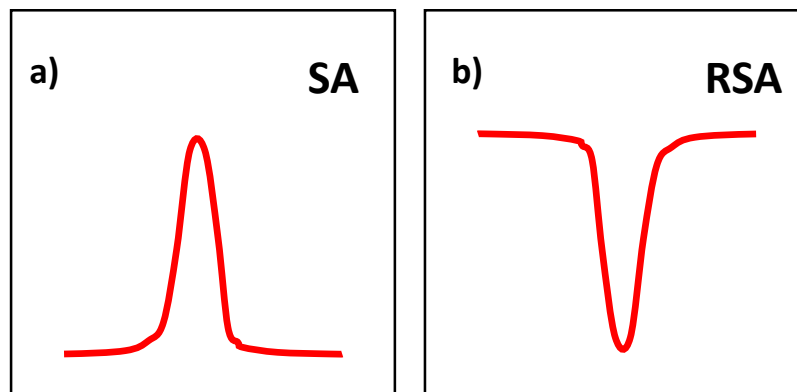

Figure 3.2: Typical OA ZS curves depicting (a) negative and (b) positive nonlinear absorption coefficient

RSA behavior in a medium is due to the phenomena such as two or multi photon absorption, excited state absorption, free carrier absorption or a combination of these mechanisms. Such mechanisms result in increased absorption due to the higher excited-

state absorption cross-section over the ground-state absorption cross-section owing to a decrease in transmission (RSA). In certain materials, the intensity of the incident beam is sufficiently high to deplete the ground state population allowing the incoming photons to be transmitted through the medium resulting in a decrease in the absorption (SA). In such situations, the ground-state absorption cross-section is higher than the excited-state absorption cross-section. In some materials these mechanisms may occur in a competitive fashion to cause a flip from RSA to SA or from SA to RSA[6-15]. It could be observed that these mechanisms produce a change in the intensity of the transmitted light which leads to the change in nonlinear absorption coefficient.

In the presence of RSA, the intensity dependent optical nonlinearity is described by the equation 3.1.

$$\alpha(I) = \alpha_0 + \beta I \tag{3.1}$$

$\alpha(I)$ is the effective (saturated) absorption coefficient, α_0 is the low-intensity unsaturated linear absorption coefficient and β is the nonlinear absorption coefficient. β can be calculated from OA ZS curves using the theoretical geometry developed by Bahae et al. For RSA curves, the normalized change in the transmitted energy $T(z)$ is given by the equation[5] 3.2.

$$T(z) = \sum_{m=0}^{+\infty} \frac{[-\beta I_0 L_{eff}/(1 + \gamma^2)]^m}{(m + 1)^{3/2}} \tag{3.2}$$

The effective thickness of the sample, L_{eff} and the peak intensity at the focus, I_0 is given by the equations 3.3 and 3.4 respectively.

$$L_{eff} = 1 - exp(-\alpha_0 L)/\alpha_0 \tag{3.3}$$

$$I_0 = E/\tau(\pi\omega_0^2) \tag{3.4}$$

where, L is the sample thickness, E is the beam energy at the sample and τ is the pulse width. The Rayleigh length z_0 is given by $z_0 = \pi\omega_0^2/\lambda$ and laser beam waist ω_0 is

given by $\omega_0 = f\lambda/D$, where f is the focal length of the lens, λ the wavelength of laser and D, the radius of the beam. The translation coordinate normalized by the Rayleigh length is denoted by $\gamma = z/z_0$.

The self-focussing nature of reverse saturable absorbers can be used to limit the optical intensity transmitted through a system. Such materials exhibit linear transmittance at low powers, but behave opaque at higher intensities. An ideal optical limiter (OL) should have a large ratio of excited-state absorption cross-section to ground-state absorption cross-section over a wide range of spectrum with a fast response time. The optical limiting performance of such materials can be analyzed with the help of transmittance vs input energy plot[16] or output fluence vs input fluence plot[17]. The transmittance vs input energy plot can be obtained from OA ZS curve data by substituting the beam waist with position dependent beam spot size as $\omega_0^2(1 + z^2/z_0^2)$ in equation 3.4. Hence, the equation can be re-written as follows.

$$I(z) = \frac{I_0}{1 + (z^2/z_0^2)} \tag{3.5}$$

The data from $z \leq 0$ presents the OL curve and the limiting threshold is determined graphically at the intersection between the linear and nonlinear parts of the OL curve.

The normalized transmittance for SA curves is given by the equation[7] 3.6.

$$T(z) = \sum_{m=0}^{+\infty} \frac{[-\alpha I_0 L_{eff}/(1 + \gamma^2)]^m}{(m + 1)} \tag{3.6}$$

where, the nonlinear absorption coefficient for homogeneous[18] and inhomogeneous broadening[14,19] systems is given by equation 3.7 and 3.8, respectively where I_s is the saturation intensity.

$$\alpha(I) = \left(\frac{\alpha_0}{1 + (I/I_s)}\right) \tag{3.7}$$

$$\alpha(I) = \left(\frac{\alpha_0}{\sqrt{1 + (I/I_s)}}\right) \tag{3.8}$$

To interpret the concurrence of RSA and SA, the effective absorption coefficient as in equation 3.9, combines the negative SA coefficient (first term) and the positive RSA coefficient (second term)[7,20,21].

$$\alpha(I) = \left(\frac{\alpha_0}{1 + (I/I_s)} + \beta I\right) \tag{3.9}$$

The imaginary part of third-order susceptibility is related to β through the equation 3.10 and is expressed in $m^2 V^{-2}$.

$$Im\ \chi^{(3)} = \frac{\beta n_0^2 \varepsilon_0 c \lambda}{2\pi} \tag{3.10}$$

Applications of RSA materials are for the purpose of shortening and smoothening laser pulses. RSA materials are also excellent optical limiters which have application in laser damage protection to human eyes and sensors. Materials with SA property find application in passive Q-switching or mode locking lasers. Such effects that occur in semiconductors are used as SA mirrors. Saturable absorbers are also useful for nonlinear filtering of the laser beam and in optical signal processing. Reverse saturable absorbers in conjunction with saturable absorbers can be used to mode-lock lasers for which gain medium have high saturation energies where the SA material cuts the leading edge of the pulse while the other cuts the trailing edge[22].

3.1.3 CLOSED APERTURE Z-SCAN

In CA ZS experimental configuration, the transmittance is measured through an aperture placed in the far field. This configuration exploits the spatial broadening and narrowing of Gaussian beams in the far field due to the self-focusing and self-defocusing effect caused by the nonlinear interaction of the laser beam with the material. The size of the aperture is represented by its linear transmittance and is usually

of the range 10 - 50 %. The position of the aperture should be in the far field i.e. greater than z_0 and the typical values range from $20z_0$ to $100z_0$. All other experimental configuration and procedure are similar to OA ZS.

The sample can be regarded as a thin lens with a variable focal lens. As the sample is scanned far away from the focus where the beam irradiance is low, no nonlinear effect predominates and hence the transmittance is constant. As the sample nears the focal profile, different features were observed for materials with different nonlinear property. As the irradiance begins to increase, the material with negative lensing effect (diverging lens), tends to collimate the beam leading to beam narrowing at the aperture. This causes an increase in the transmittance resulting in a peak in the ZS curve. At the focus, the sample produces minimal change in the transmittance behavior. Beyond the focal plane, the same defocusing effect tends to diverge the beam, leading to a beam broadening at the aperture resulting in a decrease in the transmittance. This is analogous to scanning a diverging lens instead of the sample. A representation of this picture is illustrated in figure 3.3. The green shade is the actual focal profile without the sample while the red dashed line guides the beam profile in the presence of the sample. Thus for a self-defocusing nonlinearity, the typical CA ZS curve observed is a peak at the pre-focal position followed by a valley at the post-focal position. The observance of a peak-valley in ZS curve indicates a negative nonlinear refraction.

Usually, the ZS curves have similar peak height and valley depth. Sometimes asymmetry may arise in the ZS curve due to the effect of nonlinear absorption in the CA geometry, resulting in a suppressed peak and enhanced valley. The theoretical fit of such data is performed by a procedure which takes into account the best pair of values (β,n_2) representing both results from OA and CA data. The normalized transmittance of the symmetric[23] and asymmetric peak-valley[24] ZS data is given by equation 3.11 and 3.12 respectively.

$$T(z) = 1 - \frac{8\pi\gamma}{\lambda}\frac{n_2 I_0 L_{eff}}{(\gamma^2 + 9)(\gamma^2 + 1)} \qquad (3.11)$$

$$T(z) = 1 + \frac{8\pi\gamma}{\lambda}\frac{n_2 I_0 L_{eff}}{(\gamma^2 + 9)(\gamma^2 + 1)} - \frac{\beta I_0 L_{eff}(\gamma^2 + 3)}{(\gamma^2 + 9)(\gamma^2 + 1)} \qquad (3.12)$$
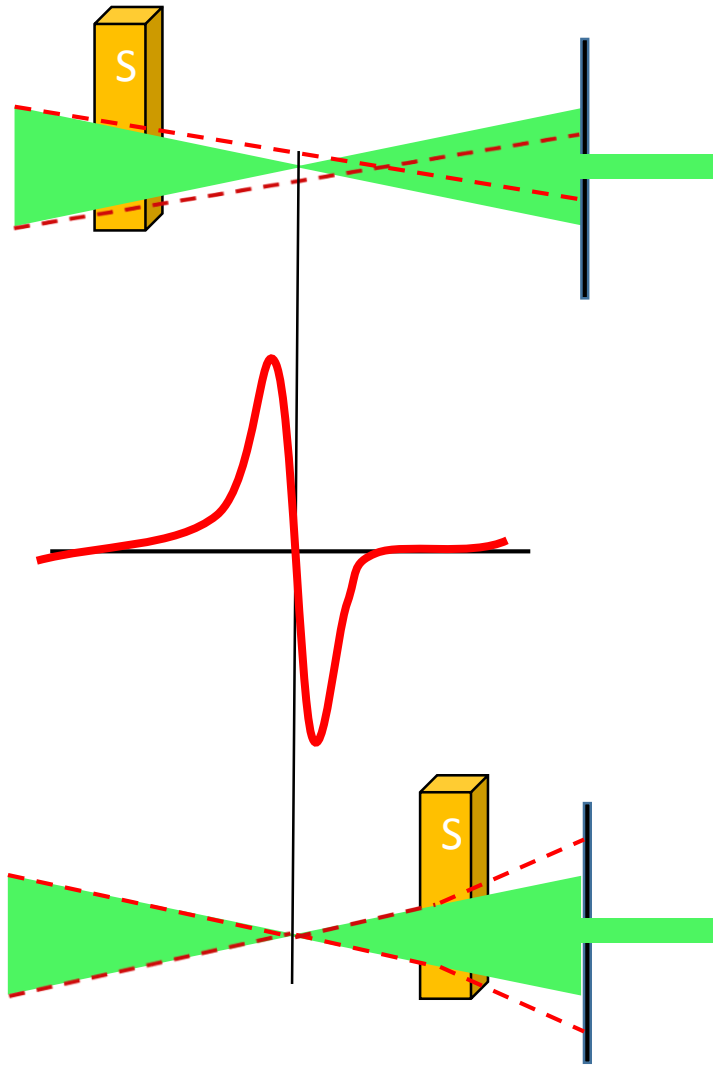
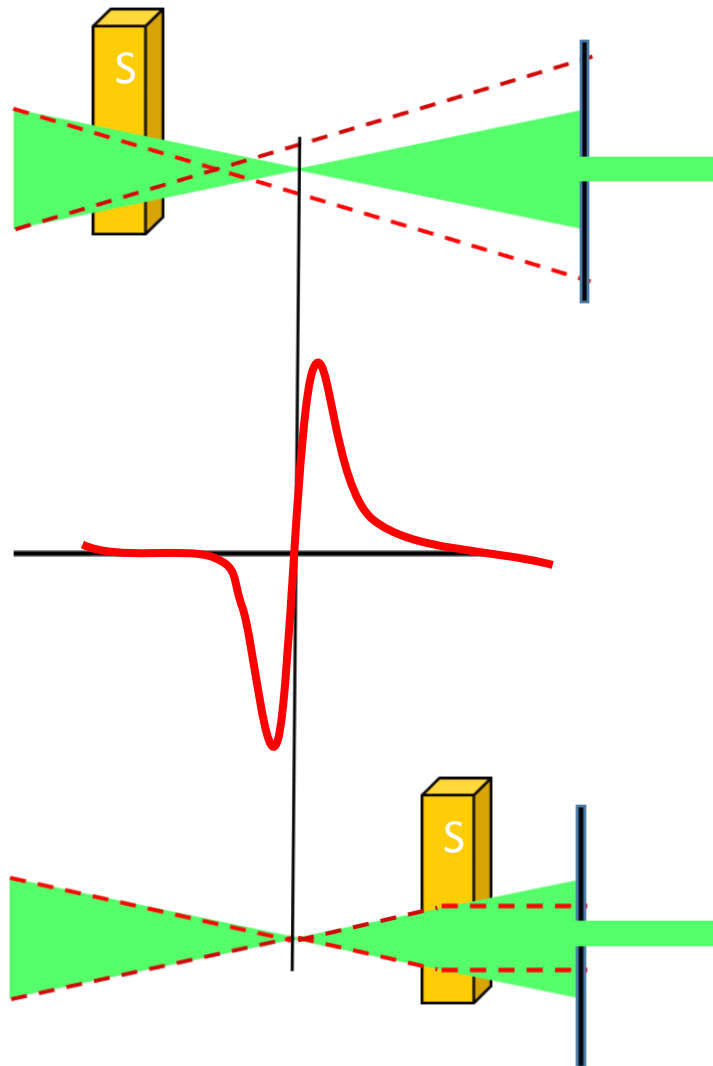Figure 3.3: Typical CA ZS curves of samples with negative lensing effect

Figure 3.4: Typical CA ZS curves of samples with positive lensing effect

For a positive lensing effect the opposite occurs, leading to a valley-peak ZS curve (see figure 3.4). The normalized transmittance of the symmetric[25] and asymmetric valley-peak[26] ZS data is given by equation 3.13 and 3.14 respectively.

$$T(z) = 1 + \frac{8\pi\gamma}{\lambda} \frac{n_2 I_0 L_{eff}}{(\gamma^2 + 9)(\gamma^2 + 1)} \tag{3.13}$$

$$T(z) = 1 - \frac{8\pi\gamma}{\lambda} \frac{n_2 I_0 L_{eff}}{(\gamma^2 + 9)(\gamma^2 + 1)} - \frac{\beta I_0 L_{eff}(\gamma^2 + 3)}{(\gamma^2 + 9)(\gamma^2 + 1)} \tag{3.14}$$

Bahae et al.[2] proposed a simpler and direct measurement of nonlinear refractive index provided the sample has a good optical quality to resolve the transmittance changes by 1%. For a phase distortion, $|\Delta\Phi_0| \leq \pi$ the nonlinear refractive index, n_2 can be calculated in SI system using the equation 3.15.

$$n_2 = \frac{\Delta T_{p-v}}{0.406 \, (1 - S)^{0.25} \, k I_0 L_{eff}} \tag{3.15}$$

where ΔT_{p-v} is the distance between normalized peak and valley transmittance and k is the propagation constant.

The n_2 value can be converted into SI system by using the following equation.

$$n_2(esu) = \frac{cn_0}{40\pi} \, n_2 \left(m^2/W \right) \tag{3.16}$$

The asymmetrical ZS curves (enhanced peak/suppressed valley or vice versa) carry nonlinear absorption effect since the CA ZS measurement is sensitive to both nonlinear absorption and nonlinear refraction. In such cases, dividing the CA data by OA data yields a ZS curve only due to nonlinear refraction resulting in a symmetrical curve as shown in figure 3.5. The n_2 value can be calculated using either of these equations 3.11, 3.13 or 3.15.
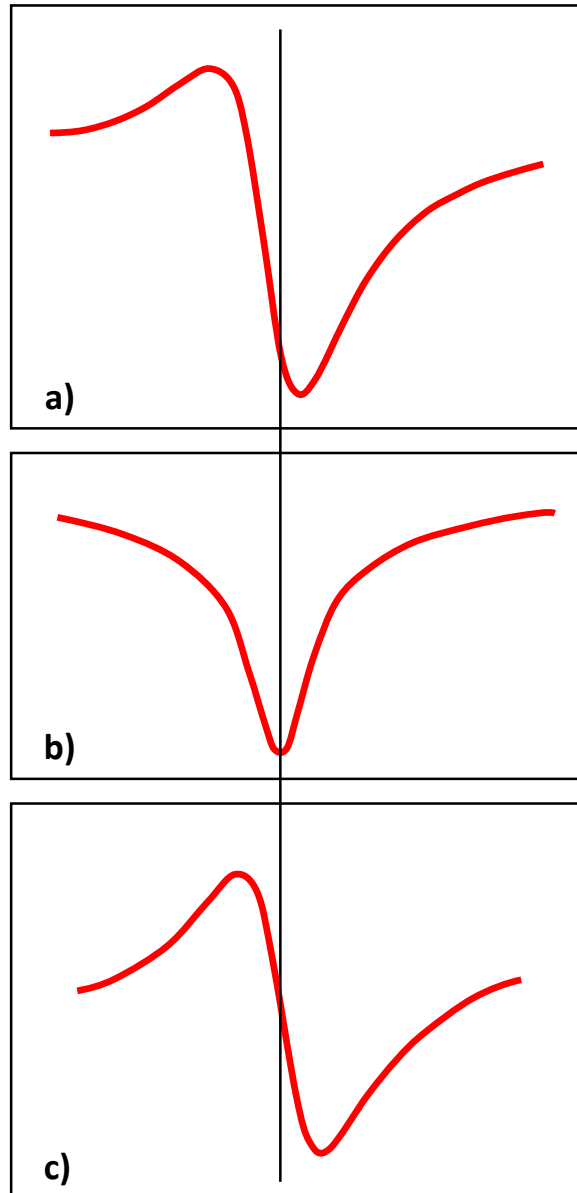
Figure 3.5: Effect of nonlinear absorption in CA ZS curve (a) and its exclusion by dividing it with OA ZS data (b) resulting in a symmetrical CA ZS curve (c)

The real part of third-order susceptibility is related to n_2 through the equation 3.17 and is expressed in $m^2 V^{-2}$. The third order nonlinear susceptibility, $\chi^{(3)}$ is calculated using the equation 3.18.

$$Re \; \chi^{(3)} = 2n_0^2 \varepsilon_0 c n_2 \qquad (3.17)$$

$$\chi^{(3)} = \left[\left(Re \; \chi^{(3)} \right)^2 + \left(Im \; \chi^{(3)} \right)^2 \right]^{1/2} \qquad (3.18)$$

Materials with high nonlinear refractive index are desirable for all-optical ultrafast switching, signal regeneration and high-speed demultiplexing applications. However, such materials have small bandgap energy and also often possess strong two-photon absorption. This may be unfavorable for certain applications in communication networks such as channel conversion.

3.2 TECHNIQUES USED IN ASE MEASUREMENT

3.2.1 THIN FILM PREPARATION

Thin films from solution processable organic materials can be prepared using various deposition techniques such as drop casting, dip coating, tape casting (doctor blade technique), spin coating, spray pyrolysis, inkjet printing and Langmuir-Blodgett technique. The thin film prepared in the present studies for fabrication of planar micro-cavity laser is by a simple drop casting technique.

3.2.1.1 Drop casting

Drop casting involves placing drops of solution on a pre-cleaned substrate and allowing solvent evaporation at either ambient or controlled environment. It is advisable to use highly cleaned substrates and to treat it with a basic NaOH solution, piranha solution, oxygen plasma or UV-Ozone to enhance the wetting properties of the substrate surface especially when water is used as the solvent. This technique is used in thin films where a thickness of hundreds of nanometer is required. The thickness is proportional to the

concentration of the solution. However, there is no provision to control the thickness of the film. The advantage of this technique, other than being simple, is that there is no wastage of material. The demerits are poor surface uniformity and evaporation time. However, evaporation rate can be controlled by increasing the temperature or by providing saturated solvent vapor atmosphere.

3.2.2 ASE EXPERIMENTAL SETUP

A typical setup, depicted in figure 3.6, for amplified spontaneous emission and lasing is discussed here. The thin film samples prepared by drop casting method was pumped by Nd:YAG laser from Spectra Physics (Quanta-Ray, LAB-190-10). The pulse duration and repetition rate of this laser are 7 ns and 10 Hz respectively. The frequency-doubled and -tripled were used to excite the thin film sample. The circular beam was transformed to a beam of stripe geometry with 1 mm x 10 mm dimensions using an aperture and cylindrical lens. A block was placed on the path of the beam to control the dimension of the beam. The thin film sample was secured firmly on a stand and was pumped transverse to the axis of the film. The emission was found emanating from the edges of the film and was collected with a 200 μm diameter fiber connected to Ocean Optics HR4000 spectrometer with a resolution of 0.21 nm. As we observed a highly directional and strong emission, no optics was used to collect the output emission to the fiber. Suitable neutral density filters were used at the pump beam and emission beam to vary the pump energy and to adjust the output intensity.

The output emission intensity was measured as a function of input pump energy, which helps us to determine the threshold energy and confirm spectral narrowing. The exponential gain coefficient was measured by Shaklee method by introducing a block to cut down the stripe geometry to 1 mm x 5 mm. The output intensities with an excitation stripe length of 10 mm and 5 mm were used to calculate gain coefficient using equation 5.4 discussed in section 5.2.
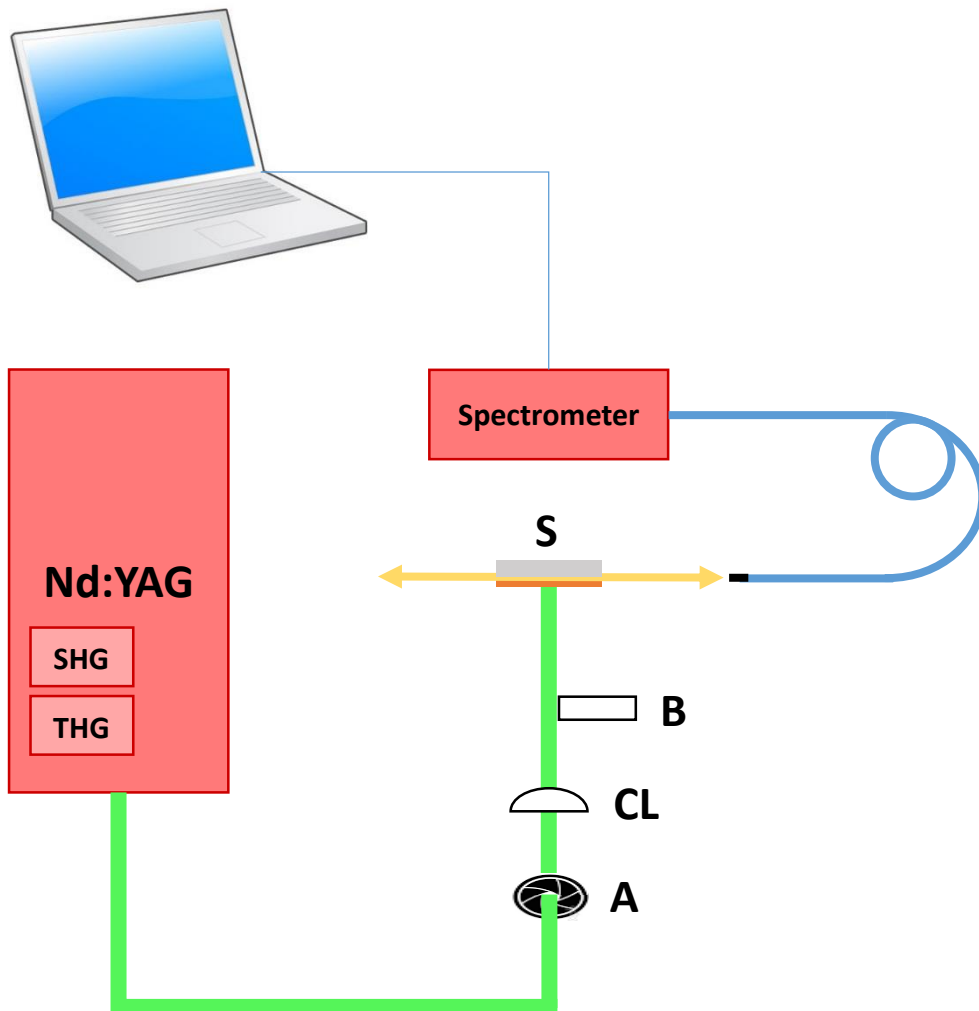
Figure 3.6: ASE experimental setup to measure emission intensity from planar microcavity.

3.3 TECHNIQUES USED IN ELECTROLUMINESCENT MEASUREMENT

3.3.1 FABRICATION OF LIGHT EMITTING DIODES

The ease of fabricating polymer light emitting diodes lies in using simple techniques for preparing thin films such as spin coating, inkjet printing etc. However for cathode deposition we used the thermal evaporation technique. The following subsections describe the fabrication techniques used in this investigation.

3.3.1.1 Spin coating

Spin coating is a common technique widely used in the preparation of thin films of few nanometers to hundred nanometers. A typical process involves dropping a few volume of the order of microliters of the material in a volatile liquid over the substrate, which is then spun at thousands of rpm. The centrifugal force on the material causes the solution to spread across the substrate finally causing it to splatter over the edge of the substrate. Further spinning at high speeds allows the volatile solvents to evaporate leaving the material uniformly spread over the entire substrate. The thickness and quality of the material depend on various parameters making the repeatability a common issue. The parameters are concentration of the material, volatility and viscosity of the solvent, volume of the material dropped, spin speed, acceleration and duration, surface tension, vapor pressure, temperature, local humidity, pretreatment of the substrate to enhance the wetting properties, etc. However, the thickness of the thin film of the same material can be varied by changing the concentration of the solution and spin speed. The solvent for the material is so chosen as to allow it to completely evaporate at the end of spinning process. Sometimes it may be required to anneal the coated substrate to ensure complete evaporation. The formation of good quality films also lies in sleight of the hand, acquired through practice.

There are two types of dispensing methods depending on the type of dispense of the material used. They are static and dynamic dispense. In static dispense, the material is first dropped on a static substrate so as to cover the whole substrate or at least on the active area. The substrate is first spun at lower speed ensuring complete coverage and then gradually ramping up to a higher speed to achieve required thickness. In dynamic

dispense, the substrate is first spun at the required speed and carefully dropping the material exactly at the center of the substrate. Both these dispense methods have their own advantages and applications.

We now discuss some of the troubleshooting of various spin coating defects

- Film too thick or too thin – Usually thickness can be varied by changing the spin speed and duration along with the concentration of the material.

- Air bubbles on the substrate – The use of proper and neat dispensing tip helps to avoid air bubbles in the material dispensed on the substrate.

- Nonuniformity –Vacuum warping of the thin substrate allows the solution to be controlled by the vacuum pulling resulting in undesired film quality. Nonuniformity also appears due to unintentional dropping of solution after dispensing or by contact made by the dispensing tip on the substrate.

- Hole in the middle – Sometimes the material is not coated on the center of the substrate. This appears when the solution is not dispensed exactly at the center of the substrate.

- Pin holes, Comet, Streaks or Flares – These irregularities appear due to any solids, such as impurities, aggregation/agglomeration or undissolved material present in the solution. It is better to ensure the use of clean pretreated substrates and completely soluble material by sonication and filtration of the solution.

- Radiative Striations – Striations[27,28] are radially oriented lines of thickness variation found on the surface of the coated thin film due to the instability in the surface tension during solvent evaporation. Although the exact reasons to these undesired effects are not well understood, addition of surfactants and co-solvents[29] can reduce striations and other coating effects.

- Uncoated areas – The uncoated areas appear if the dispensing volume is too low so as not to cover the entire substrate. Static dispensing might help in this aspect. Another reason is the non-wetting property of the substrate which can

be avoided by treatment with basic NaOH or Oxygen plasma or UV-Ozone to produce OH surface terminations.

The Manufacturer/ Model of the spin coater used in this study is Automation & Produktionstechnik GmbH, SPIN 150. The thickness of the polymer films were estimated by optical reflectance measurements using ThetaMetrisis (FR-pOrtable) with an accuracy of 1 nm.

3.3.1.2 Thermal evaporation

Thermal evaporation is a simple and common physical vapor deposition technique. A thermal evaporator uses an electric resistance heater to melt the target material (source) and evaporate it to be deposited on a substrate. This process is accomplished at a high vacuum of the order of 10^{-7} mbar. Such high vacuum is achieved by a turbo pump backed by a rotary pump. The water-cooled vacuum chamber consists of two sets of electrodes, one to carry lithium fluoride in an encased molybdenum boat and aluminum in a tungsten filament. The chamber also consists of a quartz crystal monitor (QCM) for precise measurement and control of deposition rate and thickness using a Digital Thickness Monitor (DTM). This measurement technique operates on the principle of piezoelectric effect. The RF voltage applied to the QCM allows it to resonate at its natural frequency. At constant temperature, the frequency remains stable unless the mass of the crystal varies. The mass of the QCM is increased by real-time deposition of the material, which leads to reduction of the resonant frequency and is electronically measured to compute real time deposition rate and thickness of the depositing thin film. For this computation, material density, its acoustic impedance and tooling factor are provided as deposition parameters to the DTM. The tooling factor was estimated by the equation 3.19 and was found to be 100 %.

$$Tooling\ factor = \left(\frac{D_{sc}}{D_{ss}}\right)^2 \times 100\ \% \qquad (3.19)$$

where, D_{sc} is the distance between source and crystal and D_{ss} is the distance between source and substrate

The deposition parameters for lithium fluoride and aluminum are listed below.

Table 3.1: Deposition parameters for digital thickness monitor

Material	Density (g/cm^3)	Acoustic Impedance (x 10^5 g cm^{-2} s^{-1})
Lithium Fluoride	2.64	11.41
Aluminum	2.70	8.17

The Manufacturer/Model of the thermal evaporator used to deposit lithium fluoride and aluminum is a 10 Volt, 200 Ampere system from Hind High Vacuum.

3.3.2 CHARACTERIZATION OF LIGHT EMITTING DIODES

All the light emitting diodes fabricated were tested by analyzing luminance-current density-voltage (L-J-V) characteristics and electroluminescence.

The luminance and current density were measured simultaneously by sweeping the voltage from 0 – 20 V using Keithley 2400 source measure unit (SMU). The current through the device was also measured using the source measure unit. For luminance measurement, we used a silicon amplified photodiode, PDA 36A-EC from Thor labs connected to a Keithley 2000 digital multimeter (DMM). The photodiode was calibrated using gallium nitride LED with an emission wavelength of 528 nm. The current through the device measured from SMU was converted to current density in mA/cm^2 and the photocurrent measured from DMM was converted to luminance in cd/m^2. The current density and luminance was measured simultaneously by connecting SMU and DMM to a computer through General Purpose Interface Bus, controlled by a LabView program.

The electroluminescence was measured using Ocean Optics HR4000 spectrometer with a resolution of 0.21 nm. All measurements were carried out at room temperature and in lab environment.

3.4 CONCLUSIONS

The experimental setup, techniques and calculation methods for nonlinear measurements and amplified spontaneous emission are discussed. The fabrication methods and characterization techniques of light emitting diodes are also described in detail.

REFERENCES

[1.] M S Bahae, A A Said, E W V Stryland, High-sensitivity, single-beam n_2 measurements, Opt. Lett., 14, 955, (1989)

[2.] M S Bahae, A A Said, T H Wei, D J Hagan, E W V Stryland, Sensitive measurement of optical nonlinearities using a single beam, IEEE J. Quant. Electron., 26, 760, (1990)

[3.] M S Bahae, M P Hasselbeck, Chapter 17: Third order optical nonlinearities, in Handbook of Optics: Volume IV - Optical Properties of Materials, Nonlinear Optics, Quantum Optics, M Bass, Eds., The McGraw-Hill Companies Inc., (2000)

[4.] E W V Stryland, M S Bahae, A A Said, D J Hagan, Characterization of nonlinear optical absorption and refraction, Prog. Crystal Growth and Charact., 27, 279, (1993)

[5.] E W V Stryland, M S Bahae, Z-scan measurements of optical nonlinearities, in Characterization Techniques and Tabulations for Organic Nonlinear Materials, M G Kuzyk, C W Dirk, Eds., Marcel Dekker, Inc., (1998)

[6.] T Cassano, R Tommasi, A P Meacham, M D Ward, Investigation of the excited-state absorption of a Ru dioxolene complex by the Z-scan technique, J. Chem. Phys., 122, 154507, (2005)

[7.] Y Gao, X Zhang, Y Li, H Liu, Y Wang, Q Chang, W Jiao, Y Song, Saturable absorption and reverse saturable absorption in platinum nanoparticles, Opt. Commun., 251, 429, (2005)

[8.] B Karthikeyan, M Anija, C S S Sandeep, T M M Nadeer, R Philip, Optical and nonlinear optical properties of copper nanocomposite glasses annealed near the glass softening temperature, Opt. Commun., 281, 2933, (2008)

[9.] F Li, P Lu, H Long, G Yang, Y Li, Q Zheng, Nonlinear absorption in CuPc-doped PMMA thin film in the femtosecond regime: Experimental and theoretical studies, Opt. Express, 16, 14571, (2008)

[10.] Y J Ma, J I Oh, D Q Zheng, W A Su, W Z Shen, Tunable nonlinear absorption of hydrogenated nanocrystalline silicon, Opt. Lett., 36, 3431, (2011)

[11.] B Nithyaja, H Misha, P Radhakrishnan, V P N Nampoori, Effect of deoxyribonucleic acid on nonlinear optical properties of Rhodamine 6G-polyvinyl alcohol solution, J. Appl. Phys., 109, 023110, (2011)

[12.] C P Singh, K S Bindra, S M Oak, Nonlinear optical studies in semiconductor-doped glasses under femtosecond pulse excitation, Pramana, 75, 1169, (2010)

[13.] G Sreekumar, P G L Frobel, C I Muneera, K Sathiyamoorthy, C Vijayan, C Mukherjee, Saturable and reverse saturable absorption and nonlinear refraction in nanoclustered Amido Black dye–polymer films under low power continuous wave He–Ne laser light excitation, J. Opt. A: Pure Appl. Opt., 11, 125204, (2009)

[14.] N K M N Srinivas, S V Rao, D N Rao, Saturable and reverse saturable absorption of Rhodamine B in methanol and water, J. Opt. Soc. Am. B, 20, 2470, (2003)

[15.] R Wang, Y Wang, D Han, C Zheng, J Leng, H Yang, Modeling and identification on nonlinear saturable and reverse-saturable absorptions of gold nanorods using femtosecond Z-scan technique, Chin. Opt. Lett., 10, 101902, (2012)

[16.] S A Joseph, Investigations of optical interaction process in certain photonic materials using Z-scan and thermal lens techniques, Ph. D thesis, Cochin University of Science and technology, (2006)

[17.] E W V Srtyland, Y Y Wu, D J Hagan, M J Soileau, K Mansour, Optical limiting with semiconductors, J. Opt. Soc. Am. B, 5, 1980, (1988)

[18.] A E Seigman, Chapter 4: Atomic rate equations, in Lasers, University Science Books, (1986)

[19.] M Samoc, A Samoc, B L Davies, Saturable absorption in poly(indenofluorene): a picket-fence polymer, Opt. Lett., 23, 1295, (1998)

[20.] Z Liu, Y Wang, X Zhang, Y Xu, Y Chen, J Tian, Nonlinear optical properties of graphene oxide in nanosecond and picosecond regimes, Appl. Phys. Lett., 94, 021902, (2009)

[21.] J Wang, B Gu, H T Wang, X W Ni, Z-scan analytical theory for material with saturable absorption and two-photon absorption, Opt. Commun., 283, 3525, (2010)

[22.] Y B Band, B Scharf, Engineering reverse saturable absorbers for desired wavelengths, Chem. phys. Lett., 127, 381, (1986)

[23.] S Mathew, A D Saran, B S Bhardwaj, S A Joseph, P Radhakrishnan, V P N Nampoori, C P G Vallabhan, J R Bellare, Size dependent optical properties of the CdSe-CdS core-shell quantum dots in the strong confinement regime, J. Appl. Phys., 111, 074312, (2012)

[24.] M Vivacqua, D Espinosa, A M F Neto, Application of the Z-scan technique to determine the optical Kerr coefficient and two-photon absorption coefficient of magnetite nanoparticles colloidal suspension, J. Appl. Phys., 111, 113509, (2012)

25. F Q Li, N Zong, F F Zhang, J Yang, F Yang, Q J Peng, D F Cui, J Y Zhang, X Y Wang, C T Chen, Z Y Xu, Investigations of third-order optical nonlinearity in $KBe_2BO_3F_2$ crystal by Z-scan, Appl. Phys. B, 108, 301, (2012)

26. R A Ganeev, A S Zakirov, G S Boltaev, R I Tugushev, T Usmanov, P K Khabibullaev, T W Kang, A A Saidov, Structural, optical, and nonlinear optical absorption/refraction studies of the manganese nanoparticles prepared by laser ablation in ethanol, Opt. Mater., 33, 419, (2011)

27. X D Min, X Orignac, R M Almeida, Striation-free, spin-coated sol-gel optical films, J. Am. Ceram. Soc., 78, 2254, (1995)

28. H Kozuka, Y Ishikawa, N Ashibe, Radiative striations of spin-coating films: Surface roughness measurement and in-situ observation, J. Sol-Gel Sci. Technol., 31, 245, (2004)

29. D P Birnie, Rational solvent selection strategies to combat striation formation during spin coating of thin films, J. Mater. Res., 16, 1145, (2001)

4

Effect of DNA on nonlinear optical properties of dyes

Abstract

The nonlinear optical property of DNA has been investigated earlier and had observed reverse saturable absorption due to two photon absorption property in DNA-poly vinyl alcohol system. An earlier report from our lab shows the addition of DNA flips the SA curve of Rhodamine 6G to RSA. We were interested to extend this investigation in other dyes with different nonlinear optical properties. Therefore, we chose two dyes, one that exhibits RSA and other with RSA-SA curves. This chapter presents the results on the nonlinear optical properties of these two dyes, namely PicoGreen (PG) and Triazatriangulenium (TATA) salt. This chapter also describes the effect of DNA on nonlinear optical properties of PG and TATA.

4.1 INTRODUCTION

Nonlinear optics is a branch of science that deals with the interaction of light with matter under circumstances such that the linear superposition principle is violated. Some of the nonlinear optical processes include second, third and higher optical harmonic generation; sum and difference frequency generation; optical parametric - generation, oscillation and amplification; optical Kerr effect; four-wave mixing; Raman amplification; phase conjugation; multiphoton absorption; etc. These processes lead to various applications such as harmonic generation in lasers, all-optical switching, optical data storage, optical power limiting in laser goggles, image processing and its manipulation, holography, optical solitons in optical fiber communication, electro-optical waveguides, parallel and spatial processing capabilities in optical computing and as sensitizers for photodynamic therapy in human body.

Although inorganic nonlinear optical crystals are well studied, organic nonlinear optical materials are not investigated in detail. New organic nonlinear optical materials are in great need due to their versatility and easy processability. Organic NLO materials can have non-resonant third-order nonlinear optical susceptibilities, $\chi^{(3)}$ of the order of 10^{-10} esu with femtosecond response times[1]. Delocalized π-electrons, which are free to travel along the conjugated structure or backbone of molecules and polymers, are the key factor in high nonlinearities in organic materials. Organic materials especially biomaterials that are biodegradable and biocompatible are the main topic of discussion in this thesis. The criteria for choosing optical nonlinear materials are those that present large nonlinear susceptibility, high conversion efficiency, wide transparent range, fast response and high optical damage threshold.

4.1.1 DNA AS A NONLINEAR OPTICAL MEDIUM

In this section, we discuss the earlier reports describing DNA as a biopolymer material exhibiting nonlinear optical properties.

Samoc et al.[2,3] employed Z-scan (ZS) technique using femtosecond pulses over a wide range of wavelengths to determine the complex cubic nonlinear susceptibility of aqueous DNA solution. Their results confirmed the possibility of moderate two-photon absorption in DNA at a wavelength of 530 nm, corresponding to twice the wavelength

of its main absorption peak at 260 nm. The nonlinear absorption coefficient of DNA aqueous solution was estimated to be 0.2 cm/GW. The nonlinear refractive index and real part of nonlinear susceptibility varied from 2 x 10^{-15} to 1 x 10^{-14} cm^2/W and 8 x 10^{-14} to 5 x 10^{-13} esu, respectively.

Sahraoui et al.[4] examined second and third harmonic generation from DNA complexes with NLO dyes. The second harmonic generation signals were very weak with effective $\chi^{(2)}$ values of 0.01 and 0.03 pmV^{-1}. However, they obtained significant third harmonic generation signals. The calculated third order nonlinear susceptibility values from dye-doped DNA were five times greater than the value reported using the dye only. This enhancement was attributed to the electronic interactions between π-systems of DNA and that of the dye molecules. Similar reports were published by Derkowska et al.[5] while using oxazolone derivatives with DNA complexes. The intercalation of dye molecules with DNA complexes promote charge migration and NLO activities.

Third-order optical response leads to third harmonic generation, two-photon absorption and intensity dependent refractive index, which are the basis for optical switching devices. Nithyaja et al.[6] described possible two-photon absorption at 532 nm corresponding to twice the wavelength of the absorption peak (260 nm) of DNA. The two-photon absorption coefficient, β was calculated using OA ZS experiment and was found to be 1.1 x 10^{-11} cm/W.

There are also reports of doping DNA with highly fluorescent dye such as, Rhodamine 6G (Rh6G) to measure the change in the nonlinear optical property of the dye using frequency doubled Nd:YAG laser in nanosecond and femtosecond regimes. Our group[6] had reported OA ZS experiments performed on Rh6G-PVA solution to observe SA response with TPA coefficient of -237 x 10^{-12} cm/W. Switching behavior from SA to RSA was observed on addition of DNA. The TPA coefficient was observed to change to a positive value of 540 x 10^{-12} cm/W. In another work from our group, Sreeja et al.[7] reported enhancement in the negative nonlinear refractive index by two orders of magnitude from Rh6G-PVA film on addition of DNA. Dancus et al.[8] compared ZS curves from Rhodamine B using continuous wave (slow) and femtosecond (fast) pump pulses.

From the above reported values, it could be concluded that DNA is a moderately efficient nonlinear photonic material similar to typical organic polymers. It is therefore our interest, to study the effect of DNA in various nonlinear optical dyes possessing different nonlinear mechanism.

4.1.2 PICOGREEN DYE

PicoGreen (PG) is a fluorescent dye used in biomedical research for DNA quantitation assays[9]. PG belongs to the cyanine family of fluorescent dyes which is commonly employed as a quantitation reagent used to probe and quantify nucleic acids such as double-stranded DNA (dsDNA), single-stranded DNA (ssDNA) and ribonucleic acid (RNA). This assay, as described in various manuals and protocols[10-12], is a common procedure and has gained importance as it is more sensitive than UV absorbance method. This stain can selectively bind to dsDNA with increased sensitivity (with a minimum detection range of 25 pg/ml)[13] than ssDNA or RNA. PG does not fluoresce in its pristine form, but on binding/ intercalation with double stranded DNA, the fluorescence is enhanced by 1000 fold or more. This enhancement has been exploited in DNA quantitation in solution and gels, real-time PCR, cell chromosome staining and other techniques[14]. Dragan et al.[15] have recently proposed the possible modes of binding PG dye to DNA and explained the change in quantum yield and excited state lifetime. In their paper, it was detailed that the absence of fluorescence was due to dynamic quenching process via collisional interactions and subsequent dequenching on intercalation with DNA molecules has improved the fluorescence quantum yield and excited state lifetime dramatically.

PG (IUPAC: 2- [N-bis-(3-dimethylaminopropyl)-amino]-4-[2,3-dihydro-3-methyl-(benzo-1,3-thiazol-2-yl)-methylidene]-1-phenyl-quinolinium)[16] with its molecular formula $C_{34}H_{42}N_5S$ has an average mass of 552.794983 Da[17]. The molecular structure of the dye has been determined by H. Zipper et al [Zipper, 2004] and is shown in figure 4.1. The excited state lifetime of PG is estimated to be 4 ± 3 ps, which is increased to 4.4 ± 0.01 ns on intercalation with DNA[15]. The pristine form of PG has a fluorescence quantum yield of 0.0006 which was improved by more than 1000 fold to 0.64, on intercalation with dsDNA and 0.30, on intercalation with ssDNA[13].
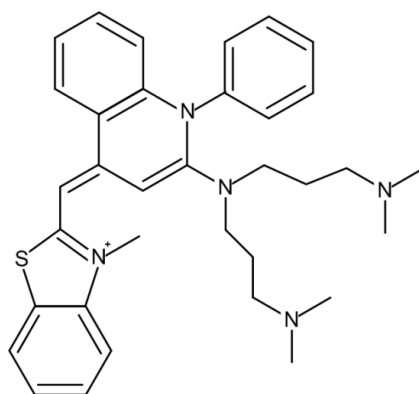
Figure 4.1: Molecular structure of PG dye

PG was made available from Invitrogen, USA. Commercially available PG reagent is in liquid form with the solvent being dimethyl sulfoxide (DMSO). The approximate concentration of the reagent was calculated to be 2.75 x 10^{-5} mol/L based on the molar extinction coefficient reported by Singer et al.[9], as 70,000 $cm^{-1}M^{-1}$. PG was stored away from light as it is susceptible to photo-bleaching due to prolonged exposure to room light. Hence, the dye was immediately subjected to investigation once removed from storage.

The linear normalized absorption spectrum of PG diluted in DMSO is shown in figure 4.2(a). The absorption spectra has a band in the visible region around 440 nm to 540 nm with its peak at 499 nm. The normalized fluorescence of PG is depicted in figure 4.2(b). The intrinsic fluorescence of free PG dye was negligible when excited at 500 nm. This is due to the dynamic quenching process via intramolecular collisional interaction, which reduces the excited-state lifetime of the order of picoseconds. When dsDNA is added to the dye, the fluorescence is enhanced many-fold with its emission peak at 535 nm as clearly seen in figure 4.2(b). This is due to the dye molecules being trapped in the groves of the DNA, which inhibits collisional interactions, resulting in an excited-state lifetime of the order of nanoseconds[15].
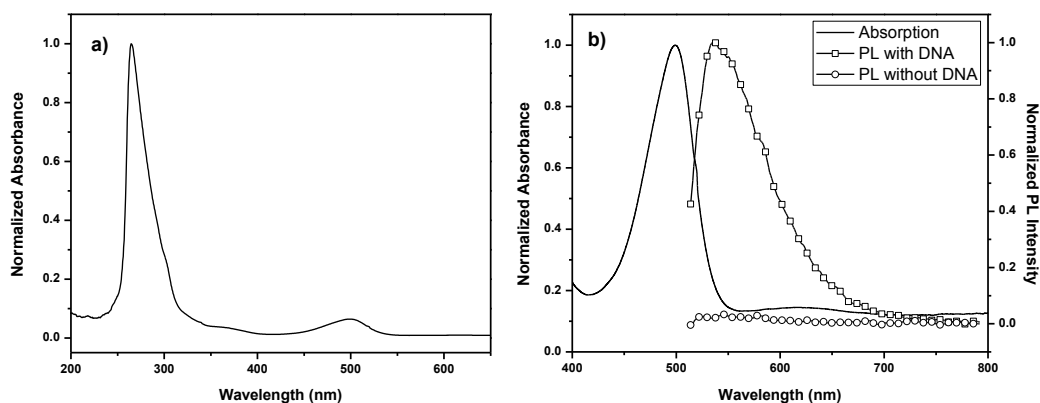
Figure 4.2: (a) Normalized linear absorption spectrum of PG dye and (b) normalized linear absorption spectra of PG:DNA complex and normalized fluorescence spectrum with and without salmon extracted dsDNA in PG dye

4.1.3 TRIAZATRIANGULENIUM SALT

Triazatriangulenium salt was synthesized at Photosciences and Photonics laboratory at Council of Scientific and Industrial Research - National Institute for Interdisciplinary Science and Technology, Thiruvananthapuram. The preparation method was referred from Laursen et al.[18]. Aqueous tetrafluoroboric acid, HBF_4 (2.5 ml) is added to tris (2,6-dimethoxyphenyl) carbinol[19] in ethanol (100 ml), to which diethyl ether and petroleum ether each of 100 ml was added. The precipitate that is formed is filtered and washed with diethyl ether. The obtained greenish black crystals, tris(2,6-dimethoxyphenyl)carbenium tetrafluoroborate, were prepared in N-methyl-2-pyrrolidone at a concentration of 200 mg/ml. n-octylamine was added to the above solution and the reaction mixture was refluxed for 24 h. After cooling, diethyl ether was added to precipitate the crystals. Recrystallization from methanol yielded thin needle-like orange-red crystals of triazatriangulenium salt (4,8,12-Tri-n-octyl-4,8,12-triazatriangulenium tetrafluoroborate). The molecular structure of the salt is shown in figure 4.3.
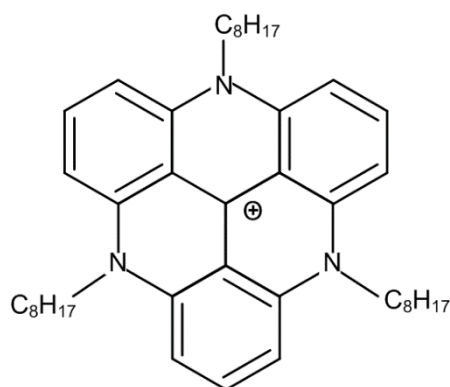
Figure 4.3: Molecular structure of synthesized TATA salt

The normalized absorption spectra of the TATA salt dissolved in acetonitrile is presented in figure 4.4(a). The absorption of the dye in the visible region extends from 450 nm to 550 nm with its dominant peak at 523 nm and a shoulder at 490 nm. The normalized fluorescence spectra of TATA salt was recorded while exciting at 523 nm. Figure 4.4(b) presents the fluorescence spectrum ranging from 540 nm to 640 nm with a peak at 564 nm. The observed spectra are in accordance with the earlier reports[18,20]. On addition of DNA, we observed that the fluorescence peak was shifted from 564 nm to the 591 nm with a considerable enhancement in fluorescence intensity.

Figure 4.5(a) and 4.5(b) give a detailed picture on the enhancement of fluorescence from TATA salt. Aqueous solution of DNA at a concentration 8.5 mg/ml was added to TATA salt in microliters. At low concentration of DNA, a steep decrease in fluorescence intensity is observed while it enhances above 50 μl of DNA concentration, as seen in figure 4.5(b). It is also noted that beyond this DNA concentration, there is a sudden red-shift in the peak fluorescence intensity followed by a gradual blue shift at a higher concentration. The red-shift and decrease in fluorescence intensity are the usual observations in fluorescence characteristics of dyes as a function of its concentration due to the nonradiative relaxation effect. At low values of DNA concentration, enhancement in the collisional interactions between dye molecules and DNA reduces the fluorescence intensity and the observed red-shift in the fluorescence spectra. As the DNA concentration is increased, the intercalation causes the dye

molecues to occupy the groves in the DNA structure, thereby reducing the nonradiative relaxation resulting in enhanced fluorescence emission.
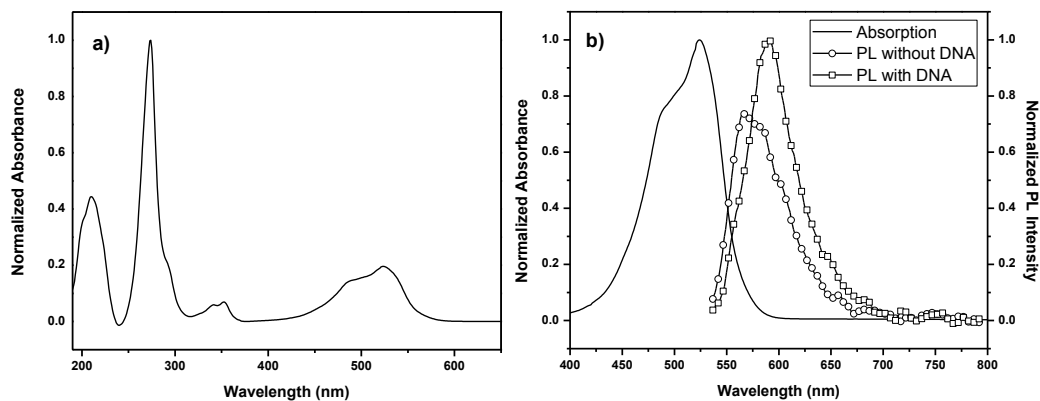

Figure 4.4: (a) Normalized linear absorption spectrum of TATA salt and (b) normalized linear absorption spectra of TATA:DNA complex and normalized fluorescence spectrum with and without salmon extracted dsDNA in TATA salt
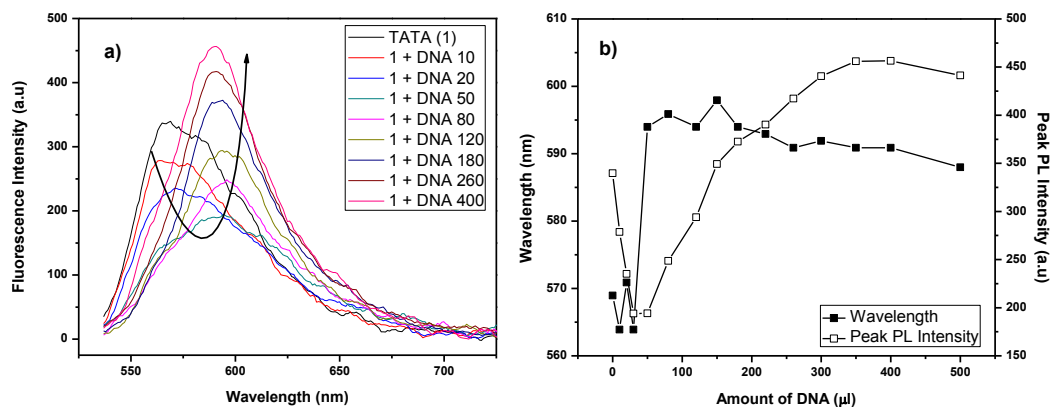

Figure 4.5: (a) Emission spectra of TATA salt at different concentration of DNA (b) Variation in emission wavelength and peak PL intensity as a function of DNA concentration

4.2 NONLINEAR OPTICAL PROPERTIES OF PICOGREEN DYE

4.2.1 NONLINEAR ABSORPTION COEFFICIENT

The original concentration of PG dye, as supplied by Invitrogen was maintained during ZS experiments. The experimental setup and data analysis described by Bahae et al.[21] are discussed in detail in section 3.1. Figure 4.6 shows the OA ZS curve of the dye at 532 nm with an incident intensity of 0.1 GW/cm^2. The picosecond lifetime of the excited state of the dye inhibits saturation at lower intensities, however at higher intensity, two photon absorption is possible due to the linear absorption peak at 260 nm. Hence an optical limiting type (reverse saturable absorption, RSA) behavior was observed with nonlinear absorption coefficient, β at 116.15 cm/GW. The experimental data was analyzed using two-photon absorption model represented by the equation 3.2. A decrease in nonlinear absorption coefficient with increased intensity of the incident laser beam was observed and the results are presented in table 4.1.
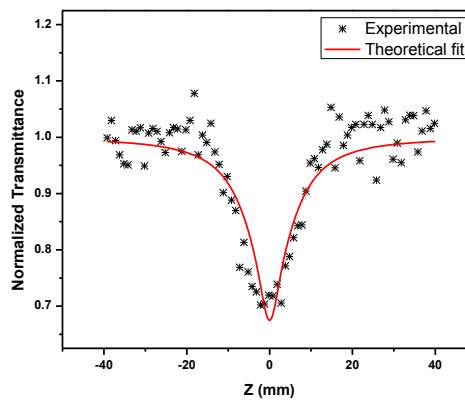

Figure 4.6: OA ZS curve of PG at an incident intensity of 0.1 GW/cm^2

Table 4.1: Key parameters related to OA ZS experiments of PG dye

Intensity, I_o (GW/cm^2)	Nonlinear absorption coefficient, β (cm/GW)	Optical limiting threshold, OL_{th} (MW/cm^2)
0.10	116.15	36.2
0.21	72.86	63.0
0.32	50.29	77.6

To confirm the role of dye in the optical limiting type behavior of the PG solution, OA ZS was performed on both pure solvent and the dye solution. As shown in figure 4.7(a), no significant nonlinear absorption was found for DMSO while PG solution showed strong nonlinear absorption with a TPA coefficient, β estimated to be 40 cm/GW at an incident laser intensity of 0.35 GW/cm^2. This confirms that the optical limiting behavior is due to the dye only.

One of the important exploits of RSA behavior in materials is its application as an optical limiter. In principle, an optical limiter is opaque to high input intensities while transparent at low light intensities. An important term in optical limiting
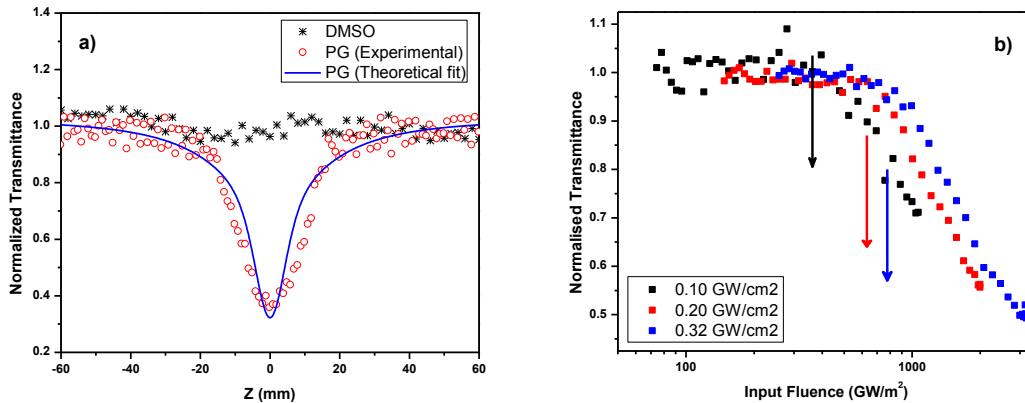

Figure 4.7: (a) Comparison of OA ZS curve of DMSO solvent and PG dye solution
(b) Optical limiting response of PG dye at various input intensities.

(OL) measurement is the limiting threshold. An ideal optical limiting material should have low limiting threshold. In the present studies, we have used OA data to extract the limiting threshold by expressing abscissa in terms of input fluence using equation 3.5 described in section 3.1.2.

Figure 4.7(b) shows the OL response of PG dye at different incident intensities and the limiting threshold was observed at 36.2 MW/cm^2 at an incident intensity of 0.1 GW/cm^2. As the incident intensity was increased, the limiting threshold was found to increase. The continuous line with an arrow in the figure indicates the approximate threshold value (OL_{th}) which is determined graphically as the intersection between the linear and nonlinear part of the OL curve. The OL thresholds at various intensities are presented in table 4.1.

4.2.2 THIRD-ORDER NONLINEAR OPTICAL SUSCEPTIBILITY

When an aperture of 20 % linear transmittance was introduced in the far field of the sample (CA ZS), the resulting transmittance exhibited self-defocusing effect with an asymmetrical peak-valley curve as shown in figure 4.8(b). This suppressed peak and enhanced valley was due to the fact that the CA measurement is sensitive to both nonlinear absorption and nonlinear refraction. Some materials such as ZnSe and BaF$_2$ showed similar asymmetrical curve as reported by Stryland et al.[22,23]. Shahriari et al have also reported a similar ZS results in silver nanofluid[24,25]. By dividing the CA data (figure 4.8(b)) by OA data (figure 4.8(a)), the ZS curve due to nonlinear refraction alone could be obtained. Figure 4.9 shows the results of dividing the CA data by the OA data at an incident intensity of 0.3 GW/cm^2.

The linear refractive index, n_0 of the PG dye was measured using Abbe refractometer and was found to be 1.46. The calculated values of nonlinear refractive index, n_2 and third-order nonlinear susceptibility, $|\chi^{(3)}|$ using equation 3.11 and 3.18 respectively, are given in table 4.2. We observed an intensity dependent third-order susceptibility.
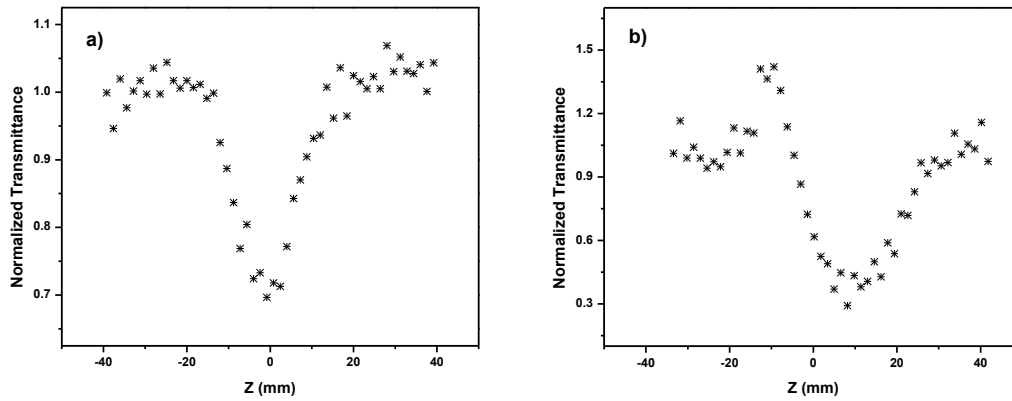
Figure 4.8: (a) OA ZS curve and (b) CA ZS curve of PG dye at an incident intensity of 0.2 GW/cm^2
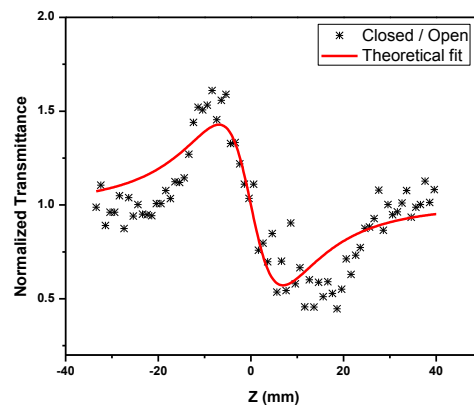

Figure 4.9: Result of division of CA ZS curve (4.8 (b)) by OA ZS curve (4.8(a))

Table 4.2: Key parameters related to CA ZS experiments of PG dye

Intensity, I_o (GW/cm^2)	Nonlinear refractive index, n_2 (cm^2/W) x10^{-12}	Third order susceptibility, $|\chi^{(3)}|$ (esu) x10^{-11}
0.1	- 1.6	9.3
0.2	- 0.9	5.2
0.3	- 0.5	3.2

Some cyanine dyes such as PC (1,1' -diethyl- 3,3,3',3' -tetramethyl-indolepentylmethinecyanine iodine) and various other cyanine (polymethine) dyes which possess considerable nonlinear absorption coefficient, nonlinear refractive indices and third order susceptibilities have been reported. Research is targeted towards identifying new materials with higher nonlinear refractive index due to their possible applications as optical limiters. In this study we introduced material, PG dye that possess a nonlinear absorption coefficient that is two orders of magnitude higher than the polymethine dyes[26] and a nonlinear refractive index and third order nonlinear susceptibilities of approximately two orders of magnitude higher than the PC solution[27].

4.3 EFFECT OF DNA ON NONLINEAR OPTICAL PROPERTIES OF PICOGREEN DYE

As discussed in section 4.1.1, DNA exhibited strong nonlinear absorption due to two-photon absorption. To study the role of DNA on the nonlinear optical property of the PG solution, we performed OA ZS studies on PG with and without DNA. Figure 4.10(a) shows the plot related to OA ZS experiment of the dye and dye intercalated DNA at an incident intensity of $0.10\,GW/cm^2$. As described earlier, the free dye showed reverse saturable absorption (RSA) behavior. At lower concentration of DNA in PG solution, it was observed that the transmitted intensity increased at the focal point relative to that in PG solution alone. As the concentration of DNA is increased, the onset of SA behavior is observed away from the focal point. The saturable absorption effect away from the focus is due to the increased excited-state lifetime caused by evading intramolecular collision by intercalation of dye molecules with DNA. A dip in the SA behavior near the focal point is observed indicating RSA at higher intensities due to the excess dye molecules that are not trapped in the groves of the DNA. It can be noted that the RSA valley decreases with increase in concentration of DNA. This indicates the presence of more than one type of nonlinear optical processes taking place in the DNA:dye complex medium. Such multiple nonlinear absorption processes were reported by various groups in different materials[28-34]. Nithyaja et al.[6] had reported a flip of SA to RSA in Rh6G as DNA concentration of DNA was increased. However, in the

present case, the flip was from RSA to SA as the concentration of DNA was increased. Figure 4.10(b) and 4.10(c) show the OA ZS experiments performed at an incident intensity of 0.23 GW/cm^2 and 0.32 GW/cm^2 respectively. Though the SA effect (the humps that flank the central RSA) increased with the concentration of DNA, it decreased with increase in the overall incident intensity at the focus. From the figure 4.10, it could also be observed that the onset of nonlinear effect starts at lower intensities as the concentration of DNA is increased.
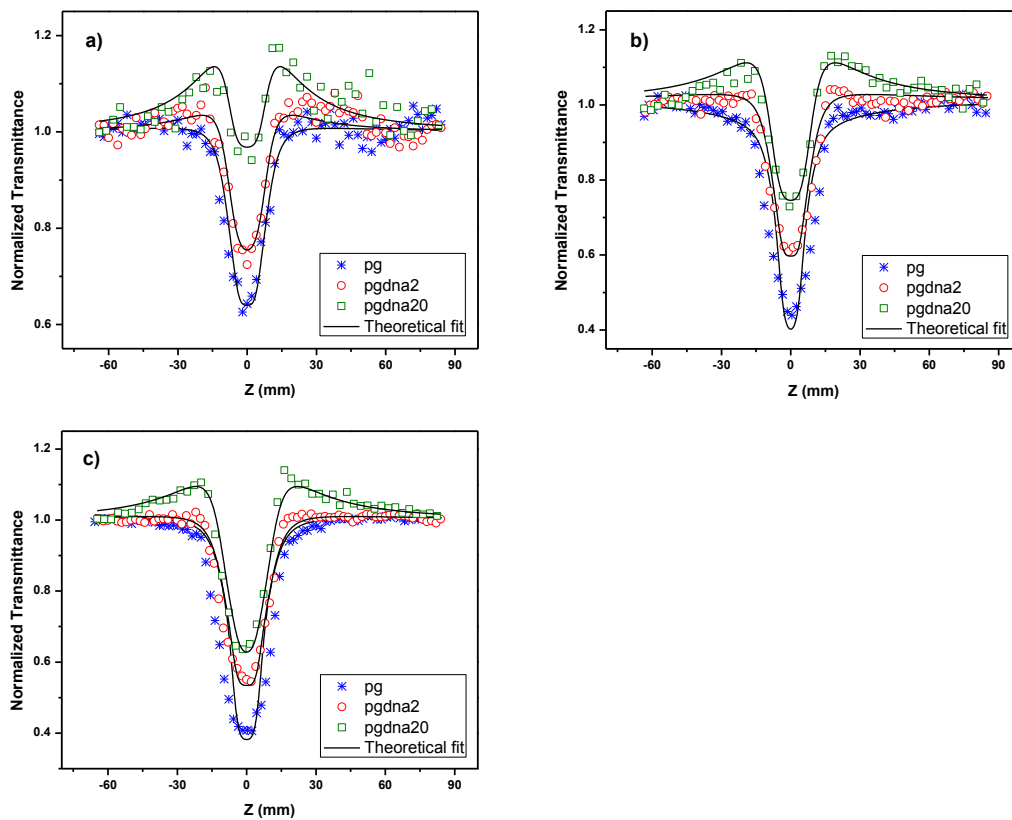

Figure 4.10: OA ZS curve of PG (pg) and PG dye intercalated DNA at a concentration of 2 g/L (pgdna2) and 20 g/L (pgdna20) at an incident intensity of (a) 0.10 GW/cm^2 (b) 0.23 GW/cm^2 and (c) 0.32 GW/cm^2.

Theoretical fit for the above experimental plots was obtained by using two-photon absorption geometry described by equation 3.6 and 3.9, from which I_s and β are calculated. The values of these parameters are presented in Table 4.3. It could be observed that the TPA coefficient, β of the PG dye varied from 113.05 cm/GW at 0.10 GW/cm^2 to 42.94 cm/GW at 0.32 GW/cm^2. This was in agreement with our earlier results presented in table 4.1. At 0.10 GW/cm^2, β reduced to 51.17 cm/GW on addition of DNA and remained constant as the incident intensity was increased. It could be found that the TPA coefficient of the dye decreased as the incident intensity was increased, but for the dye intercalated DNA the coefficient remained constant with respect to incident intensity.

Table 4.3: Key parameters related to OA ZS experiments of PG and PG:DNA complex

Sample	Incident Intensity, I_o (GW/cm^2)	Nonlinear absorption coefficient, β (cm/GW)	Saturation Intensity, I_s (MW/cm^2)
pg*		113.05	25.46
pgdna2*	0.10	98.27	27.74
pgdna20*		51.17	62.69
pg*		52.28	55.07
pgdna2*	0.23	52.96	51.48
pgdna20*		51.79	61.94
pg*		42.94	67.05
pgdna2*	0.32	40.29	67.67
pgdna20*		48.66	65.92

* **pg – PicoGreen dye; pgdna2 – PicoGreen doped in 2g/L DNA; pgdna20 – PicoGreen doped in 20g/L DNA**
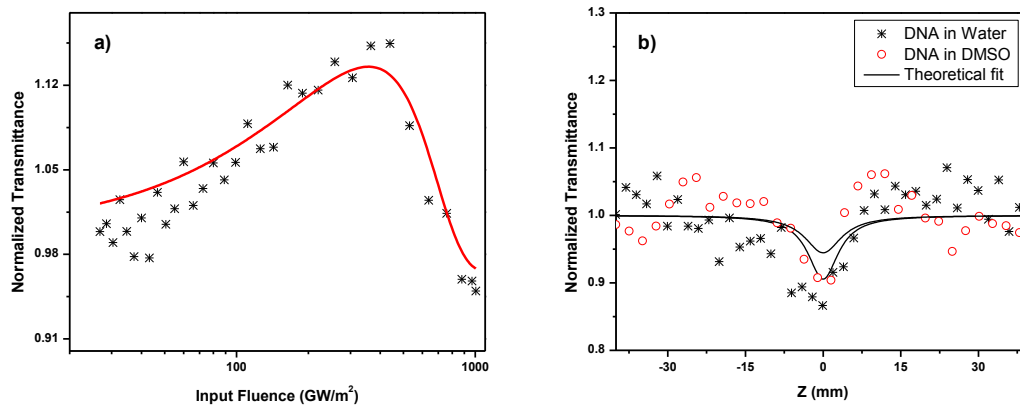
Figure 4.11: (a) Normalized transmittance of PG at an incident intensity of 0.10 GW/cm^2 as a function of input fluence (b) Comparison of OA ZS curve of DNA in distilled water and DMSO

In figure 4.11(a), the normalized transmittance is plotted against input intensity. This data was extracted from the OA ZS curve of DNA (20 g/L) doped in PG dye at an input intensity of 0.10 GW/cm2 at the focus. The displacement of the sample from the focus, z in the ZS plot is converted to input intensity using the formula described by equation 3.5. From this plot, it could be understood that at lower input intensities the transmittance increased while above a critical value (37.5 MW/cm^2) the transmittance decreased. This effect could be exploited in many dye-based optoelectronic devices such as an optical switch. With the variation of transmitted intensity observed in DNA doped in dye, it is important to check the effect of DNA on the solvent. Aqueous DNA solution (15 g/L) was prepared by dissolving DNA in both single distilled water and DMSO and were subjected to OA ZS. Figure 4.11(b) shows the RSA behavior of DNA in both the solvents. From the observations, it has been found that there was only a minor change in their nonlinear absorption. This might be due to a slight difference in the concentration of DNA.

4.4 NONLINEAR OPTICAL PROPERTIES OF TRIAZATRIANGULENIUM SALT

4.4.1 NONLINEAR ABSORPTION COEFFICIENT

OA ZS experiments were performed on the synthesized TATA salt detailed in section 4.1.3. We used the same experimental setup and laser source as used to measure the nonlinear optical properties of PG dye. Both PG dye and TATA salt have significant optical absorption at 266 nm, so both shall exhibit two-photon absorption induced nonlinear optical effect. The OA ZS curve of TATA salt at a concentration 1.00 mg/ml at an incident intensity of 0.29 GW/cm^2 is shown in figure 4.12. We observed an RSA type behavior near the focus, flanked by SA behavior away from the focus. The SA and RSA behavior is due to the single photon absorption and two photon absorption at 532 nm, respectively. Initially the single photon absorption saturates the excited state of the dye, and as the intensity increases the two photon absorption dominates the former process resulting in a RSA valley. Theoretical curve fit was performed on the obtained experimental data using two-photon absorption model and its coefficient, β was calculated using the equation 3.6 and 3.9. This plot was similar to OA ZS curve of PG dye intercalated in DNA. Similar results have been reported in various materials as discussed in section 4.3. To understand the nature of the nonlinear effect of salt, OA ZS was performed at various concentrations and incident intensities.

Figure 4.13(a) depicts the OA ZS curve of TATA salt at a concentration of 0.23 mg/ml by varying the incident intensity of laser from 0.11 GW/cm^2 to 0.34 GW/cm^2. The nonlinear absorption coefficient was calculated using equation 3.9 and presented in table 4.4. The TPA coefficient for the salt at a concentration of 1 mg/ml at an incident intensity of 0.11 GW/cm^2 was estimated to be 811 cm/GW. Figure 4.13(b) shows the OA ZS curve of TATA salt by varying the concentration of the salt viz. 0.23 mg/ml, 0.55 mg/ml and 1.00 mg/ml, at an incident laser intensity of 0.30 GW/cm^2. It was found that as the concentration of the dye was increased the transmitted light across the intensity profile also increased. It could be observed that there is a considerable increase in the TPA coefficient, β as the concentration of the salt is increased. It could also be perceived that the TATA salt exhibited intensity dependent nonlinear absorption coefficient at higher concentration of the salt (1 mg/ml). However at low

concentrations, the TPA coefficient remained constant with varying incident intensities.
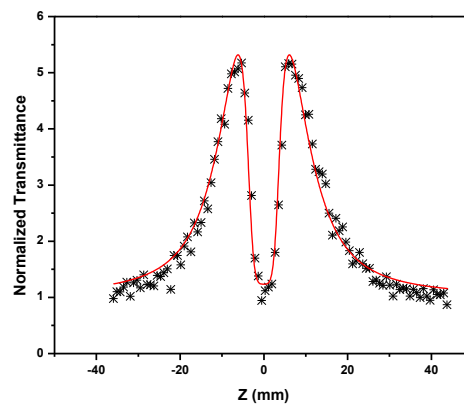

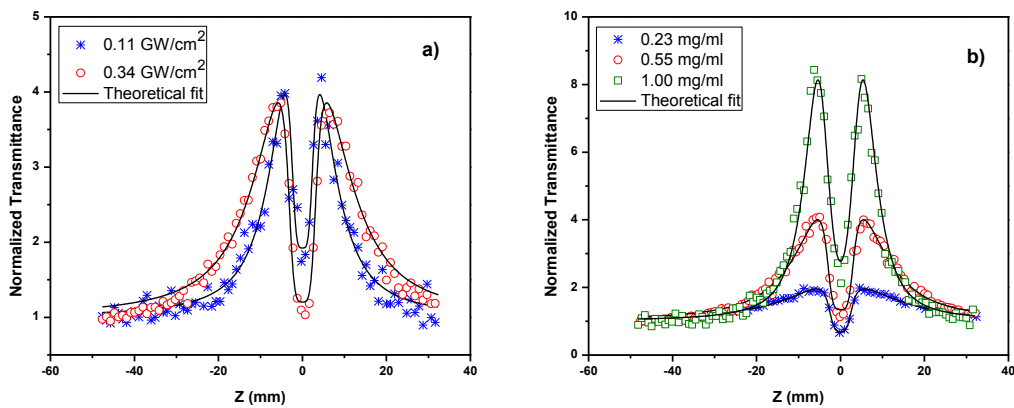Figure 4.12: OA ZS curve of 1.00 mg/ml concentrated TATA salt in acetonitrile at an incident intensity of 0.29 GW/cm^2

Figure 4.13: OA ZS curve of TATA salt (a) at different incident intensities at a concentration of 0.23 mg/ml and (b) at different concentration of the salt at an incident intensity of 0.30 GW/cm^2

4.4.2 THIRD-ORDER NONLINEAR SUSCEPTIBILITY

CA ZS experiments revealed nonlinear refractive index and third order nonlinear susceptibility of the TATA salt. With a 10 % linearly transmitting aperture, the ZS curve plot showed SA effect away from the focus (figure 4.14(b)), like in OA ZS curve (figure 4.14(a)). This is due to the fact that the measurement was sensitive to both nonlinear refraction and nonlinear absorption. To cancel this effect, the data was subjected to similar treatment as in PG dye case. The resulting curve was an asymmetrical peak-valley as shown in figure 4.15 which indicates a negative refractive index. Equation 3.12 which involves two-photon absorption term and optical Kerr effect term was used to fit the experimental data. The best pair of values of β and n_2 were used that represents both the results from the OA and CA ZS curves simultaneously.

The linear refractive index, n_0 of the TATA salt was measured using Abbe refractometer and was found to be 1.34. The calculated values of nonlinear absorption coefficient, β and nonlinear refractive index, n_2 are depicted in table 4.4. The third-order nonlinear susceptibility, $\chi^{(3)}$ was calculated from β and n_2 using the equation 3.10, 3.17 and 3.18 described in chapter 3, and was found to be 5.31×10^{-18} m^2/V^2 for a salt concentration of 1 mg/ml at 0.11 GW/cm^2 incident intensity. It is clear from the table 4.4, that the nonlinear effect of TATA salt enhances with the increase in the salt concentration at low incident intensities.
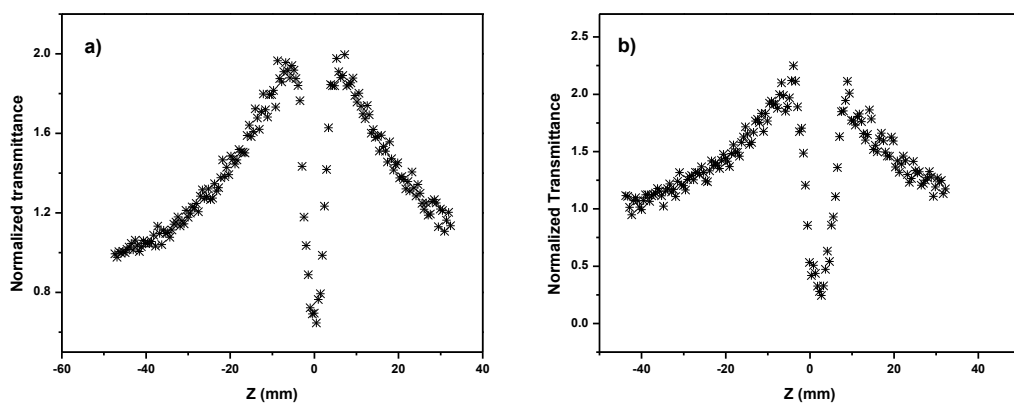

Figure 4.14: (a) OA ZS curve and (b) CA ZS curve of TATA salt at a concentration of 0.23 mg/ml at an incident intensity of 0.11 GW/cm^2
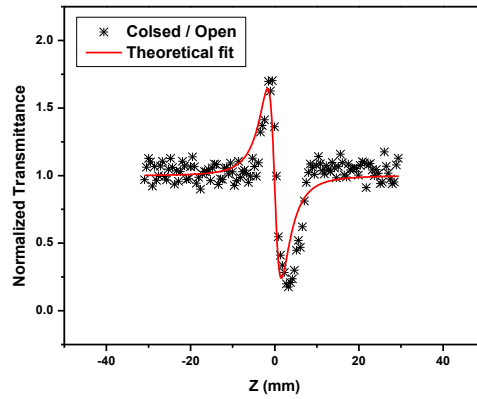
Figure 4.15: Result of division of CA ZS curve (4.14(b)) by OA ZS curve (4.14(a))

Table 4.4: Key parameters related to ZS experiments of TATA salt

TATA salt concentration, C (mg/ml)	Incident Intensity, I_o (GW/cm^2)	Nonlinear absorption coefficient, β (cm/GW)	Nonlinear refractive index, n_2 (cm^2/W) x 10^{-12}
0.23		74.84	-2.321
0.55	0.11	101.70	-4.279
1.00		810.89	-5.713
0.23		75.23	-1.324
0.55	0.30	55.55	-0.982
1.00		370.83	-0.642
0.23		71.54	-1.424
0.55	0.34	57.09	-1.423
1.00		333.30	-0.611

4.5 EFFECT OF DNA ON NONLINEAR OPTICAL PROPERTIES OF TRIAZATRIANGULENIUM SALT

To study the nature of nonlinearity in TATA salt doped in DNA, we chose the following weight ratios of TATA salt with DNA viz. 1:0, 1:5, 1:10 and 1:20. We fixed the concentration of TATA salt in the final solution at 0.5 mg/ml.

To prepare 1:10 sample, 25 μl of 20 mg/ml of DNA aqueous solution is made to 50 μl by adding water and then added to 200 μl of 1 mg/ml TATA salt solution. Similarly, for 1:0, 1:5 and 1:20, 0 μl, 10 μl and 50 μl of DNA solution is made up to 50 μl by adding water respectively. The OA ZS experiments were performed on these samples at an incident intensity 0.25 GW/cm^2. It could be observed from the figure 4.16, that the SA peak reduced as the concentration of DNA is increased. The TPA coefficient, β was calculated by theoretically fitting the experimental data using equation 3.6 and 3.9. Table 4.5 lists the TPA coefficient of all the samples. Similar to the PG:DNA case, the TPA coefficient reduces as DNA concentration increases.
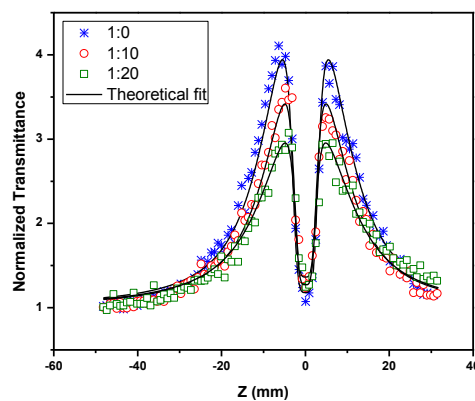

Figure 4.16: OA ZS curve of TATA salt and TATA salt doped in DNA of varying concentrations viz. 100 mg/ml and 200 mg/ml at an incident intensity of 0.25 GW/cm^2

Table 4.5: Key parameters related to OA ZS experiments of TATA salt and
TATA:DNA complex with the salt concentration of 1 mg/ml

DNA Conc., C (mg/ml)	Incident Intensity, I_o (GW/cm^2)	Nonlinear absorption coefficient, β (cm/GW)
0		110.25
50		85.35
100	0.25	82.07
200		78.69

4.6 CONCLUSIONS

We investigated two different dyes, PicoGreen and Triazatriangulenium salt, for their
nonlinear optical property using a simple and efficient transmission ZS technique to
measure nonlinear absorption coefficient and nonlinear refractive index. The TATA
salt was synthesized by reflux method while the PG dye was procured from Invitrogen,
USA. The dyes were so chosen that it has an absorption in the UV (260 nm) region and
to possess fluorescence enhancement by doping it in DNA aqueous solution. Both the
dyes show enormous enhancement in fluorescence in the presence of DNA. The
absorption in the UV region shall enable two-photon absorption at 532 nm. We also
chose the dyes to have different nonlinear property such as an RSA curve (PG) and an
RSA in SA flip (TATA) to compare it with the earlier reports from Rhodamine dye
with an SA curve. The nonlinear absorption coefficients of PG and TATA were
calculated using the two-photon model and was found to have a value of the order of
~100 cm/GW and ~800 cm/GW, respectively. The nonlinear refractive indices of both
the dyes were calculated and found to be of the order of 10^{-12} cm^2/W. In comparison
with the materials discussed in Bahae et al.[35], it could be concluded that PG and TATA
would be desirable for all-optical switching applications.

On introduction of DNA to these dyes, the samples exhibited a decrease in nonlinear absorption coefficient. These results were similar to the one reported by Nithyaja et al.[36], where DNA was used as a stabilizing agent in the preparation of silver nanoparticles. It could be also observed that on increasing the concentration of DNA, the SA effect was dominant in PG dye while the SA effect reduced in TATA salt. From the ZS data presented in this chapter, it could be concluded that DNA plays an important role in the nonlinear behavior of PG and TATA dyes. The multiple nonlinear mechanisms involved in the dyes in the presence of DNA could be exploited in developing various photonic devices, especially in optical switching.

REFERENCES

1. R W Boyd, G L Fischer, Nonlinear optical materials, in Encyclopedia of Materials: Science and Technology, Elsevier, p. 6237, (2001)

2. M Samoc, A Samoc, Grote J G, Complex nonlinear refractive index of DNA, Chem. Phys. Lett., 431, 132, (2006)

3. A Samoc, M Samoc, J G Grote, A Miniewicz, B L Davies, Optical properties of deoxyribonucleic acid (DNA) polymer host, Optical Materials in Defence Systems Technology III, edited by Grote J G, Kajzar F, Lindgren M, Proc. of SPIE, 6401, 640106, (2006)

4. B Sahraoui, M Pranaitis, D Gindre, J Niziol, V Kažukauskas, Opportunities of deoxyribonucleic acid complexes composites for nonlinear optical applications, J. Appl. Phys., 110, 083117, (2011)

5. B Derkowska, O Krupka, V Smokal, B Sahraoui, Optical properties of oxazalone derivatives with and without DNA-CTMA, Opt. Mater., 33, 1429, (2011)

6. B Nithyaja, H Misha, P Radhakrishnan, V P N Nampoori, Effect of deoxyribonucleic acid on nonlinear optical properties of rhodamine 6G-polyvinyl alcohol system, J. Appl. Phys., 109, 023110, (2011)

7. S Sreeja, B Nithyaja, D Swain, V P N Nampoori, P Radhakrishnan, S V Rao, Nonlinear optical studies of DNA doped rhodamine 6G-PVA films using picosecond pulses, Optics and Photonics Journal, 2, 135, (2012)

8. I Dancus, V I Vlad, A Petris, I Rau, F Kajzar, A Meghea, A Tane, Nonlinear optical properties of Rh610 sensitized DNA-CTMA characterized by Z-scan, ROMOPTO 2012: Tenth Conference on Optics: Micro to Nanophotonics III, edited by Vlad V I, Proc. of SPIE, 8882, 88820D, (2013)

9. V L Singer, L J Jones, S T Yue, R P Haugland, Characterization of PicoGreen reagent and development of a fluorescence-based solution assay for double-stranded DNA quantitation, Anal. Biochem., 249, 228, (1997)

10. Quant-iT PicoGreen dsDNA Reagent and Kits, Manuals, Invitrogen

11. PicoGreen assay for dsDNA, Protocol ND-3300, Thermo Scientific

12. C Labarca, K Paigen, A simple, rapid, and sensitive DNA assay procedure, Anal. Biochem., 102, 344, (1980)

13. G Cosa, K S Focsaneanu, J R N McLean, J P McNamee, J C Scaiano, Photophysical properties of fluorescent DNA-dyes bound to single- and double-stranded DNA in aqueous buffered solution, Photochem. Photobiol., 73, 585, (2001)

14. S J Ahn, J Costa, J R Emanuel, PicoGreen quantitation of DNA: effective evaluation of samples pre- or post-PCR, Nucleic Acids Res., 24, 2623, (1996)

15. A I Dragan, J R Casas-Finet, E S Bishop, R J Strouse, M A Schenerman, G D Geddes, Characterization of PicoGreen interaction with dsDNA and the origin of is fluorescence enhancement upon binding, Biophys. J., 99, 3010, (2010)

16. H Zipper, H Brunner, J Bernhagen, F Vitzthum, Investigations on DNA intercalation and surface binding by SYBR Green I, its structure determination and methodological implications, Nucleic Acids Res., 32, e103, (2004)

17. ChemSpider CSID: 17230578

18. B W Laursen, F C Kerbs, Synthesis, structure, and properties of azatriangulenium salts, Chem. Eur. J., 7, 1773, (2001)

19. J C Martin, R G Smith, Factors influencing the basicities of triarylcarbinols. The synthesis of sesquixanthydrol, J. Am. Chem. Soc., 86, 2252, (1964)

20. S Dileesh, K R Gopidas, Photoinduced electron transfer in azatriangulenium salts, J. Photochem. Photobiol. A, 162, 115, (2004)

21. M S Bahae, A A Said, E W V Stryland, High-sensitive, single-beam n_2 measurements, Opt. Lett., 14, 955, (1989)

22. M S Bahae, A A Said, T Wei, D J Hagan, E W V Stryland, Sensitive measurement of optical nonlinearities using single beam, IEEE j. Quant. Electron., 26, 760, (1990)

23. E W V Stryland, M S Bahae, A A Said, D J Hagan, Characterization of nonlinear optical absorption and refraction, Prog. Crystal Growth and Charact., 27, 279, (1993)

24. E Shahriari, W M M Yunus, Effect of particle size on nonlinear refraction and absorption of Ag nanoparticles, D. J. Nanomater. Bios., 5, 939, (2010)

25. E Shahriari, W M M Yunus, Single beam Z-scan measurements of nonlinear refraction and nonlinear absorption coefficients in silver nano-fluid, Am. J. Engg. & Applied Sci., 3, 98, (2010)

26. R A Ganeev, R I Tugushev, A A Ishchenko, N A Derevyanko, A I Ryasnyansky, T Usmanov, Characterization of nonlinear optical parameters of polymethine dyes, Appl. Phys. B., 76, 683, (2003)

27. H Kang, Y Yuan, Z Sun, Z Wang, Nonlinear optical properties of a self-organized dye thin film, Chin. Opt. Lett., 5, 428, (2007)

28. S V Rao, N K M N Srinivas, D N Rao, Nonlinear absorption and excited state dynamics in Rhodamine B studied using Z-scan and degenerate four wave mixing techniques, Chem. Phys. Lett. 361, 439, (2002)

29. N K M N Srinivas, S V Rao, D N Rao, Saturable and reverse saturable absorption of Rhodamine B in methanol and water, J. Opt. Soc. Am. B. 20, 2470, (2003)

30. Y C Gao, X R Zhang, Y L Li, H F Liu, Y X Wang, Q Chang, W Y Jiao, Y L Song, Saturable absorption and reverse saturable absorption in platinum nanoparticles, Opt. Commun., 251, 429, (2005)

31. Z B Liu, Y Wang, X L Zhang, Y F Xu, Y S Chen, J G Tian, Nonlinear optical properties of graphene oxide in nanosecond and picosecond regimes, Appl. Phys. Lett., 94, 021902, (2009)

32. R R Rojo, L Stranges, A K Kar, M A M Rojas, W H Watson, Saturation in the near-resonance nonlinearities in a triazole-quinone derivative, Opt. Commun., 203, 385, (2002)

33. J He, W Ji, G H Ma, S H Tang, H I Elim, W X Sun, Excitonic nonlinear absorption in CdS nanocrystals studied using Z-scan technique, J. Appl. Phys., 95, 6381, (2004)

34. T Cassano, R Tommasi, A P Meacham, M D Ward, Investigation of the excited-state absorption of a Ru dioxolene complex by the Z-scan technique, J. Chem. Phys., 122, 154507, (2005)

35. E W V Stryland, M S Bahae, Z-scan measurements of optical nonlinearities, in Characterization Techniques and Tabulations for Organic Nonlinear Materials, M G Kuzyk, C W Dirk, Eds., Marcel Dekker, Inc., (1998)

36. B Nithyaja, H Misha, V P N Nampoori, Synthesis of silver nanparticles in DNA template and its influence on nonlinear optical properties, Nanosci. Nanotechnol., 2, 99, (2012)

5

Effect of DNA in lasing medium

Abstract

DNA is known to enhance the photoluminescence of fluorescent dyes. This enhancement can be attributed to various mechanisms associated with the type of bonding or intercalation of dye molecules with DNA. Here, we have used PicoGreen dye, which on addition of DNA enhances its fluorescence by more than 1000 fold. This enormous enhancement in fluorescence interested us to take up amplified spontaneous emission (ASE) studies, which could lead us to the development of DNA based lasing medium. We observed strong emission in the yellow region of the visible spectrum, with ASE threshold at ~ 2-3 mJ/cm^2. The degradation of the dye under intense laser beam was also investigated and is found par with available organic dyes.

5.1 INTRODUCTION

Ever since the identification of DNA by Friedrich Meischer[1] in 1869 and subsequent discovery of its molecular structure by James Watson and Francis Crick[2] in 1953, DNA has been known as a carrier of inheritance in every living organism. The hereditary information is stored in the DNA as a code, which is determined by the order or sequence of the four nucleobases. Till a decade ago, research in DNA has been associated with genetic engineering, medicine and microbiology. Fluorescence labelling based DNA sequencing (determining the order of nucleobases in a DNA strand) methods paved way for interaction between DNA and Photonics, which led to a new field termed as 'DNA Photonics'[3-6]. Presently, DNA has been exploited in various fields of photonics, optoelectronics and nanotechnology. Such bio-derived materials from nature can provide 'green' technology for a sustainable future.

DNA is found to enhance the fluorescence of lasing dyes when attached/ intercalated/ inserted into its strands, thus inhibiting the aggregation of dye molecules. DNA, being cheaper, renewable, biodegradable and transparent is a suitable candidate as a host material for lasing/fluorescent dyes[7,8]. First reports on using DNA in lasing medium were made by Ogata et al.[9-11] in 2000, who presented an interesting claim of amplified spontaneous emission in organic dye molecules viz. rhodamine 6G (Rh6G), pyrromethene 556, 4-[4-(dimethylamino) stylyl]-1-docterylpyridinium bromide (DMASDPB, sometimes referred as Hemi22) when doped in DNA:CTMA. The doping assisted the disassociation of dye molecules in the strands of DNA that led to the increase in fluorescence enhancement. Under higher excitation intensities, spectral narrowing and super-linear response of output intensity was observed. Later, Ogata et al. designed optical fiber amplifiers by gel-spinning method using DNA lipid complex doped with europium based rare earth chelates[12] and 4-{4-(dibutylamino)-styryl}-1-methylpyridinium iodide (DBASMPI, sometimes referred as Hemi1)[13]. This demanded the necessity to investigate the properties of DNA:CTMA complex for the use in optical and optoelectronic applications. Hagen et al.[14] investigated the electrical and optical properties of DNA:CTMA complex. They found that the complex was highly transparent in the visible range, low optical loss, thermally stable up to 200 °C and could tailor the resistivity by varying the molecular weight of DNA. Surprisingly the complex exhibited properties that are more suitable for an optical material - such as

refractive index, electrical conductivity, and dielectric breakdown field as discussed in chapter 2. Following, this several groups started to explore this interesting and promising optical biopolymer by doping it with various dyes to fabricate solid-state dye lasers. Steckl and Grote et al.,[15-20] investigated a number of lasing dyes viz. europium bromide, 4-(4-[Bis-(2-chloro-ethyl)-amino]-styryl)-1-methyl-pyridinium tosylate (BASPT) and sulforhodamine 640 in planar waveguides and distributed feedback laser (DFB) structures.

Kawabe et al.[21-25] continued to explore the use of hemicyanine dye DMASDPB and weakly fluorescent quinolone derived carbocyanine dyes, DiQC2 with DNA:CTMA complex. The dyes were so chosen that it has strong fluorescence enhancement on intercalation/ disassociation with DNA:CTMA. Light amplification from DNA:CTMA:dye was perceived along with spectral narrowing in the emission spectra when excited at higher intensities and was compared with PMMA as the host material. In order to observe lasing from these dyes, optical resonators were incorporated by fabricating the dyes on a DFB grating plates. Tunability of emission wavelength was also achieved by the use of dynamic grating realized by the interference of two lasing pump beams. In another work[26,27] reported by same group fabricated bi-layered devices consisting of pyridine 1/DNA:CTMA and disperse red 1/PMMA. The device was excited with a pump beam while using two interfering beams for grating formation to observe a tunable lasing at around 680 nm. They also developed a simple immersion technique[28-31] of staining dyes to undoped DNA:CTMA films. This technique yielded highly concentrated films of Hemi 22, Hemi1 and Eosin Y, which otherwise could not be fabricated by conventional techniques. They also discovered that the emission properties of Eosin Y changed by using different surfactants such as Benzylcetyldimethylammonium (BCDA), Methyltrioctylammnonium (MTOA) and Dimethyldistearylammonium (DMDA) instead of CTMA.

Mysliwiec et al.[32-39] used surface relief grating as distributed bragg reflectors (DBR) to realize lasing from organic laser dyes such as Rh6G, spiropyran and 3-(1,1-dicyanoethenyl1)-1phenyl-4,5dihydro-1H-pyrazole (DCNP) doped in DNA:CTMA as well as pure DNA films. Recently they had demonstrated tunable lasing from Rh6G[40] based on aggregate formation by varying the concentration of the dye molecules. Hung et al.[41] and Lin et al.[42] claimed low threshold and high gain, when Rh6G was loaded in

DNA modified by benzyltrimethylammonium (BTMA) surfactant instead of predominantly used CTMA. It was proposed that BTMA aided efficient energy transfer which led to the improved performance. Nithyaja et al.[43] has used DNA from herring sperm doped with Rh6G in polyvinyl alcohol matrix to observe enhancement in ASE intensity with a decrease in lasing threshold. From the above reports, it could be perceived that DNA plays as a good host material for most of the lasing dyes. Similar studies were demonstrated with Rhodamine B dye by Rujoiu et al.[44]. It additionally enhances the fluorescence of the dyes and have good film forming capabilities. These advantages make DNA an alternative over other conventionally used host materials such as PMMA and PVA.

In the present work, we introduce Picogreen (PG) dye as a lasing medium. PG is a fluorescent probe, generally used in biomedical research for quantitation of double and single stranded DNA and RNA. PG, an asymmetrical cyanine dye, does not fluoresce in its pristine form, but on binding with double stranded DNA, the fluorescence enhanced by 1000 fold or more[45]. This enhancement has been exploited in DNA quantitation in solution and gels, real-time PCR, cell chromosome staining and other techniques[46]. It has been found to be more efficient way to quantify DNA over other conventional methods such UV-visible spectroscopy or over other fluorescent probes such as Hoechst 33258. PG can be used to detect dsDNA as little as 1 ng/ml and require very small amount of sample. Dragan et al.[47] have recently proposed the possible modes of binding to DNA and explained the change in quantum yield and excited state lifetime. In their paper it was detailed that the negligible fluorescence was due to dynamic quenching process and subsequent dequenching by intercalation with DNA molecules due to the immobilization of dye molecules due to electrostatic interaction has improved the fluorescence quantum yield and excited state lifetime dramatically. This enormous enhancement in fluorescence made us interested to take up the amplified spontaneous emission studies, which could lead us to the development of a new active lasing medium.

Most of the works reported in respect of DNA lipid complex with lasing emission in the orange – red region. In this chapter, we present the results on yellow emitting PicoGreen as a lasing dye in the presence of DNA:CTMA lipid complex. An optimum weight ratio of DNA and PG mixture was measured at which it exhibited maximum

fluorescence. We then prepared a thin film by drop casting a mixture of DNA:CTMA and PG and allowed to dry in the vacuum. Absorption and fluorescence spectroscopy studies were performed on thin film samples that gave an insight into its emission properties. The samples were excited by nano-second laser to study the validity of the dye as a lasing material. Additionally the exponential gain coefficient and photostability of the dye were also analyzed.

5.2 THEORY OF AMPLIFIED SPONTANEOUS EMISSION

The three important prerequisites of a laser are gain medium, population inversion and optical resonator. The phenomena of lasing action begin with the absorption of a photon by an electron at ground level and its subsequent excitation to an excited level (stimulated absorption), consuming the energy of the photon it absorbed. On spending its lifetime at the excited level, the electron decays to the ground level and thereby emitting a photon with an energy equal to the bandgap between the excited state and ground level (spontaneous emission) and thus satisfying the law of conservation of energy. However, while at the excited state, had the electron encountered a photon of specific frequency, the electron de-excites to the ground level faster than the normal radiative decay process and thereby emitting a photon with its phase correlated to the photon it encountered (stimulated emission), satisfying both laws of conservation of energy and momentum. The incident photon is not absorbed by the excited electron, but is radiated back along with the emitted photon thus providing amplification. This process cascades a chain reaction to generate thousands of photons of similar characteristics to that of the incident photon. Both spontaneous emission and stimulated emission occur in a competitive fashion. Sometimes the spontaneously emitted photon may stimulate an excited electron to radiate a photon similar in characteristics (identical phase, frequency, polarization and direction) to the first few photons generated by the spontaneous emission. Such a process of amplifying the spontaneously emitted photons by the process of stimulated emission in a single-pass through a gain medium is known as Amplified Spontaneous Emission (ASE).

When the first requirement of a laser is provided i.e. an active medium, amplification of light or optical gain is achieved by stimulated emission. In addition to the gain

medium, if the second requirement is achieved i.e. population inversion by pumping sufficient and appropriate energy to the active medium, the stimulated emission dominates the spontaneous emission. The first two requirements impose a limitation on the output gain which is dependent on stimulated emission cross section, population density difference and effective gain length. The stimulated emission cross section of a particular laser transition is essentially a constant for a medium and the population density difference is limited in any particular energy level[48]. Hence the third requirement, optical resonator cavity when provided, applies feedback to allow the light to take multiple passes inside the gain medium, a way of extending the effective length of the gain medium and thus improving the gain, directionality, monochromaticity and coherence of the output laser beam.

Here the amplification is achieved due to the gain medium while the domination of stimulated emission is due to the population inversion. The resonator cavity extends the active medium to improve the gain by many-fold. To identify a gain medium, an efficient way is to confirm ASE. The important condition for ASE is to have sufficient number of excited state molecules at the metastable state or upper laser level. Some lasing medium have exceptionally high gain that they do not require optical resonator, yet emit very bright and spatially coherent beam due to their high amplification of spontaneous emission. They are termed as mirror-less lasers and are used where no temporal coherence is required. Some of the available mirror-less lasers are N2 laser (337 nm), H2 laser (120 nm), He-Ne laser (3.39 m), He-Xe laser (3.51), few pulsed excimer lasers, high-gain dye laser amplifiers, high-gain semiconductor diode laser[49]. The enormously large and powerful natural lasers which occur in interstellar space are also examples of mirror-less or ASE laser systems.

In spontaneous emission (fluorescence/thermal emission) decay of excited state electrons happens without any external influence. This emission although centered on a single wavelength, they have large linewidth ranging from a few tens to hundreds of nanometer. The individual photons do not have phase correlation between them and they emanate in random direction. In contrast, amplified spontaneous emission possess distinct features that are intermediate between a laser and a conventional light source. The features are (1) moderate directionality – stimulated emission emits in the same direction as the incident photon, yet resonators can achieve low divergence beam as

that of laser oscillator; (2) spectral narrowing – This narrowing is due to the fact that stimulated emission generates photons of similar frequency as that of the incident photon. However, in systems of planar microcavity or cuvette cavity, the planar/ cuvette faces act as resonators to provide particular mode propagation with high gain that enhances the narrowing to the order of subnanometer as in lasing; (3) limited coherence – ASE exhibits low temporal coherence due to the spontaneous emission, but may be spatially coherent depending on the circumstances; (4) super-linear response of output intensity – This super-linear response with respect to input energy implies the amplification taking place in the gain medium; (5) intense output beam – the emitted output light consists of a beam due to low divergence; (6) saturation gain – ASE occurs in materials with high gain without the aid of resonators. It is necessary to have gain amplification for the medium to lase.

Mathematically gain is defined as the natural logarithm of ratio of number of photons emitted to the number of photons absorbed. The gain as dictated by Shank's technique[50] is calculated by measuring ASE intensity as a function of excitation length of the pump beam at the same wavelength. In this technique, a laser beam of stripe geometry is used to pump the sample using a cylindrical lens. The output ASE intensity was measured with a given length, L and L/2. The length of the stripe is varied by using a beam block. According to the theory described by Shaklee et al.[51], the rate of change in the fluorescence intensity with respect to the stripe length is given by

$$\frac{dI}{dx} = AP_0 + gI \qquad (5.1)$$

where, I is the fluorescence intensity propagating along x axis

A is a constant related to spontaneous emission cross section

P_0 is the pump intensity

g is the net gain (g = g′ - α)

g′ is the gain due to stimulated emission, and

α is the net optical loss

The solution to equation 5.1 is

$$I = \frac{AP_0}{g(\lambda)} \exp\left[g(\lambda)L - 1\right] \qquad (5.2)$$

where, L is the stripe length

For a stripe length of L/2, the equation 5.2 changes to

$$I = \frac{AP_0}{g(\lambda)} \exp\left[g(\lambda)L/2 - 1\right] \qquad (5.3)$$

From equation 5.2 and 5.3, the gain could be deduced as

$$g = \frac{2}{L} \ln\left[\frac{I_L}{I_{L/2}} - 1\right] \qquad (5.4)$$

To validate a dye as a gain medium, it is necessary to confirm the following features as discussed by Samuel et al.52. ASE can be considered as lasing without optical feedback and this phenomenon strongly increases the chance of lasing action.

- The output beam will have a narrow linewidth emission of the order of few nanometers.

- A distinct threshold is observable in output intensity with respect to the input power.

- A distinct threshold is observable in linewidth of the emission spectra with respect to the input power.

- The emitted light consists of a beam with low divergence.

In some cases where lasing modes are observed, it would require additional measurements such as polarization and temporal coherence of the emitted light to investigate the nature of light emission. In such cases the characteristics of emission will largely depend on the various other factors including the type of resonators, the

alignment of the cavity that define the particular mode competition, the resonator losses and the time period to repopulate the excited states which depend on the fluorescence lifetime.

We confirm the observance of ASE and lasing action in the gain medium consisting of DNA:CTMA:PG thin film on a glass substrate considering the points discussed by Samuel et al.[52]. We therefore, present necessary and sufficient evidence of spectral narrowing, a distinct threshold in linewidth and output intensity and the lasing output beam.

5.3 FABRICATION OF PG:DNA THIN FILM

Marine derived DNA (extracted from salmon testes) and CTAB [hexadecyltrimethylammonium bromide] were procured from Sigma-Aldrich, USA. PG dye was supplied by Invitrogen, USA. The molecular structure, International Union of Pure and Applied Chemistry (IUPAC) name [2-(n-bis-(3-dimethylaminopropyl)-amino)-4-(2,3-dihydro-3-methyl-(benzo-1,3-thiazol-2-yl)-methylidene)-1-phenyl-quinolinium] and molecular mass (552.5 Da) were determined by Dragan et al.[47]. The optical properties such as absorption and fluorescence spectroscopy of PG has already been given in Section 4.1.2. As already discussed, DNA in its fibrous form is soluble only in water. It can be made soluble in organic solvents by attaching a surfactant, CTAB. The DNA:CTMA (DC) lipid complex was prepared as described elsewhere (detailed in chapter 2). DNA was prepared in distilled water at a concentration of 20 mg/ml. DC lipid complex was prepared in butanol at a similar concentration.

It is known that DNA enhances the fluorescence of PG through a de-quenching process. In order to use DNA-PG as a lasing medium, it is necessary to estimate the optimum concentration of DNA with respect to PG at which the photoluminescence is maximum. To investigate this optimum concentration, PG solution was prepared with varying amount of DNA. The weight ratio of DNA:CTMA (DC) with respect to PG was varied from 2 to 5000 in nine different samples. Figure 5.1 shows the fluorescence peak intensity of different samples at a wavelength 530 nm. The samples were excited at 500 nm. From the observed plot, it could be found that DC:PG with weight ratio of 50:1
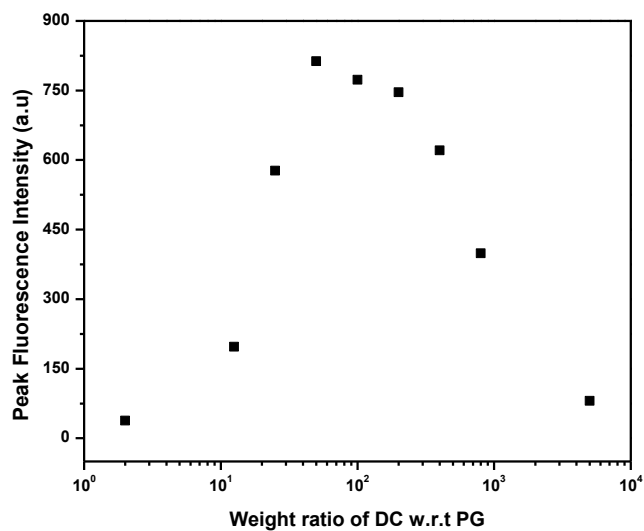
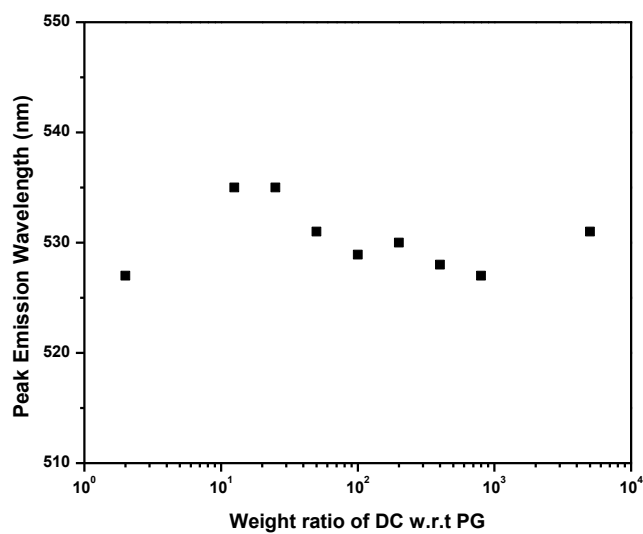Figure 5.1: Variation of peak fluorescence intensity of different weight ratios of DC with respect to PG

Figure 5.2: Variation of peak emission wavelength of different weight ratios of DC with respect to PG

Figure 5.3: Photograph of pure DNA (left) and modified DNA (DNA:CTMA, right) film

showed maximum fluorescence. This weight ratio was used in fabricating thin film that was further used for ASE measurements. The variation in the peak emission wavelength in all the samples were recorded and depicted in figure 5.2. Thin films of DNA and DC were prepared by drop casting method, as described in Section 3.2.1.1. We found that the DC film produced better optical quality than DNA film (see Figure 5.3). The opacity of the DNA film was higher than DC film, which could possibly affect the transmission of emitted light from lasing dyes.

Hence, we chose DC film. PG dye was used as received and no further purification and dilution was made. To prepare dye doped DC film, DC lipid complex was added to PG dye in a volume ratio of 2:1 and drop casted on a clean glass substrate. The corresponding weight ratio of DNA with respect to PG was estimated to be 40:1, approximately close to the ratio at which the fluorescence enhancement is maximum. The film was allowed to dry in vacuum chamber at 40 °C for 2 hours. The annealing in vacuum was necessary to evaporate DMSO at a lower temperature and thus not degrading DNA. The film

Figure 5.4: Photograph of bilayer DNA-PG film (top left) and bilayer DC-PG film (top right) prepared by immersion technique; DNA:PG (bottom left); and DC:PG film (bottom right) prepared by drop casting technique.

was stored at room temperature for further lasing studies. We also prepared bilayer films where first DC film was drop casted and annealed. We further casted PG dye solution over the DC film, similar to the immersion technique followed by Suzuki et al.[28]. In their paper, DC film was immersed in a dye solution for 24 hours, showed discoloration of dye solution and significant coloring of the transparent film. The immersion technique yielded films of higher concentration over the conventional casting method. However in this case, the film fabricated did not produce a better

quality film. Figure 5.4, shows four films prepared from DNA (left) and DC (right) by immersion technique (top) and drop casting method (bottom). The thin film prepared by casting a mixture of DC and PG yielded uniform and better quality film and therefore, was the only film subjected to further studies. This film will henceforth be referred to as the sample film. The thickness and refractive index of the sample film were measured using ellipsometer and was estimated to be 0.35 μm and 1.511 respectively.

5.4 OPTICAL AMPLIFICATION IN PG:DNA THIN FILM

The experimental technique followed is detailed in Section 3.2.2. We irradiate the thin film sample by a 10 mm stripe geometry of second and third harmonic frequencies from an Nd:YAG laser of 10 Hz repetition rate with a pulse duration of 7 ns. The stripe geometry was achieved using an aperture and a cylindrical lens. The experimental setup is shown in figure 3.6. The pump laser beam was irradiated normally on to the sample and the output emission from the thin film was collected using an optical fiber connected to Ocean Optics (HR4000) spectrophotometer, without using any collecting lens. The power of laser beam was measured using Newport 1918-R optical meter along with an 818E-10-25-F model Newport detector.

The normalized optical absorption and normalized fluorescence spectra along with ASE spectrum from the sample is presented in figure 5.5. The UV-absorption of the sample film exhibit two spectrally distinct wavelengths with its peak at 300 nm and 506 nm which is attributed to the absorption regions of DC and PG, respectively. The fluorescence spectrum, when excited at 355 nm, reveals a broad peak ranging from 515 nm to 586 nm (at the half-maxima), with its peak at 550 nm. The full-width at half-maximum (FWHM) was measured and found to be 68.67 nm. We further measured fluorescence when excited using third harmonic frequency (355 nm) from an Nd:YAG laser. At an energy density of 15.4 mJ/cm^2, a dominant peak was observed ranging from 554 nm to 564 nm (at half-maxima) with the peak at 559 nm. This shift from the conventional fluorescence peak is due to the particular mode oscillation corresponding to 559 nm. The FWHM of the ASE spectrum was measured to be 12.16 nm. This

reduction in FWHM is associated with the observance of spectral narrowing, which is due to the high gain of the active medium.
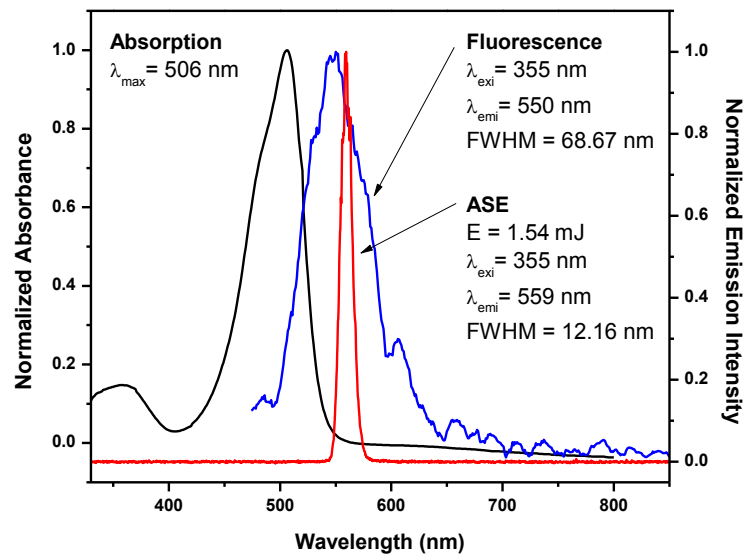

Figure 5.5: Normalized spectra of absorption, fluorescence and amplified spontaneous emission from DC:PG thin film

For ASE measurements, the sample was irradiated with second harmonic frequency (532 nm) from Nd:YAG laser. A stripe geometry laser beam of cross section 10 mm x 1 mm was used to pump the thin film sample and the output emission was collected from the edge of the film as shown in figure 3.6. The energy density of the laser beam was varied from 1 mJ/cm^2 to 180 mJ/cm^2 and the output was measured corresponding to each fluence. Characterization of their emission profiles exhibited a growing peak, centered at 568 nm. At low pump energy density of 1.9 mJ/cm^2, the FWHM recorded was 67.9 nm which was approximately equal to the bandwidth observed from the conventional spectrofluorometer. As the pump energy density was increased beyond 3 mJ/cm^2, we observed a tendency of spectral narrowing along with a super-linear response of output intensity with respect to the input energy density. The ASE outputs

presented in figure 5.6 were obtained with energy densities at 0.60, 1.55, 12.3 and 17.6 mJ/cm^2 and the corresponding FWHM for the spectra were 37.9, 21.68, 18.07 and 13.26 nm. Figure 5.7 and 5.8, shows the dependence of FWHM and output ASE intensity as a function of input energy density using a laser pump beam of wavelength 532 nm. As the figure 5.7 reveals, the FWHM rapidly decreased to 17.45 nm at 24 mJ/cm^2 and to 13.26 nm at 176.2 mJ/cm^2. From figure 5.8, there appears a distinct lasing threshold at 3 mJ/cm^2.
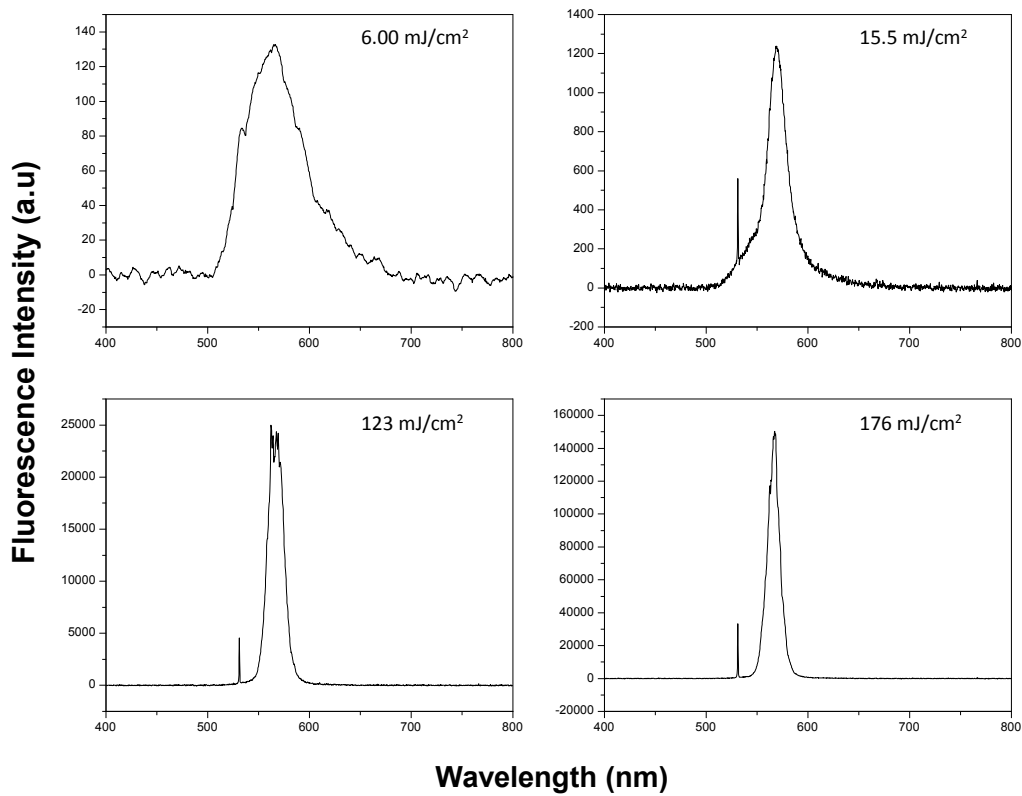
Figure 5.6: Emission profiles from DC:PG film under 532 nm excitation at energy densities of 6, 15.5, 123 and 176 mJ/cm^2
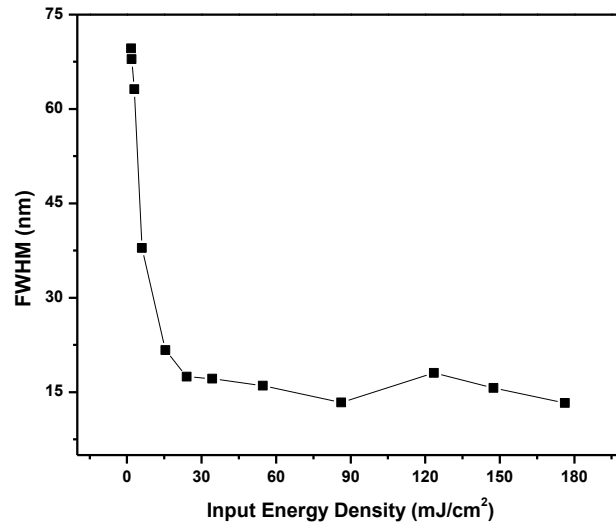
Figure 5.7: Dependence of FWHM parameter on energy density using 532 nm pump beam
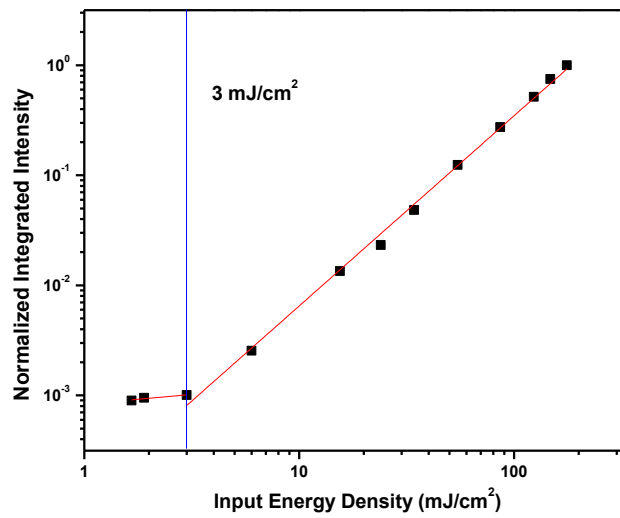
Figure 5.8: Dependence of ASE intensity on energy density using 532 nm pump beam (threshold at 3 mJ/cm^2)

Citing the presence of DNA, which could help in resonant energy transfer with PG, the thin film sample was irradiated with third harmonic frequency (355 nm) of Nd:YAG laser. Here as the pump energy density was varied from 0.1 mJ/cm^2 to 65 mJ/cm^2, we observed an emission profile with its peak centered at 559 nm. At a low energy density of 0.2 mJ/cm^2, the observed emission spectrum showed a linewidth of 67.9 nm. Beyond a pump energy density of 1.7 mJ/cm^2, a super-linear response of output intensity with respect to the input energy density was observed along with a spectral narrowing.
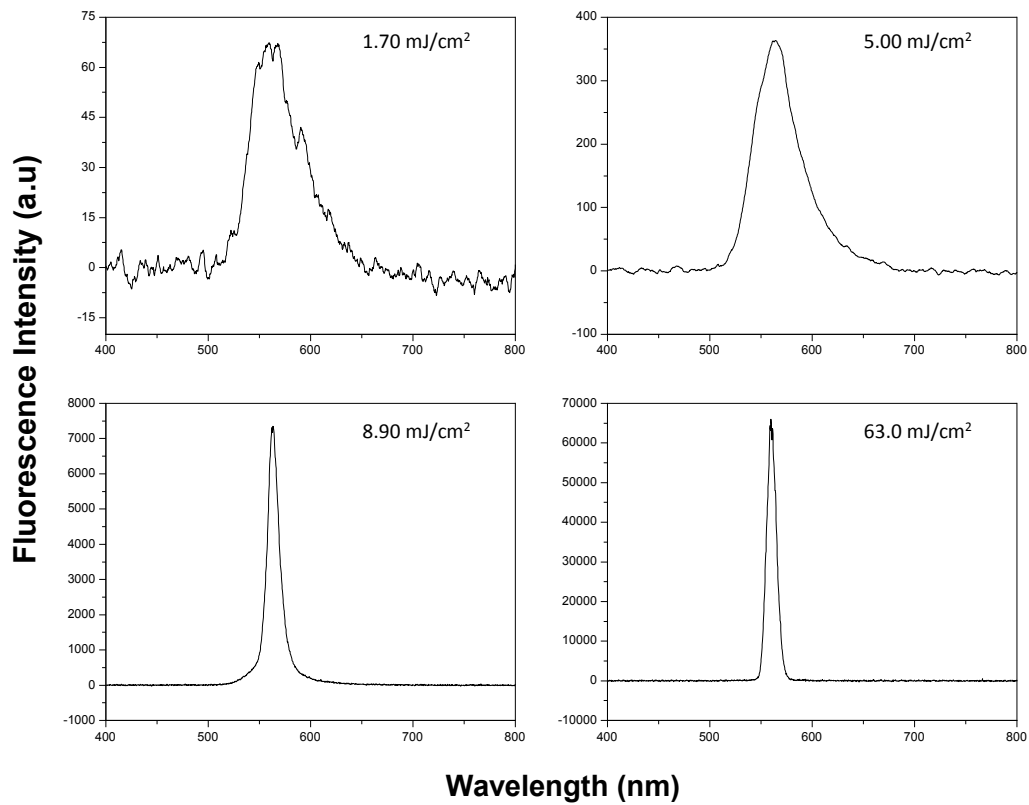
Figure 5.9: Emission profiles from DC:PG film under 355 nm excitation at energy densities of 1.7, 5, 8.9 and 63 mJ/cm^2

The ASE outputs presented in figure 5.9 were obtained with energy densities at 1.7, 5, 8.9 and 63 mJ/cm^2 and the corresponding FWHM for the spectra were 59.04, 47.26, 12.85 and 5.71 nm. Figure 5.10 and 5.11, shows the dependence of FWHM and output ASE intensity as a function of input energy density using a laser pump beam of wavelength 355 nm. As depicted in figure 5.10, the FWHM at 7.1 mJ/cm^2 was 13.93 nm and at 63 mJ/cm^2, it was 5.71 nm. Similar to 532 nm irradiation, a distinct lasing threshold was perceived from figure 5.11 at 1.7 mJ/cm^2.
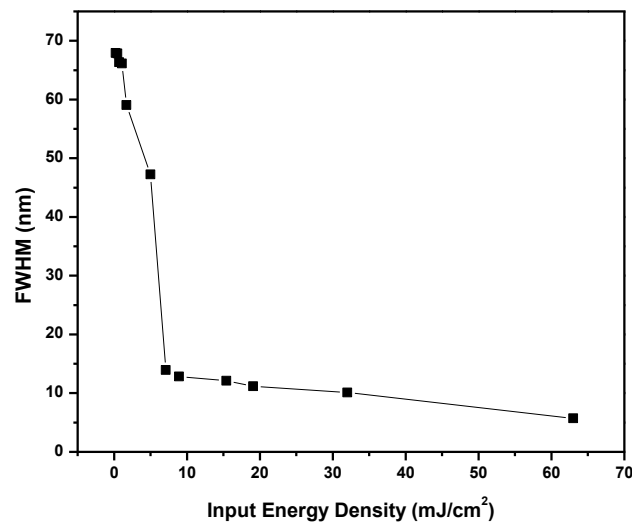
Figure 5.10: Dependence of FWHM parameter on energy density using 355 nm pump beam

Figure 5.12 shows the dependence of integrated ASE intensity as a function of input energy density for an excitation wavelength of 355 and 532 nm. It could be observed that PG:DC thin film exhibited a lower ASE threshold and higher efficiency when excited with 355 nm.
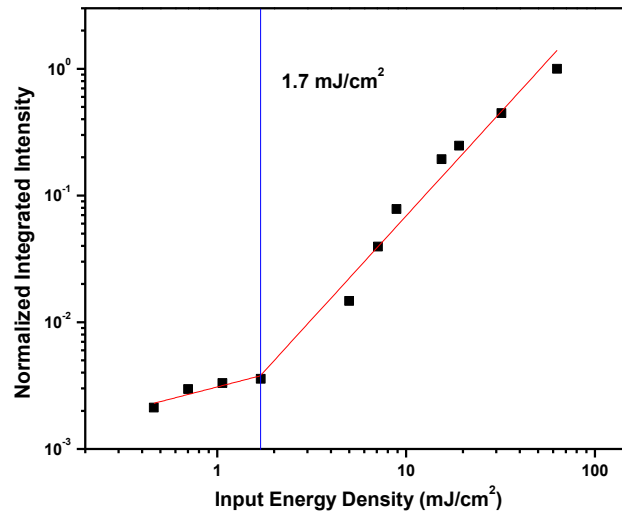
Figure 5.11: Dependence of ASE intensity on energy density using 355 nm pump beam (threshold at 1.7 mJ/cm^2)
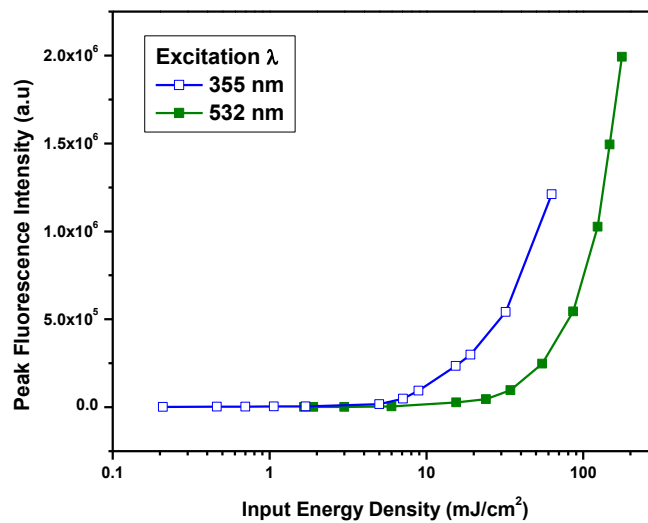

Figure 5.12: Comparison of dependence of ASE intensity with respect to input energy density for an excitation wavelength of 355 nm and 532 nm
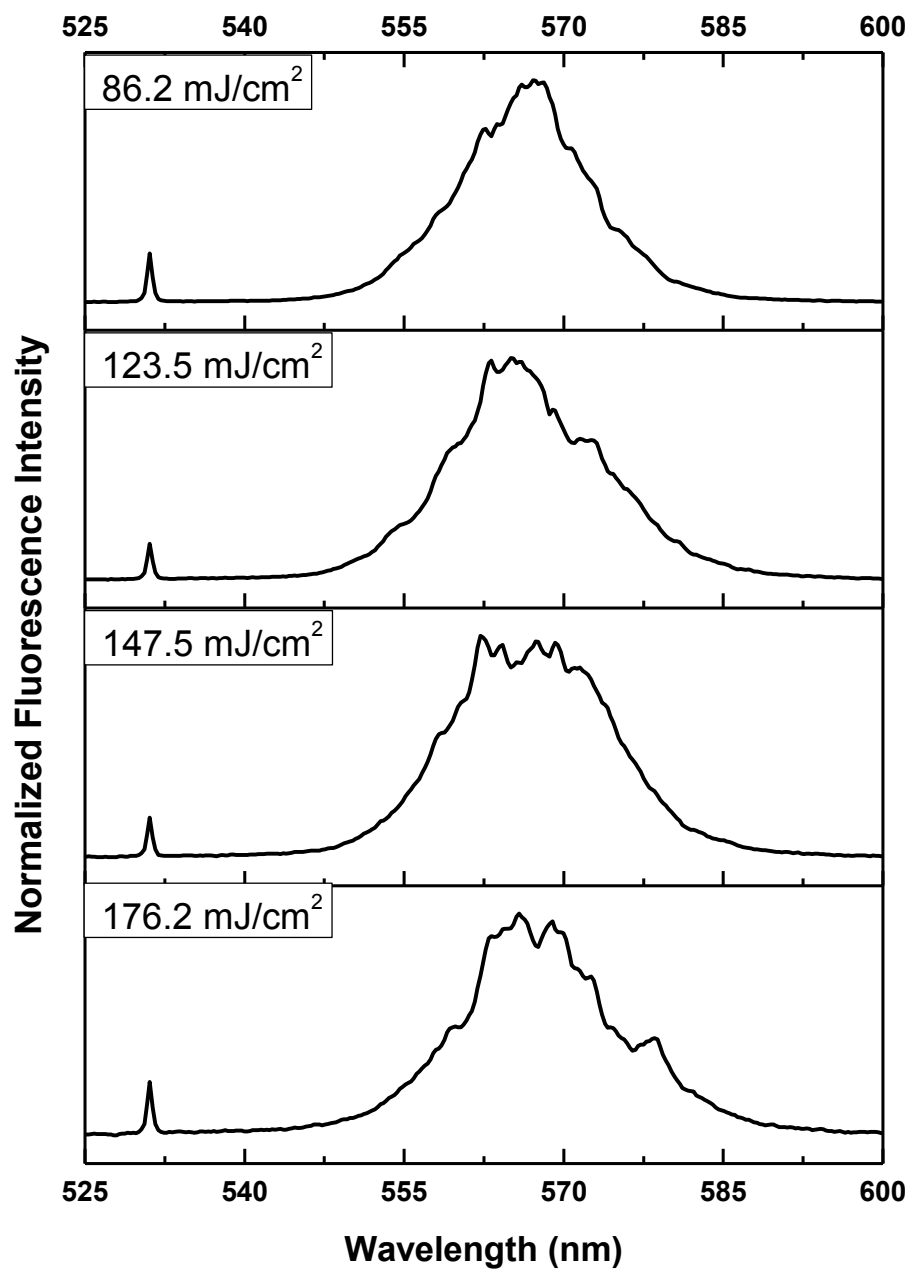
Figure 5.13: Detailed spectral structures under 532 nm excitation at energy densities of 86.2, 123.5, 147.5 and 176.2 mJ/cm^2
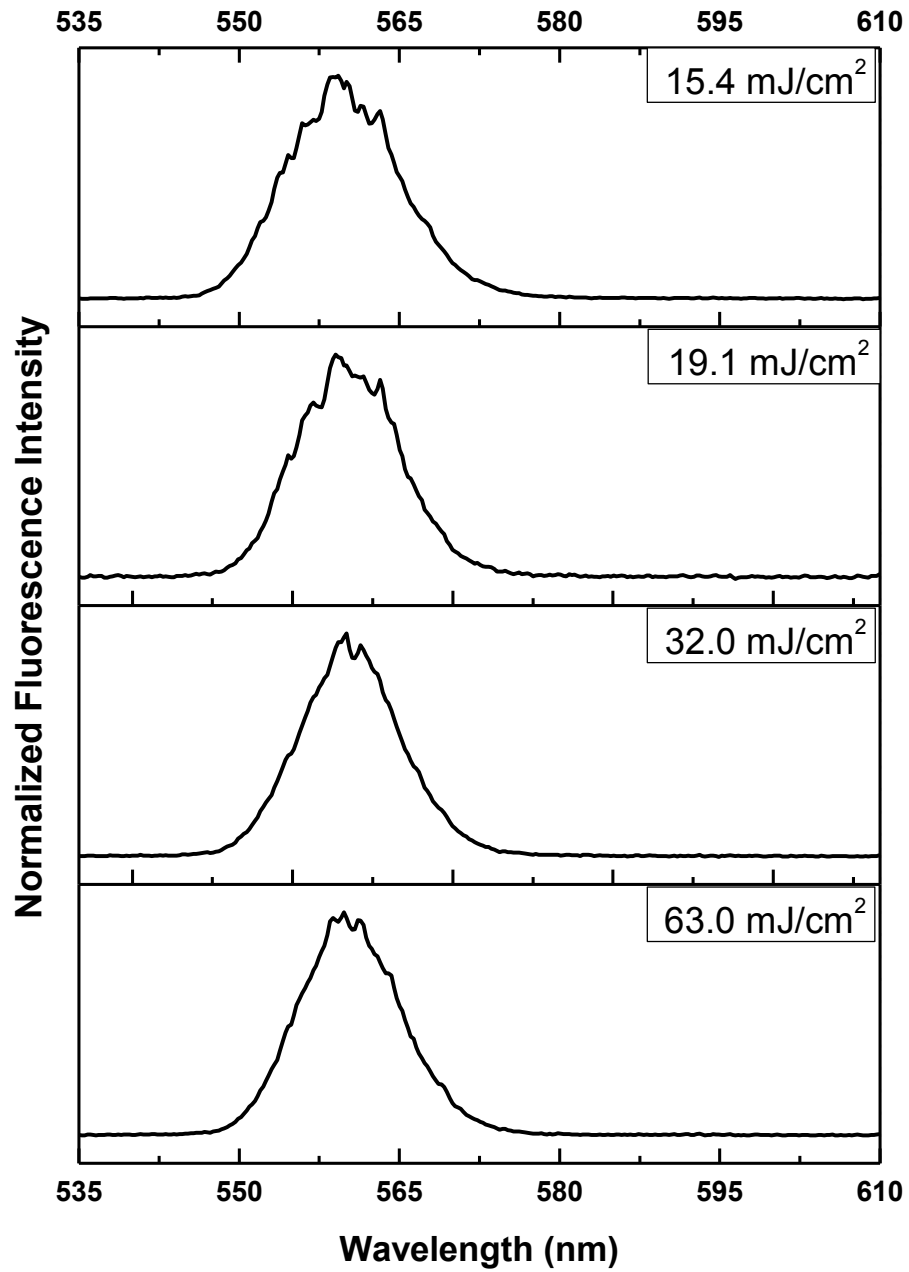
Figure 5.14: Detailed spectral structures under 355 nm excitation at energy densities of 15.4, 19.1, 32 and 63 mJ/cm^2

Figure 5.13 shows the ASE spectra from DC:PG film under 532 nm excitation at energy densities of 86.2, 123.5, 147.5 and 176.2 mJ/cm^2. At higher intensities, the spectrum appears to exhibit mode structures. We could observe modulation structures from resolution limited spectrometer ranging from 562 nm to 579 nm. But on careful inspection of the ASE spectra, we see that the modes appear to be random. This may be due to the possibility of aggregation of dye molecules. The spikes that were clearly visible in the spectra excited with 147.5 mJ/cm^2 may be due to the surface roughness of the thin film. Similar results were also obtained from the thin film while using 355 nm pump beam. Figure 5.14 depicts the ASE spectra from DC:PG under 355 nm excitation at energy densities of 15.4, 19.1, 32.0 and 63.0 mJ/cm^2. Here the spectrum ranges from 555 nm to 563 nm. However by providing suitable cavity design and excitation, it could be possible to tune the lasing wavelength from 555 nm to 579 nm.

The exponential gain coefficient was calculated by Shaklee method (described in section 5.2) by introducing a block to the laser pump beam. The initial beam geometry was 10 mm x 1 mm. The intensity measured at an excitation strip length of 10 mm is denoted by I_L. A block was placed so as to alter the beam geometry to 5 mm x 1mm, at which the intensity is denoted by $I_{L/2}$. The exponential gain coefficient, γ was calculated using the equation 5.4 and was found to be 4.7 cm^{-1} while using 532 nm excitation. At 355 nm excitation, the gain coefficient was found to be 5.2 cm^{-1}.

5.5 PHOTO STABILITY OF PICOGREEN

Another important factor is the photo-degradation of PG, which will determine its practical applicability as a lasing medium. While using a pump beam of 532 nm pulses at 1.5 mJ and measuring the output spectrum for every 15 seconds, we estimated that the output intensity was reduced to 50 % of its initial value after 215 excitation pulses. Figure 5.15 shows the temporal stability of ASE signals when excited at 532 nm. The peak intensity was measured at 569 nm and are normalized in the plot. With the available literature, we conclude that this value is typical for an organic dye. We show the photograph of the observed output beam on a white screen when excited at 355 nm (see figure 5.16 and 5.17). The observance of green output light, which is otherwise yellow is due to the fluorescence from the white sheet of paper used as a screen.
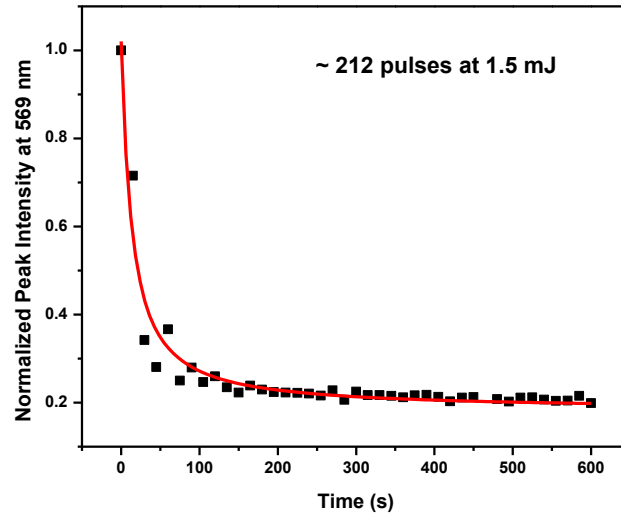
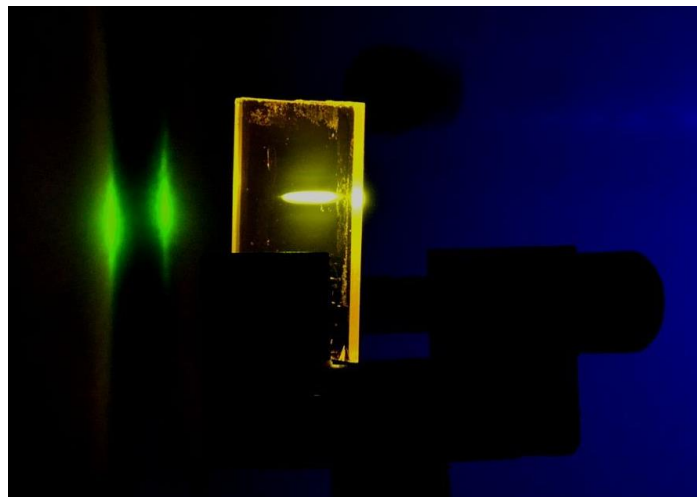Figure 5.15: Dependence of ASE intensity on time for DC:PG film

Figure 5.16: Photograph of yellow emission from DC:PG film when irradiated at 355 nm. The green color is due to the fluorescence emission from the white paper (screen)
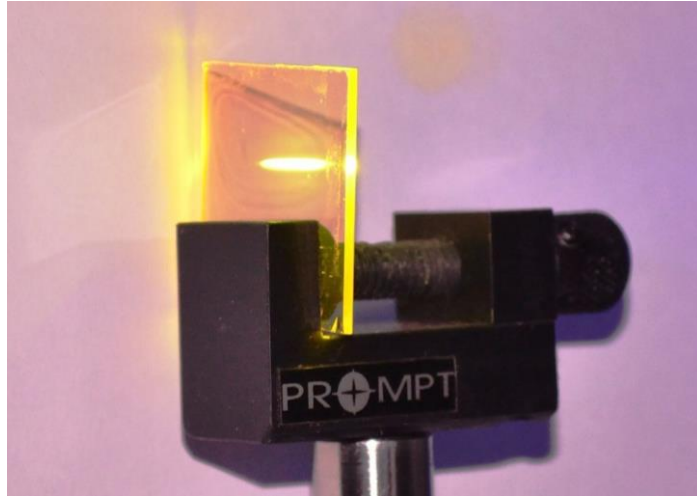
Figure 5.17: Photograph of yellow emission from DC:PG film under ambient light

To quantify the performance of dye, an elaborate comparison has been made with DNA-based other cyanine and hemicyanine dyes and a common lasing dye, Rh6G. Dyes with weak fluorescence yield shows enhanced performance on doping it with DNA. Our results were compared with the reports referred in section 5.1 and were presented in table 5.1. We could infer from the table that the PG:DC film exhibited very low ASE threshold (ρ) without the aid of distributed feedback (DFB) structures or surface relief gratings (SRG). The gain (γ) of the cyanine and hemicyanine dyes were not reported and hence a comparison could not be made. In comparison with rhodamine dye, the gain from PG:DC was slightly lesser.

Table 5.1: Comparison of dye doped DNA complex available from earlier reports
with our results from PG:DC complex

Dyes/ Sample configuration	Pumping Source	ASE performance	Reference
PicoGreen-DNA:CTMA film	λ = 532 (355) nm (ns)	ρ = 3 (1.7) mJ/cm^2 γ = 4.7 (5.2) cm^{-1} λ = 568 (559) nm $\Delta\lambda$ = 13.26 (5.71) nm	Present study

Rhodamine 6G			
Rh6G-DNA:CTMA film	λ = 532 nm (ns)	ρ = 2 mJ/cm^2 λ = 595 nm $\Delta\lambda$ = 15 nm	Kawabe et al. [9,10]
Rh6G-DNA:CTMA film	λ = 532 nm (ns)	ρ = 5.77 mJ/cm^2 γ = 8.49 cm^{-1} λ = 572 nm $\Delta\lambda$ = 6.61 nm	Hung et al.[41]
Rh6G-DNA:CTMA film	λ = 532 nm (ns)	ρ = 3.1 mJ/cm^2 γ = 2 cm^{-1} $\lambda \approx$ 592 nm $\Delta\lambda \approx$ 10 nm	Mysliwiec et al. [32,33]
Rh6G-DNA:CTMA film with photochromic polymer (lasing with SRG)	λ = 532 nm (ns)	ρ = 3 (1.8) mJ/cm^2 λ = 605 (590) nm $\Delta\lambda$ = 5 nm	Mysliwiec et al. [35]
Rh6G-DNA film	λ = 532 nm (ns)	ρ = 4.5 mJ/cm^2 γ = 6.5 cm^{-1} λ = 587 nm $\Delta\lambda$ = 16 nm	Mysliwiec et al. [37]
Rh6G-DNA:CTMA film	λ = 532 nm (ns)	ρ = 3.6 $\pm$ 0.4 mJ/cm^2 λ = 579, 587, 593 nm	Mysliwiec et al. [40]
Rh6G-DNA-PVA film	λ = 532 nm (ns)	ρ = 150 mJ/cm^2 λ = 565 nm $\Delta\lambda$ = 5 nm	Nithyaja et al. [43]
Rh6G-DNA:CTMA-Ormocer	λ = 505 nm (fs)	λ = 600 nm $\Delta\lambda$ = 15 nm	Gupta et al. [17]
SRh 640-DNA:CTMA film	λ = 532 nm (ns)	ρ = 95 μJ/cm^2 λ = 605 nm $\Delta\lambda \approx$ 10 nm	Yu et al. [19,20]
Hemicyanine dye			
DMASDPB-DNA:CTMA film	λ = 532 nm (ns)	ρ = 0.5 mJ/cm^2 λ = 625 nm $\Delta\lambda$ = 20 nm	Kawabe et al. [11]

DMASDPB-DNA:CTMA film (immersion/ conventional technique)	λ = 532 nm (ns)	ρ = 0.3/10 mJ/cm^2 $\lambda \approx$ 625/605 nm $\Delta\lambda$ = 14/24 nm	Kawabe et al. [28,29]
DMASDPB-DNA:CTMA (solution in Littrow cavity/ film in DFB structure)	λ = 532 nm (ns)	ρ = 10/1.5 mJ/cm^2 $\lambda \approx$ 629/605 nm $\Delta\lambda$ = 4/- nm	Chida et al. [22,25]
DMASDPI-DNA:CTMA film	λ = 532 nm (ns)	ρ = 1 mJ/cm^2 $\lambda \approx$ 615 nm $\Delta\lambda \approx$ 6 nm	Yoshida et al. [53]
Cyanine dyes			
DiQC$_2$(1)-DNA:CTMA film DiQC$_2$(3)-DNA:CTMA film with DFB structures	λ = 532 nm (ns)	ρ = 3 mJ/cm^2 ρ = 6 mJ/cm^2	Chida et al. [24]
DiSC$_2$(3)-DNA:CTMA film (method1/ method2) [21]	λ = 532 nm (ns)	ρ = 7.5/ 2 mJ/cm^2	Honda et al. [21]
Other dyes			
Pyridine 1-DNA:CTMA film	λ = 532 nm (ns)	ρ = 10 mJ/cm^2 λ = 675 nm	Chida et al. [27]
Spiropyran-DNA:CTMA film	λ = 355 nm (ns)	ρ = 8.6 mJ/cm^2 γ = 6 cm^{-1} λ = 680 nm $\Delta\lambda$ = 6 nm	Mysliwiec et al. [34]
DCNP-DNA:CTMA film (without/ with SRG grating)	λ = 532 nm (ns)	ρ = 17/11 mJ/cm^2 γ = 10/12-15 cm^{-1} λ = 637/ 643.5 nm $\Delta\lambda$ = 7/ $\leq$ 1 nm	Mysliwiec et al. [36]

5.6 CONCLUSIONS

In summary, we investigated a new dye for lasing at 560-570 nm using deoxyribonucleic acid, which not only acts as a host matrix for the dye but also as fluorescence enhancer through dynamic dequenching process. We have therefore fabricated modified DNA lipid complex intercalated with PG dye thin film and observed amplified spontaneous emission at 568 nm and 559 nm while exciting at second and third harmonic frequencies respectively from an Nd:YAG laser. We also observed modes ranging from 555 nm to 579 nm and also propose probable tunable emission by utilizing proper cavity structure and excitation wavelength. We estimated an ASE threshold at 3 and 1.7 mJ/cm^2 when excited at 532 and 355 nm pump beam respectively. We also observed spectral narrowing with a lowest FWHM recorded was 13.26 and 5.7 nm when excited at 532 and 355 nm pump beam respectively. The film of 0.35 μm thick could sustain approximately 215 pulses of 1.5 mJ, 532 nm laser radiation before the emission degrades to 50% of the initial intensity. Though we find an exponential gain coefficient of ~ 5.0 cm^{-1} in our PG:DC samples, which is at par with most of the organic dyes. Here, we see that the DNA not only acts as a host material but plays an important role in the luminescence of the dye molecules that could lead to the development of DNA based lasers.

REFERENCES

[1.] F Miescher, Ueber die chemische Zusammensetzung der Eiterzellen, Med. Chem. Unters., 4, 441, (1871)

[2.] J D Watson, F H C Crick, A Structure for Deoxyribose Nucleic Acid, Nature, 171, 737, (1953)

[3.] J A Hagen, J G Grote, N Ogata, J S Zetts, R L Nelson, D E Diggs, F K Hopkins, P P Yaney, L R Dalton, S J Clarson, DNA Photonics, Organic Photonic Materials and Devices VI, edited by J G Grote, T Kaino, Proc. SPIE 5351, 77, (2004)

[4.] J G Grote, D E Diggs, R L Nelson, J S Zetts, F K Hopkins, N Ogata, J A Hagen, E Heckman, P P Yaney, M O Stone, L R Dalton, DNA Photonics [Deoxyribonucleic acid], Mol. Cryst. Liq. Cryst., 426, 3-17, (2005)

[5.] F D Lewis, DNA Photonics, Pure Appl. Chem., 78, 2287-2295, (2006)

[6.] Y-W Kwon, D H Choi, J-I Jin, Optical, electro-optic and optoelectronic properties of natural and chemically modified DNAs, Polym. J., 44, 1191, (2012)

7. A J Steckl, DNA – a new material for photonics?, Nat. Photonics, 1, 3, (2007)

8. A J Steckl, H Spaeth, H You, E Gomez, J Grote, DNA as an optical material, Opt. Photonics News, 22, 34, (2011)

9. Y Kawabe, L Wang, T Koyama, S Horinouchi, N Ogata, Light amplification in dye doped DNA-surfactant complex films, Linear, Nonlinear, and Power-Limiting Organics, edited by M Eich, M G Kuzyk, C M Lawson, R A Norwood, Proc. of SPIE, 4106, 369, (2000)

10. Y Kawabe, L Wang, S Horinouchi, N Ogata, Amplified spontaneous emission from fluorescent-dye-doped DNA-surfactant complex films, Adv. Mater. 12, 1281, (2000)

11. Y Kawabe, L Wang, T Nakamura, N Ogata, Thin-film lasers based on dye-deoxyribonucleic acid-lipid complexes, Appl. Phys. Lett., 81, 1372, (2002)

12. L Wang, K Ishihara, H Izumi, M Wada ,G Zhang, T Ishikawa, A Watanabe, S Horinouchi, N Ogata, Strongly luminescent rare-earth ion-doped DNA-CTMA complex film and fiber materials, Materials and Devices for Optical and Wireless Communications, edited by C J Chang-Hasnain, Y Xia, K Iga, Proc. of SPIE, 4905, 143, (2002)

13. M Ozaki, Y Kagami, M Wada, N Ogata, K Mito, T Ishikawa, S Horinouchi, Function of plastic optical fiber composed of DNA compound, Nanophotonics, Nanostructure, and Nanometrology, edited by X Zhu, S Y Chou, Y Arakawa, Proc. of SPIE. 5635, 194, (2005)

14. J A Hagen, Enhanced luminous efficiency and brightness using DNA electron blocking layers in bio-organic light emitting diodes, PhD thesis, University of Cincinnati, (2006)

15. J G Grote, E M Heckman, D E Diggs, J A Hagen, P P Yaney, A J Steckl, S J Clarson, G S He, Q Zheng, P N Prasad, J S Zetts, F K Hopkins, DNA-based materials for electro-optic applications: current status, Nonlinear Optical Transmission and Multiphoton Processes in Organics III, edited by A T Yeates, Proc. of SPIE, 5934, 593406-1, (2005)

16. G S He, Q Zheng, P N Prasad, J G Grote, F K Hopkins, Infrared two-photon-excited visible lasing from a DNA-surfactant-chromophore complex, Opt. Lett., 31, 359, (2006)

17. P Gupta, P P Markowicz, K Baba, J O'Reilly, M Samoc, P N Prasad, J G Grote, DNA-Ormocer based biocomposite for fabrication of photonic structures, Appl. Phys. Lett. 88, 213109, (2006)

18. Z Yu, J A Hagen, J G Grote, A J Steckl, Red photoluminescence emission of laser dye doped DNA and PMMA, Organic Photonic Materials and Devices VIII, edited by J G Grote, F Kajzar, N Kim, Proc. of SPIE, 6117, 61170N, (2006)

19. Z Yu, Y Zhou, D J Klotzkin, J G Grote, A J Steckl, Stimulated emission of sulforhodamine 640 doped DNA distributed feedback (DFB) laser devices, Organic Photonic Materials and Devices IX, edited by J G Grote, F Kajzar, N Kim, Proc. of SPIE Vol. 6470, 64700V, (2007)

20. Z Yu, W Li, J A Hagen, Y Zhou, D Klotzkin, J G Grote, A J Steckl, Photoluminescence and lasing from deoxyribonucleic acid (DNA) thin films doped with sulforhodamine, Appl. Opt., 46, 1507, (2007)

21. M Honda, N Nakai, M Fukuda, Y Kawabe, Optical amplification and laser action in cyanine dyes doped in DNA complex, Nanobiotronics, edited by E M Heckman, T B Singh, J Yoshida, Proc. of SPIE, 6646, 664609, (2007)

22. T Chida, Y Kawabe, Tunable dye lasers based on DNA-surfactant-dye complexes, Nanobiosystems: Processing, Characterization, and Applications IV, edited by N Kobayashi, F Ouchen, I Rau, Proc. of SPIE. 8103, 81030P, (2011)

23. Y Kawabe, K I Sakai, DNA based solid-state dye lasers, Nonlinear Optics and Quantum Optics, 43, 273, (2011)

24. T Chida, Y Kawabe, Tunable DFB lasers based on DNA-surfactant-dye complexes, Nanobiosystems: Processing, Characterization, and Applications V, edited by N Kobayashi, F Ouchen, I Rau, Proc. of SPIE, 8464, 84640E, (2012)

25. T Chida, Y Kawabe, Hemicyanine-DNA-complex: Application to solid-state dye lasers, Nonlinear Optics and Quantum Optics, 45, 85, (2012)

26. Y Kawabe, T Chida, T Matsuoka, K Fukuzawa, K Tada, Grating formation in bi-layered DNA-complex devices: Application to thin-film tunable dye lasers, Nanobiosystems: Processing, Characterization, and Applications VI, edited by N Kobayashi, F Ouchen, I Rau, Proc. of SPIE, 8817, 881707, (2013)

27. T Chida, Y Kawabe, Transient grating formation in azo-doped polymer and its application to DNA-based tunable dye laser, Opt. Mater. 36, 778, (2014)

28. T Suzuki, Y Kawabe, Light amplification in DNA-surfactant complex films stained by hemicyanine dye with immersion method, Opt. Mater. Express, 4, 1411, (2014)

29. Y Kawabe, T Suzuki, Y Iisaka, Light amplification and lasing from dyes doped in DNA-complex thin films prepared by soaking method, Nanobiosystems: Processing, Characterization, and Applications VII, edited by N Kobayashi, F Ouchen, I Rau, Proc. of SPIE, 9171, 91710G, (2014)

30. Y Kawabe, T Suzuki, Y Iisaka, Light amplification in DNA and other polyion complexes stained with simple immersion technique, Nonlinear Optics and Quantum Optics, 47, 211, (2015)

31. Y Suzuki, Y Kawabe, Optical amplification in DNA-surfactant complexes incorporating hemicyanine dyes with long and short alkyl chains, Nanobiosystems: Processing, Characterization, and Applications VIII, edited by N Kobayashi, F Ouchen, I Rau, Proc. of SPIE, 9557, 955709, (2015)

32. J Mysliwiec, L Sznitko, B Smoczynska, S Bartkiewicz, A Miniewicz, B Sahraoui, F Kajzar, Applications of the DNA-based material for lasing and dynamic holography, Organic Photonic Materials and Devices XI, edited by R L Nelson, F Kajzar, T Kaino, Proc. of SPIE, 7213, 72130I (2009)

33. J Mysliwiec, L Sznitko, A Miniewicz, F Kajzar, B Sahraoui, Study of the amplified spontaneous emission in a dye-doped biopolymer-based material, J. Phys. D: Appl. Phys., 42, 085101, (2009)

34. J Mysliwiec, L Sznitko, S Bartkiewicz, A Miniewicz, Z Essaidi, F Kajzar, B Sahraoui, Amplified spontaneous emission in the spiropyran-biopolymer based system, Appl. Phys. Lett. 94, 241106 (2009)

35. J Mysliwiec, L Sznitko, A Sobolewska, S Bartkiewicz, A Miniewicz, Lasing effect in a hybrid dye-doped biopolymer and photochromic polymer system, Appl. Phys. Lett., 96, 141106, (2010)

36. L Sznitko, J Mysliwiec, P Karpinski, K Palewska, K Parafiniuk, Biopolymer based system doped with nonlinear optical dye as a medium for amplified spontaneous emission and lasing, Appl. Phys. Lett. 99, 031107 (2011)

37. I Rau, A Szukalski, L Sznitko, A Miniewicz, S Bartkiewicz, F Kajzar, B Sahraoui, J Mysliwiec, Amplified spontaneous emission of Rhodamine 6G embedded in pure deoxyribonucleic acid, Appl. Phys. Lett., 101, 171113, (2012)

38. J Myslieiec, L Sznitko, K Cyprych, A Szukalski, A Miniewicz, F Kajzar, I Rau, Random lasing in bio-polymeric dye-doped systems, Nanobiosystems: Processing, Characterization, and Applications VI, edited by N Kobayashi, F Ouchen, I Rau, Proc. of SPIE, 8817, 88170A, (2013)

39. A Camposeo, P D Carro, L Persano, K Cyprych, A Szukalski, L Sznitko, J Mysliwiec, D Pisignano, Physically transient photonics: Random versus Distributed feedback lasing based on nanoimprinted DNA, ACS Nano 8, 10893, (2014)

40. K Cyprych, Z Kopczyńska, F Kajzar, I Rau, J Mysliwiec, Tunable wavelength light emission and amplification in Rhodamine 6G aggregates, Adv. Device Mater., 1, 69, (2015)

41. Y C Hung, C H Su, H W Huang, Low threshold amplified spontaneous emission from dye-doped DNA biopolymer, J. Appl. Phys., 111, 113107, (2012)

42. T Y Lin, C Y Chang, C H Lien, Y W Chiu, W T Hsu, C H Su, Y S Wang, Y C Hung, Preparation and characterization of DNA-aromatic surfactant complexes for optoelectronic applications, Organic Photonic Materials and Devices XIII, edited by R L Nelson, F Kajzar, T Kaino, Y Koike, Proc. of SPIE, 7935, 79350E, (2011)

43. N Balan, M Hari, V P N Nampoori, Selective mode excitation in dye-doped DNA polyvinyl alcohol thin film, Appl. Opt., 48, 3521, (2009)

44. T B Rujoiu, A Petris, V II Vlad, I Rau, A M Manea, F Kajzar, asing in DNA-CTMA doped with Rhodamine 610 in butanol, Phys. Chem. Chem. Phys., 17, 13104, (2015)

45. V L Singer, L J Jones, S T Yue, R P Haugland, Characterization of PicoGreen reagent and development of a fluorescence-based solution assay for double stranded DNA quantitation, Anal. Biochem., 249, 228, (1997)

46. S J Ahn, J Costa, J R Emanuel, PicoGreen Quantitation of DNA: Effective Evaluation of Samples Pre-or Post-PCR, Nucleic Acids Res., 24, 2623, (1996)

47. A I Dragan, J R C Finet, E S Bishop, R J Strouse, M A Schenerman, D C Geddes, Characterization of PicoGreen interaction with dsDNA and the origin of its fluorescence enhancement upon binding, Biophys. J., 99, 3010, (2010)

48. W T Silvast, Laser Fundamentals, Chapter 7.6, 247, Cambridge University Press, New Delhi, (2004)

49. A E Siegman, Lasers, University Science Books, (1986)

50. C V Shank, A Dienes, W Silfvast, Single pass gain of exciplex 4-Mu and Rhodamine 6G dye laser amplifiers, Appl. Phys. Lett., 17, 307, (1970)

51. K L Shaklee, R F Leheny, Direct determination of optical gain in semiconductor crystals, Appl. Phys. Lett., 18, 475, (1971)

52. I D W Samuel, E B Namdas, G A Turnbull, How to recognize lasing, Nat. Photonics, 3, 546, (2009)

53. J Yoshida, H Takano, S Narisawa, S Takenaka, N Nakai, M Fukuda, N Ogata, Thin film dye lasers based on DNA-lipid complex materials, Nanobiotronics, edited by E M Heckman, T B Singh, J Yoshida, Proc of SPIE, 6646, 664608, (2007)

6

Effect of DNA in polymer LEDs

Abstract

Biopolymer based materials are of great interest in organic electronics and photonic devices due to their combined advantage of biodegradability, renewable resource of a biomaterial and easy processing techniques of a polymer. With the discovery of charge transport in DNA, it has been successfully incorporated as a hole transporting layer and electron blocking layer in light emitting diodes. We have fabricated an all-polymer solution processable LED using fluorene based polymers as active light emitting polymer. This chapter discusses the performance of Bio-LED in terms of output light brightness. The brightness was enhanced from 430 cd/m² to 1925 cd/m² by incorporating DNA as an electron blocking layer.

6.1 INTRODUCTION

Organic light emitting diode has been of great interest in recent years due to its application in high-efficiency solid-state lighting and high quality flat-panel displays[1]. However OLEDs require new materials for charge injection, charge transport, charge blocking and light emission that could improve their performance in terms of efficiency, brightness, stability and lifetime. Such materials require to possess specific optical and electrical properties that are well suited to carry out the specific task in the OLED device structure. Natural electronics is a developing area of research that explores naturally occurring or nature derived biomaterials to replace traditional synthetic materials in solid state organic electronics. As described in chapter 2, marine derived DNA extracted from salmon fish shows unique optical and electrical properties necessary for an electron-blocking layer (EBL) in OLED. DNA as the EBL has proved to increase the efficiency and luminance of organic light emitting diodes and promises a great future as a photonic material in OLEDs.

Following initial reports of electrical conductivity in DNA[2-13], the biomolecule was first applied to organic light emitting diodes by Kobayashi et al.[14] in 2001 followed by Koyama et al.[15] in 2002. They used DNA as a template or as a host material for lumophores confirming that the charge carriers could be injected and transported in the biomaterial. In 2004, Koyama et al.[16] prepared organic solvent soluble DNA complex to be used as a separate buffer layer in organic light emitting diodes for explaining the electrical conductivity. However, no significant improvement in device performance was achieved. Investigating this unsuccessful device performance, Grote and Steckl studied the properties[17] of DNA lipid complex and closely examinied the Highest Occupied Molecular Orbital (HOMO) and Lowest Unoccupied Molecular Orbital (LUMO) levels and understood that the complex exhibited electron blocking and hole transporting capabilities in light emitting diodes. These properties are discussed in detail in the next section. By using the biomaterial complex as an electron blocking layer, the devices showed increased performance in terms of brightness, lifetime and efficiency. With this understanding, numerous reports followed involving small molecules[18-26], nanoparticles[27-30] and polymer[31-34] based light emitting diodes. Hagen at al.[18,19] used small molecules viz. tris-(8-hydroxy quinoline) aluminum (Alq$_3$) and *N*, *N*′-bis(naphthalene-1-yl)- *N*, *N*′-bis(phenyl) benzidine (NPB) as active emissive layers

to fabricate BioLEDs, which performed 10x efficient, 30x brighter and 3x longer life than the control devices.

In addition to narrow and tunable emission from Quantum Dots, they exhibit high external quantum efficiency especially with core/shell configuration. Sun et al.[27,28] incorporated the effect of DNA in double-shell CdSe/CdS/ZnS (core/shell/shell) quantum dot. They also demonstrated deposition of DNA complex using matrix assisted pulsed laser evaporation (MAPLE) technique along with the conventional spin coating technique. MAPLE technique retains the chemical and structural integrity of the biomaterial while producing high quality uniform film. DNA as EBL was also incorporated in PFO/MEH:PPV based copolymer[31] to demonstrate white light emitting diodes with reduced turn-on voltage.

Kobayashi at al.[20-22] developed a voltage-controlled color tunable LED using a bilayer consisting of a lumophore doped in water soluble DNA/polyaniline complex and Alq$_3$ as emissive layers. The tunability ranged from green to red region as the voltage was varied from 5 V to 18 V. The tunability was attributed to the shift in the recombination sites from Alq3 to the rubidium based lumophore.

Mathur at al.[32,33] fabricated polymer LEDs with PFO and MEH:PPV as emissive layers to observe two-fold increase in the luminance. They also developed UV LEDs from ZnO nanorods[29] with the help of DNA as electron blocking layer.

Zalar et al.[34] explored to use DNA complex as electron injection/ hole blocking layer in polymer light emitting diodes with aluminum as cathode. Usually low work function materials such as Barium (Ba) and Calcium (Ca) are used as buffer layer to match the LUMO level of electroluminescent semiconducting conjugated polymers along with stable metal electrodes (Al, Au or Ag). DNA based devices exhibited enhanced performance in terms of turn-on voltage and luminous efficiency over their control device without DNA layer. This performance was comparable with devices using Ba/Al as cathode.

Hung at al.[23,30] tailored the material properties of DNA complex layer by varying the amount of aromatic surfactant and by incorporating metal nanoparticles such as Ag and

Au in the complex. Such modified DNA layer made significant improvement in luminance and current efficiency.

It was known that the base pairs of DNA were responsible for charge transport rather than the sugar phosphate backbone. This inspired Gomez et al.[25,26] to use the nucleobases to improve the performance of BioLEDs. The properties of Adenine, Guanine, Cytosine, Thymine and Uracil were studied and incorporated in organic light emitting diodes as electron blocking/hole transporting and hole blocking layer/electron transporting configurations. Of all the nucleobases, Adenine based devices proved to be efficient in terms of efficiency and current transporting capabilities.

In this work we focused on developing an all-polymer BioLED for optimizing the thickness of DNA complex layer to extract maximum performance from the devices. For this purpose we varied the thickness of DNA layer from ~30 nm to 5 nm by varying the spin parameters and concentration of the complex. The performance was rated by maximum luminance.

6.2 DNA AS HOLE TRANSPORTING AND ELECTRON BLOCKING LAYER

As mentioned in the last section, DNA has been introduced to organic light emitting devices as a non-emitting host material for small molecule dyes. However, such device structures were unsuccessful. DNA based OLED devices proposed by Kobayashi et al.[14], and Koyama et al.[15] showed the feasibility of using the biopolymer in light emitting devices, but without any significant improvement in the performance of the devices. Hirata et al.[16] demonstrated various device structures in which the DNA-CTMA layer was incorporated to take different roles in organic light emitting diodes. Better performance was achieved in the device where DNA-CTMA was incorporated between hole transporting layer and emissive layer concluding that DNA-CTMA preferentially transports holes and barring electron injection from the adjacent carrier transport layer. This interesting work led the scientists and researchers to explore the properties of DNA-CTMA layer.

By closely examining Hirata's work, it became clear that DNA-CTMA may have the properties of an electron blocking layer. The HOMO level of DNA-CTMA is located at 5.6 eV. This efficiently aids the hole transportation from PEDOT:PSS (HOMO - 5.2 eV) to the emissive iridium based polyvinyl carbazole layer (HOMO – 5.7 eV). Additionally the LUMO level at 0.9 eV also aids by providing a large barrier to block the flow of electrons and thereby increasing the electron-hole recombination in the emissive layer. The DNA-CTMA layer provided a step barrier of 1.3 eV with the emissive layer, the LUMO of which is located at 2.2 eV. Thus the prime location of HOMO and LUMO level of DNA-CTMA helps to inject hole and electrons into the emissive layer, leading to an efficient recombination. This property had led to an increase in enhanced brightness and improved efficiency in DNA based organic light emitting devices. Hagen et al.[18] conveniently demonstrated organic light emitting diodes using DNA-CTMA complex as electron blocking layer.

There are several other crucial factors that make DNA-CTMA a promising material for the design of optoelectronic thin film device applications. Being transparent in the visible and near infra-red region helps the cause of using transparent conductive ITO. Low optical loss with suitable refractive index helps DNA-CTMA to be used in optical waveguide devices. This biopolymer complex is thermally stable upto 225 °C, which makes it much more viable than other polymers such as polycarbonate and polymethyl methacrylate. DNA efficiently transports electrical charge and helps to operate DNA-CTMA based devices at low voltages. The electrical resistivity of DNA can be tailored by varying its molecular weight. Simple techniques such as spin coating and inkjet printing could be used to fabricate DNA-CTMA thin films, which would effectively reduce the cost of devices.

6.3 POLYMERS USED IN FABRICATION OF BIO-LED

All the polymers except the biopolymer DNA are reviewed in the following sections. The biopolymer have been adequately discussed in chapter 2 and section 6.2. We have used three polymers viz. (1) hole transporting PEDOT:PSS; (2) active PFO:F8BT blend; and (3) electron injecting PFN.

6.3.1 Hole Transporting Layer - PEDOT:PSS

We used poly(3,4-ethylenedioxythiophene)-poly(styrenesulfonate), commonly known as PEDOT:PSS as hole transporting layer in all the devices. The structure of PEDOT:PSS is depicted in figure 6.1. This polymer is commonly used for hole transporting in many polymer based light-emitting diodes due to the following advantages. One of the important factor of these interfacial buffer layer is to provide suitable step barrier for the transport of holes and electrons to the emissive layer. The ITO has a work function of 4.7 eV while the emissive layer has an HOMO level at 5.8 eV. The HOMO level of PEDOT:PSS falls at 5.2 eV which bridges the gap between anode and emissive layer. This makes the polymer a good hole transporter. Additionally the polymer smoothens the surface of ITO, so that the emissive layer could be coated over a smoother surface. The polymer is also transparent which helps to aid the use of transparent anode to extract light from the diode.

6.3.2 Active Emissive Layer – PFO:F8BT

Conjugated polymers attracted interest from the scientific community and found their first application in light emitting diodes. Initially poly(p-phenylene vinylenes) were of main interest, but were later turned to polyfluorenes. Polyfluorenes consists of repeating units of two coplanar benzene rings with a central carbon having two hydrogen bonds that breaks the planarity with the benzene rings. These class of polymers are of great interest in academic and industrial research due to their conjugated nature, high fluorescence quantum yield, good charge transport properties, high net gain and electroluminescence property. In fact they are the only class of conjugated polymers, whose emission can be tuned throughout the visible region by staining it with chromophoric constituents. Among the polyfluorenes poly(9,9-dioctylfluorene) (PFO, also known as F8), and a derived copolymer, poly(9,9-dioctylfluorene-altbenzothiadiazole) (F8BT), are the most well-studied light emitting polymers. Such derived polyfluorenes are of particular interest because they contain a rigid biphenyl unit – which emits in the blue region due to their large bandgap, and the possible substitution of side chains at the C9 position of the fluorene group – which improves the solubility, emission tunability and processability for applicability in polymer light emitting diodes[35].

In this study we have used blends based on PFO and F8BT as active light emitting material. The structure of PFO and F8BT is shown in figure 6.1. The reason for using this particular blend is two-fold[36]. One is that the charge motilities of these two polymers are complementary to each other. PFO efficiently conducts holes while the latter conducts electrons. The other is that there is a strong overlap between the emission of PFO and absorption peak of F8BT. This results in efficient energy transfer from PFO to F8BT. In a study conducted by Lidzey et al.[37], it was concluded that there appears a particular ratio of the polymer blends to sufficiently allow complete Förster resonant energy transfer from PFO to F8BT. This ratio was considered in this current investigation.

6.3.3 ELECTRON INJECTION LAYER - PFN

The electron injection layer used for this study was poly [(9,9-bis(3'-(N,N-dimethylamino)propyl)-2,7-fluorene)-alt-2,7-(9,9-dioctylfluorene), PFN. This copolymer is a polyfluorene based polymer containing fluorene unit and amino end groups to their side chains. The structure of PFN is depicted in figure 6.1. The synthesis of this aminoalkyl-substituted polyfluorene copolymer is reported by Huang et al.[38]. PFN is soluble in most organic solvents such as toluene, chloroform, tetrahydrofuran and xylene, but insoluble in dimethyl sulfoxide and water. It is thermally stable upto 250 °C. As an emitting layer, this polymer luminesce at around 500 nm with a maximum quantum efficiency of 0.38 %.

Charge injection and charge transport are the limiting factors of device efficiency and operating lifetime. In polymer light emitting diodes, charge injection and transport in most light emitting polymers are limited by its LUMO level. Hence it is necessary to use low-work function metals such as Ca and Ba along with high-work function metal cathodes such as Al, Ag and Au. However, these low-work function metals are highly sensitive to air and can degrade the lifetime of the devices. PFN has proved[39] to enhance the electron injection in various light emitting polymers viz. MEH:PPV, P:PPV and PFO resulting in highly efficient polymer light emitting diodes, whose performance are comparable to those that use Ca and Ba as with cathodes. Xiao et al.[40] has reviewed the use of polyfluorene based cathode interfacial layers for efficient polymer solar cells.
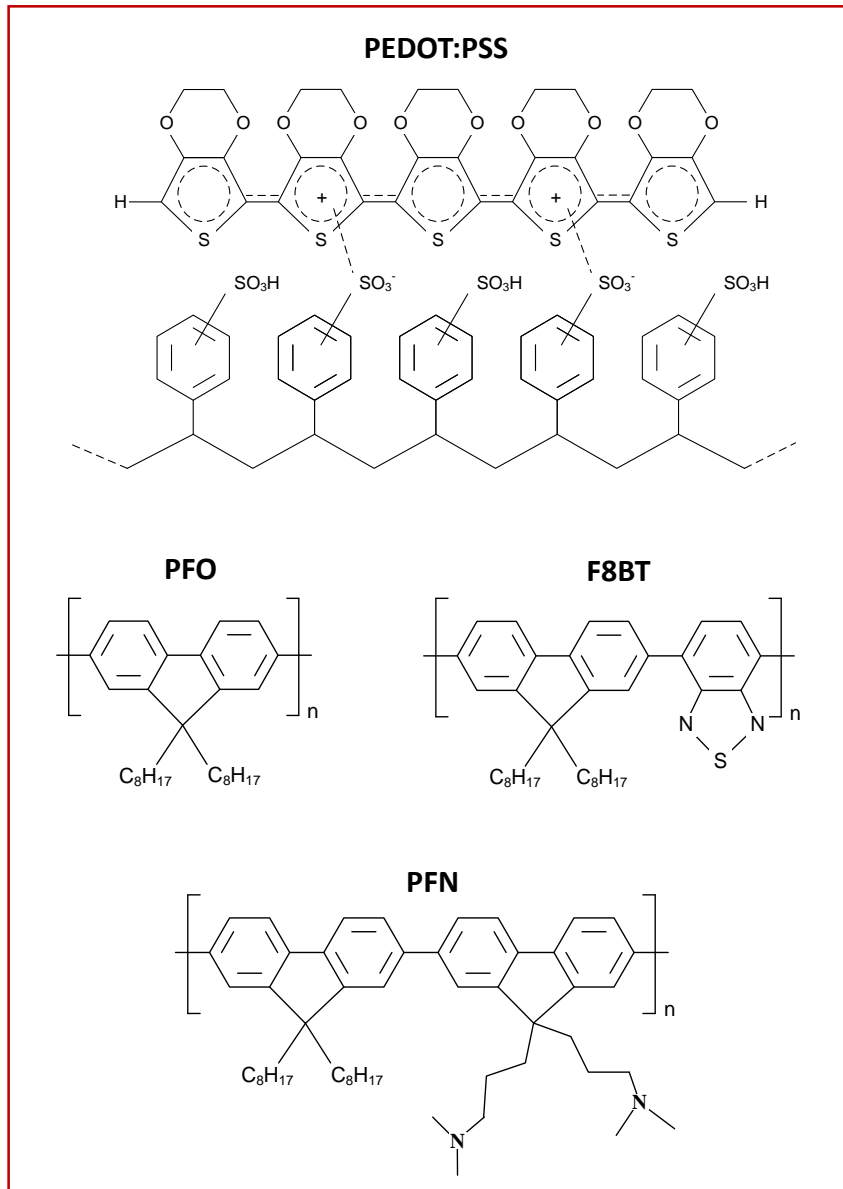
Figure 6.1: Molecular structure of PEDOT:PSS, PFO, F8BT and PFN.

6.4 DEVICE FABRICATION OF ALL POLYMER BIO-LED

Light-emitting diodes were prepared layer by layer on pre-cleaned non-patterned ITO glass substrates. The ITO coated over the glass substrates was used as a common anode and was cut into 1" x 1" square substrates. The sheet resistance of the ITO is 8-12 Ω/sq and the thickness of the coating is 120-160 nm with a surface roughness of 30-45 nm, as informed by the manufacturer. The ITO surface may not be smooth and contain large spikes. These spikes may project out to the overlying polymer layers and along with diffusion of metal cathode to the polymers shall pose problem of shorting. Therefore a part of the ITO was etched from the substrates (see figure 6.2). The metal cathode shall be coated over the etched portion with some portions overlapping with anode ITO. The overlapped potion shall form the active area of the light-emitting diode. The portion of the ITO to be protected from etching is covered with cello-pane tape. Care should be taken to see that the edges of the tape are sealed properly and no bubbles remain under the tape. The substrate is then immersed in concentrated nitric acid (HNO_3) for about three minutes. The etching of ITO could be observed by viewing the substrates at an angle. Care should be taken to remove the substrates in time and not to soak in the acid for more than five minutes. This will allow the tape to be affected by the acid as it may sweep through the tape. The substrates were removed and dipped in water. The cello-pane tape is removed immediately and washed with copious water. The fabrication procedure starts with laborious cleaning procedure. Such an elaborate cleaning procedure is necessary for good device performance and to avoid black spots on the active area of the device. The dust particles shall also pose problems of surface wetting properties and create pinholes or comet streaks. The substrates were handled with the help of tweezers. The cleaning procedure start with rubbing the ITO surface with undiluted laboratory detergent to remove any visible dirt, markings or dust particles. The substrates were then placed in a cleaning rack and immersed completely in a beaker containing diluted laboratory detergent. The beaker is placed in an ultra-sonicator bath and sonicate it for about 30 minutes. This is followed by ultra-sonication in deionized water, acetone, isopropyl alcohol and ethanol for 30 minutes each. Every time the solvent is changed, the substrates were rinsed/sprayed with the successive solvent to be cleaned with. After ultra-sonication with all the solvents, the cleaning rack along with the substrates were transferred to an empty beaker and placed in drying oven at 60 °C

for about an hour (usually overnight, a day before the device fabrication). The substrates were again cleaned by blowing nitrogen gas through a nozzle to remove any foreign substances. The substrates were then treated with ultra-violet radiation along with ozone gas using a UV-O$_3$ cleaner (UVOCS Inc., Model: T10X10/OES/E). This treatment will help to remove any organic contaminants and increase surface wetting properties for the hydrophilic hole transporting layer for adhesion to the substrate. Once the substrates were subjected to UV/O3 treatment, the substrates were immediately transferred to the glove box filled with nitrogen. This shall avoid any reabsorption of water vapor or oxygen to the surface from atmosphere. This completes the cleaning procedure. It is best to commence fabrication procedure immediately. In case of delay the substrates were stored on a hot plate at 120 °C with the ITO surface facing up, until the coating of the first polymer.

The first layer deposited was PEDOT:PSS as hole transporting layer by spin coating. The PEDOT:PSS was procured from Sigma Aldrich, USA. The polymer was used as received and without any dilution. The polymer was filtered using a rubber-free syringe and a PVDF syringe filter of pore size 0.45 μm. The filtered polymer was further stirred for two hours prior to coating. The polymer was spin coated by dynamic coating procedure detailed in section 3.3.1.1. The parameter for the coating is 5000 rpm for 30 seconds. The polymer film was then annealed on a hot plate at 150 °C for 5 minutes which ensured removal of excess solvent. These parameters yielded a film thickness of 80 nm, measured by optical reflectance system using Theta-Metrisis FR-pOrtable.

In Bio-LED the second layer was DNA:CTMA. The DNA:CTMA was prepared as described in section 2.3. The DNA:CTMA was dissolved in butanol at a concentration of 1 mg/ml and 0.7 mg/ml. Four different devices were fabricated by dynamically coating the above mentioned two concentrations of DNA:CTMA, each at 5000 rpm and 10000 rpm for 20 seconds. The DNA films were annealed at 80 °C for 5 minutes. The thickness of the DNA films fabricated were 29 nm, 27 nm, 17 nm and 17.5 nm; and were named Device B, C, D and E respectively. A device without DNA:CTMA layer, named Device A, was also fabricated to serve as a control device.

The next layer was the active polymer PFO:F8BT. The PFO and F8BT polymers were prepared separately in toluene at a concentration of 15 mg/ml. The two polymers were

filtered separately using a PTFE syringe filter of pore size 0.2 μm and then mixed in a volume ratio of 19:1 to prepare a blend of PFO and F8BT. This co-polymer yielded a thickness of 55 nm when it was dynamically spin coated at 8000 rpm for 20 seconds. The annealing was done at 80 °C for 10 minutes.

The last polymer, PFN was coated over the active co-polymer. PFN was prepared in methanol at a concentration of 2 mg/ml. A few drops of acetic acid was used to improve the solubility of PFN. The polymer solution was filtered using PTFE syringe filter of pore size 0.20 μm. PFN was coated dynamically at 2000 rpm for 15 seconds. Using the above parameters, the thickness of the PFN film was estimated to be 45 nm.

Table 6.1: Spin coating parameters of various polymers used in BioLED

Polymer	Concentration (mg/ml)	Rotation		Annealing		Thickness of the film (nm)
		Speed (rpm)	Time (s)	Temperature (°C)	Time (minutes)	
PEDOT:PSS	As received	5000	30	150	5	80
DNA:CTMA	1 1 0.7 0.7	5000 10000 5000 10000	20	80	5	29 27 17 17.5
PFO:F8BT	15	8000	20	80	10	55
PFN	2	2000	15	-	-	45

Care has been taken to choose the solvents of successive layers, such that the underlying layer is not washed away. The polymers were properly filtered using suitable filter for the solvents, to ensure uniform coating and smooth films. The edge of the substrates were cleaned using a cotton bud dipped in chlorobenzene, to expose the part of the ITO for anode contact.

Finally, the polymer coated substrates were removed from the nitrogen glove box and transferred to vacuum chamber of the thermal evaporation system. The polymer coated

substrates were placed with the polymer layers facing down on a shadow mask containing cathode strips with wide end apertures. The substrates were placed such that one of the wide end aperture overlaps with the unetched ITO substrate surface to make an active area of 0.09 cm^2. The pressure in the vacuum chamber was brought down to 3×10^{-6} Torr using a turbo pump backed by a rotary pump. Lithium fluoride was first coated as a buffer layer that helps to reduce the work function of the metal cathode. A very thin layer of 2 nm was coated at the rate of 0.1 Å/s, measured using digital thickness monitor with the help of piezoelectric crystal. At last the metal cathode was coated without breaking the vacuum. We used aluminum of thickness 100 nm at the rate of 1 Å/s as metal cathode.

These devices were immediately encapsulated to protect the active area from reacting with oxygen or moisture. We used a specialized UV curable epoxy from Ossila Limited, UK to seal a coverslip over the active area. Curing is done by irradiating the device with UV light for about 30 minutes. Thereafter the devices were immediately characterized at laboratory atmosphere in air. The characterization set up to measure luminance-current density-voltage curves and electroluminescence was detailed in section 3.3.2. The final device structure of BioLED is depicted in figure 6.2, with its energy level diagram shown in figure 6.3. Figure 6.4a and 6.4b shows the actual photograph of the device before encapsulation.
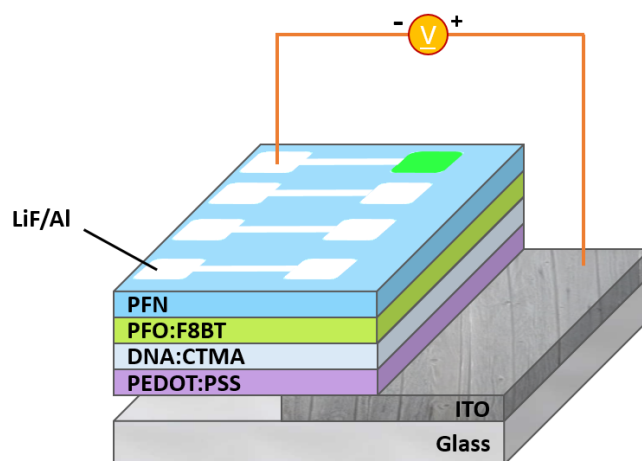
Figure 6.2: Device structure of BioLED incorporating DNA:CTMA as EBL.
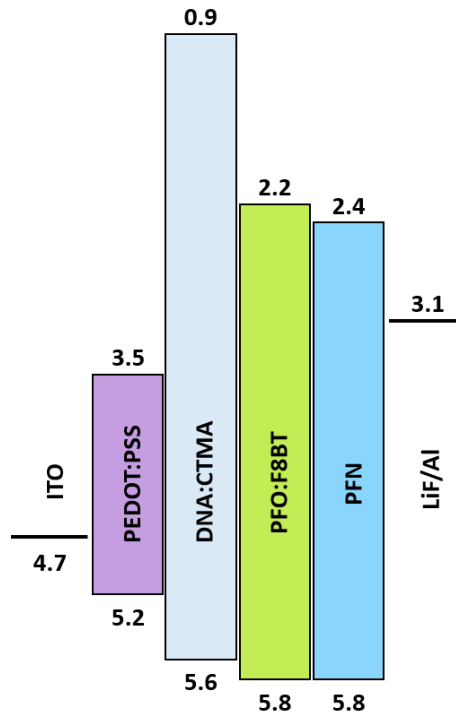
Figure 6.3: Energy level diagram of BioLED incorporating DNA:CTMA as EBL.
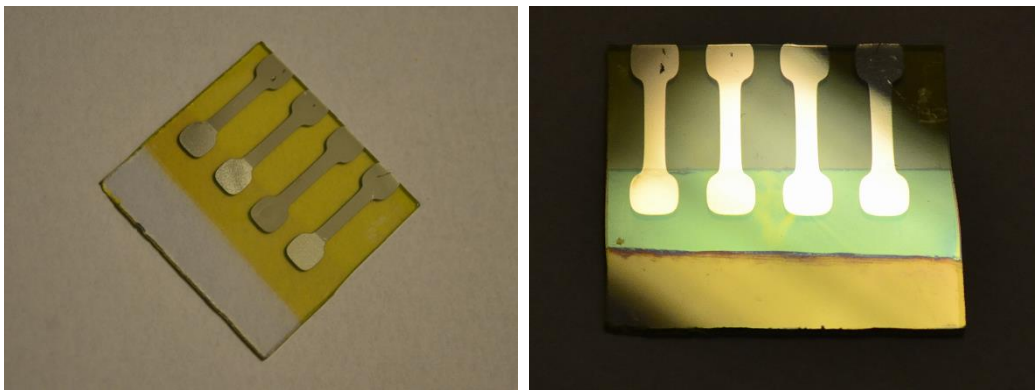
Figure 6.4: (a) Actual photograph of the final device before encapsulation (b) Reflection from the device shows the cleaned common anode at the bottom with the lower end of the cathode strip overlapping the underlying ITO layer.

6.5 PERFORMANCE OF BIO-LED

All the materials used in this device structure except for the electrodes are polymers. Here, the transparent ITO is used as anode with a work function of 4.7 eV while PEDOT:PSS, a well known polymer, is used to transport holes effectively due to its matching HOMO level with the ITO substrate. The biopolymer, DNA:CTMA is used as an electron blocking layer to control the flow of electrons from cathode directly to anode and help the recombination sites localized in the active light emitting material. The active layer is a blend of two polymers, a blue emitting PFO and green emitting F8BT. The emission is by fluorescence decay due to the absorption of photons emitted by the recombination of holes and electrons in the π and π^* band of the polymer. PFN is an aminoalkyl substituted polyfluorene co-polymer employed as cathode interfacial layer which helps to avoid the use of low work function metals such as Ca or Ba, that are susceptible to moisture and oxygen. Though the presence of PFN in the device reduced the brightness, the efficiency was much improved. A thin layer of Lithium Fluoride (LiF) was coated prior to the deposition of Aluminum without breaking the vacuum to alter the work function of
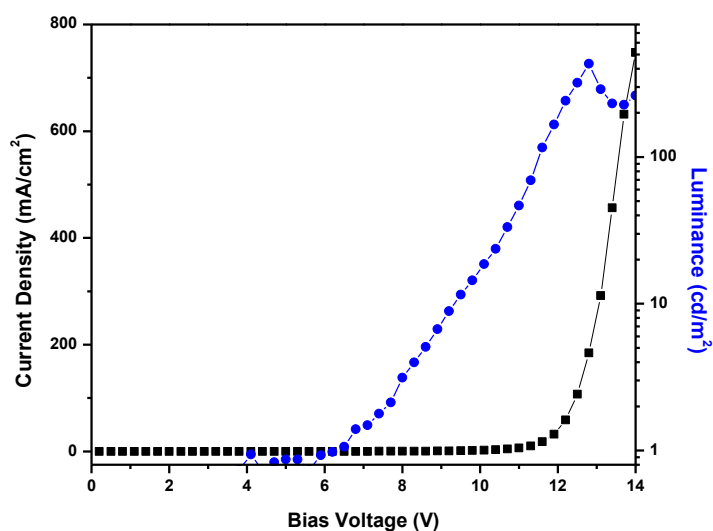
Figure 6.5: j-L-V characteristics of device A (control device).
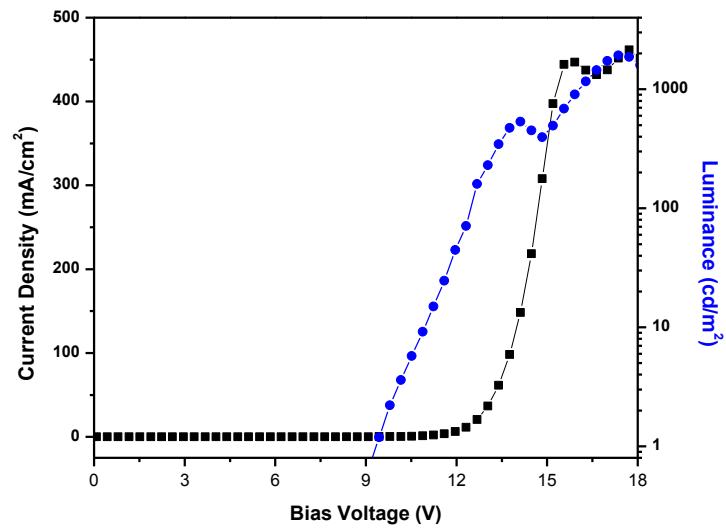
Figure 6.6: j-L-V characteristics of device E (BioLED).
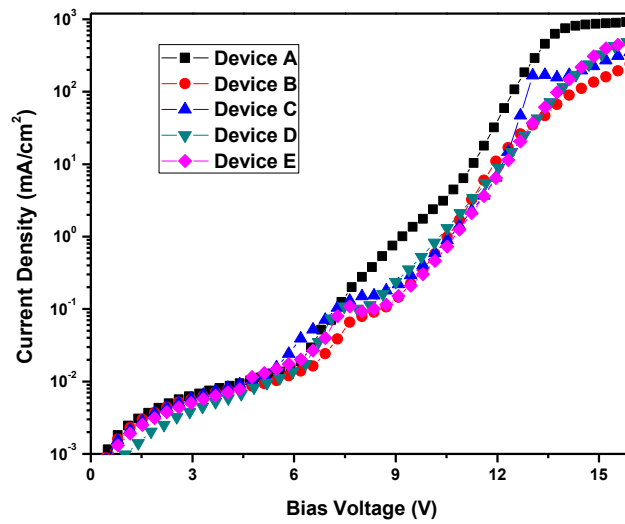
Figure 6.7: j-V characteristic of device A (control device) and B, C, D and E (BioLED) of varying DNA:CTMA thickness.
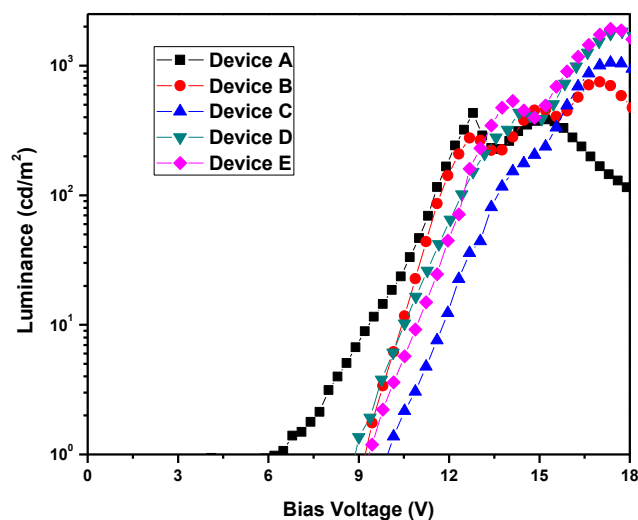
Figure 6.8: L-V characteristic of device A (control device) and B, C, D and E (BioLED) of varying DNA:CTMA thickness.

Aluminum from 4.7 eV to 3.1 eV. We have also confirmed that combined contribution of PFN and LiF increased the efficiency compared to a device with either PFN or LiF.

The L-j-V (Luminance – Current density – Voltage) characteristic of PFO:F8BT based device with and without DNA layer (Device **A** and **E**) is shown in figure 6.5 and 6.6 respectively. All the devices were cycled from 0 V to 20 V with a resolution of 0.3 V, while simultaneously recording the current through the device and the photocurrent from the photo diode. The current through the device was converted to current density knowing the active area of the device, and the photocurrent was converted to luminance by calibrating the photodiode with the help of a standard LED. On comparing the luminance plots in figures 6.5 and 6.6, it is evident that the brightness was improved by incorporating the biopolymer.

The current density dependence on the applied voltages of all the devices **A** to **E** are displayed in figure 6.7. We see that the device **A**, with no DNA:CTMA layer has higher current density and attained a maximum at ~ 900 mA/cm^2 above 14 V. Above 7 V the

current density of the devices with EBL dropped considerably and above 14 V, we could observe the current density was dependent on the thickness of the DNA:CTMA layer. Here, the device **B** has the thickest DNA:CTMA layer (29 nm) while the device **D** has lowest DNA:CTMA layer (17 nm). This drop in the current density could be attributed to the increase in the overall resistance of the devices in accordance with the presence of DNA:CTMA layer and its thickness. The linear behavior of log of current density with respect to the bias voltage shows the stable operation of diodes.

A comparative plot of the luminous performances of all the devices are depicted in figure 6.8. We could observe that the turn on voltage of device **A** is 6.5 V, while the devices with DNA:CTMA layer was around 9-10 V. However the interesting feature we perceive is that the maximum luminance values are obtained for devices with DNA:CTMA layer. The maximum luminance of device **A** was achieved at 432 cd/m^2 at 12.8 V; the device **B** reached 748 cd/m^2 at 17 V; device **C** reached 1056 cd/m^2 at 17.3 V; device **D** reached 1831 cd/m^2 at 17.7 V; and device **E** reached 1924 cd/m^2 at 17.3 V. It could be noted that the maximum luminance was achieved at higher voltages for devices with DNA:CTMA layer in comparison with devices without DNA:CTMA layer. The observed luminance
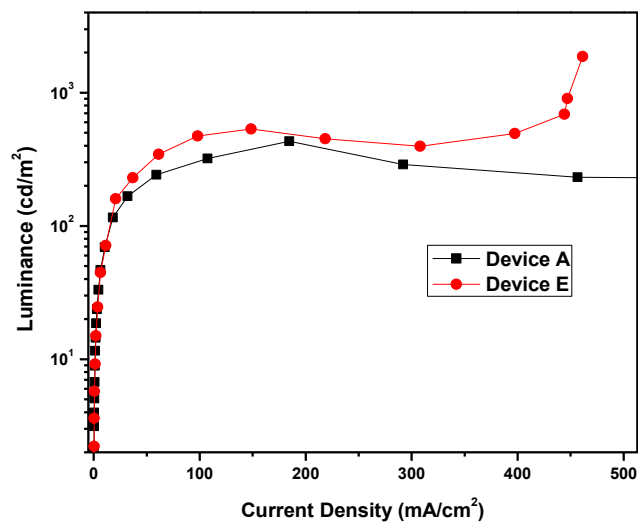

Figure 6.9: Current density vs Luminance plot of device A (control device) and device E (BioLED).

from PFO:F8BT based devices with DNA:CTMA layer was enhanced by more than 4 times over the device without DNA complex layer.

Figure 6.9 shows the luminance performance as a function of current density for device **A** and device **E**. The DNA:CTMA incorporated device showed improved luminance performance above 20 mA/cm^2. At a typical current density of 460 mA/cm^2 the device with DNA:CTMA layer showed an 8 fold increase in luminance over the device without EBL. This enhanced performance of the DNA:CTMA based device is attributed to the combination of HOMO and LUMO levels of DNA that efficiently transports holes to the active polymer while blocking electrons from cathode to directly flow towards anode.

In a separate set of experiments, the thickness of DNA complex layer was reduced to ~5 nm by varying the concentration of the lipid complex extracted from the same batch of DNA:CTMA used in earlier experiments. However, such devices showed a loss in the performance weighted by the brightness of the OLED. Figure 6.10 shows a drop in the luminance by 50 % in the device with 5.5 nm DNA:CTMA and by 25 % in the device with 5 nm DNA:CTMA layer over the devices without DNA complex layer. This decrease in performance may be due to the reduced hole injection from PEDOT:PSS to the active layer leading to a charge imbalance at the recombination site. Figure 6.11 shows the emission characteristics of device **E** at 17 V, where the brightness was maximum. We also found that there was no variation in the electroluminescence spectra of the devices with and without DNA:CTMA. The electroluminescence from PFO:F8BT blend ranges from 500 to 600 nm with its peak at 534 nm. Figure 6.12 shows the actual photograph of the emission from DNA:CTMA based light emitting diode (device **E**) at 17 V. The color of the light emitted from a light emitting diode can be classified by coordinates (x,y) in the color space chromaticity diagram as proposed by the International Commission on Illumination (CIE, 1931). The CIE 1931 color chromaticity coordinates were obtained from the EL spectra and found to be (0.33,0.61). This is mapped in color space as depicted figure in 6.13.
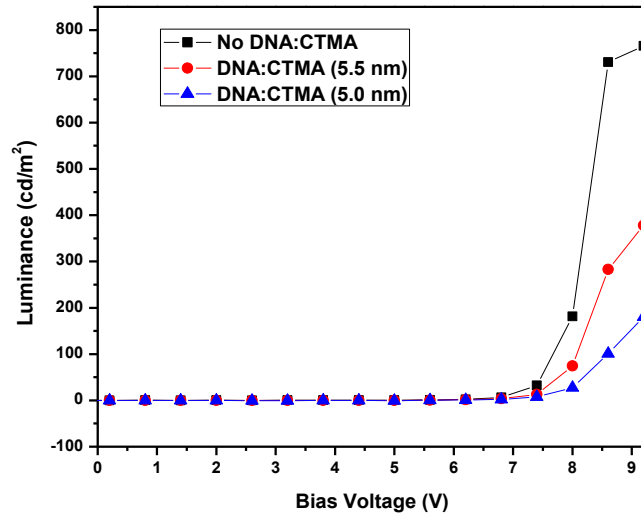
Figure 6.10: Luminance characteristic of devices with thin (~5 nm) DNA:CTMA as electron blocking layer.
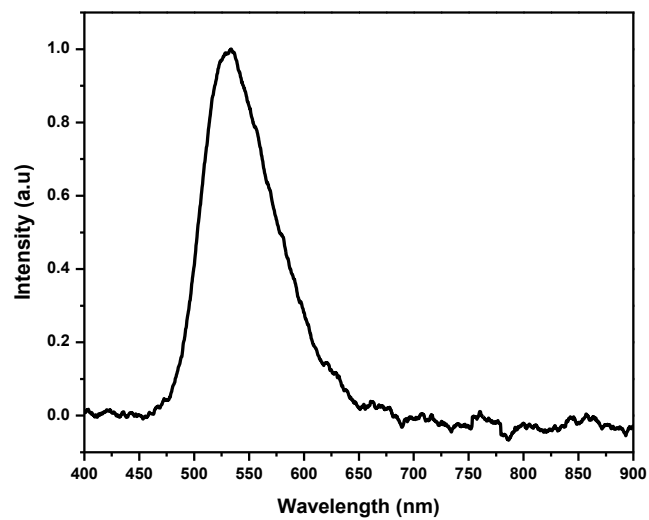

Figure 6.11: Electroluminescence spectra of device E (BioLED) at 17 V.
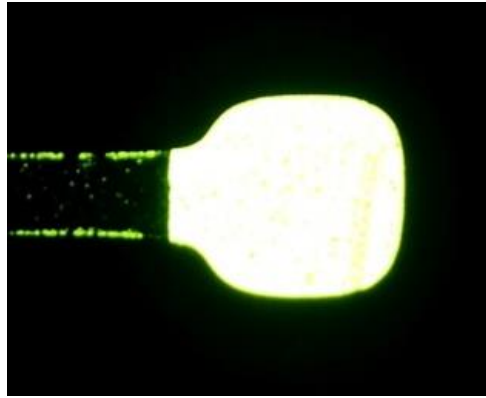
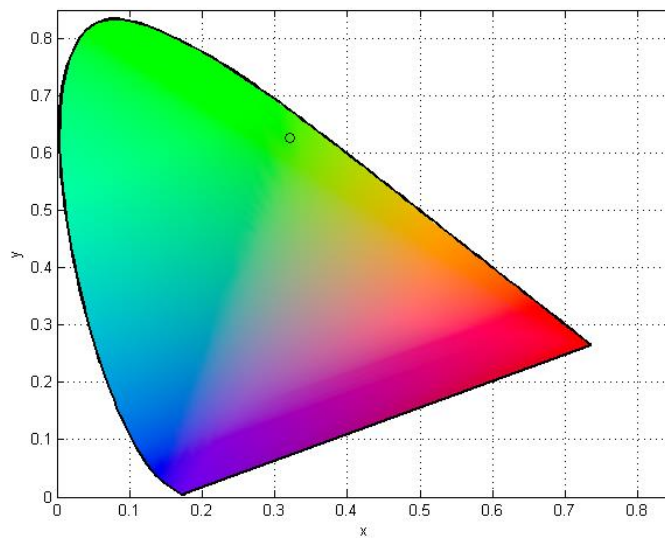Figure 6.12: Actual photograph of green emission from device E at 17 V.

Figure 6.13: CIE 1931 color chromaticity diagram with color co-ordinates of device E obtained from emission spectra (fig. 6.10).

6.6 CONCLUSIONS

In summary, we have incorporated DNA as electron blocking layer in PFO:F8BT based all solution processable polymer light emitting diode. With the prime position of HOMO and LUMO level of DNA complex, improved performance was achieved. The devices with DNA of thickness 17.5 nm exhibited increased brightness by four fold over the devices without DNA. The performance of the devices diminished when the thickness of DNA complex was reduced below 17.5 nm. On increasing the thickness of DNA complex, the luminance was decreased due to the efficient transport of holes. On the other hand, decreasing the thickness of DNA complex, improved the transport of excess of holes leading to a charge imbalance at the recombination site.

REFERENCES

1. R F Service, Organic LEDs look forward to a bright, white future, Science, 310, 1762, (2005)

2. C J Murphy, M R Arkin, Y Jenkins, N D Ghatlia, S H Bossmann, N J Yurro, J K Barton, Long-range photoinduced electron transfer through a DNA helix, Science, 262, 1025, (1993)

3. D N Beratan, S Priyadarshy, S M Risser, DNA: insulator or wire?, Chemistry & Biology, 4, 3, (1998)

4. Y Okahata, T Kobayashi, K Tanaka, M Shimomura, Anisotropic electric conductivity in an aligned DNA cast film, J. Am. Chem. Soc., 120, 6165, (1998)

5. H W Fink, C Schönenberger, Electrical conduction through DNA molecules, Nature, 398, 407, (1999)

6. S O Kelley, J K Barton, Electron transfer between bases in double helical DNA, Science, 283, 375, (1999)

7. D Porath, A Bezryadin, S de Vries, C Dekker, Direct measurement of electrical transport through DNA molecules, Nature, 403, 635, (2000)

8. M Tang, Electrical Conductivity in oriented DNA, REU Proceedings, National Nanofabrication Users Network, Pennsylvania University, 62, (2000)

9. B Giese, J Amaudrut, A-K Köhler, M Spormann, S Wessely, Direct observation of hole transfer through DNA by hopping between adenine bases and by tunnelling, Nature, 412, 318, (2001)

10. H Watanabe, C Manabe, T Shimotani, M Shimizu, Single molecule DNA device measured with triple-probe atomic force microscope, Appl. Phys. Lett., 79, 2462, (2001)

11. C Dekker, M Ratner, Electronic properties of DNA, Physics World, August 2001, 29, (2001)

12. E Wilson, DNA charge migration no longer an issue, C&EN, 79, 29, (2001)

13. D Klotsa, R A Römer, M S Turner, Electronic Transport in DNA, Biophys. J., 89, 2187, (2005)

14. N Kobayashi, S Uemura, K Kusabuka, T Nakahira, H Takahashi, An organic re-emitting diode with a water-soluble DNA-polyaniline complex containing Ru(bpy)32+, J. Mater. Chem., 11, 1766, (2001)

15. T Koyama, Y Kawabe, N Ogata, Electroluminescence as a probe for electrical and optical properties of deoxyribonucleic acid, Organic Light-Emitting Materials and Devices V, edited by Z H Kafafi, Proc. of SPIE, 4464, 248, (2002)

16. K Hirata, T Oyamada, T Imai, H Sasabe, C Adachi, T Koyama, Electroluminescence as a probe for elucidating electrical conductivity in a deoxyribonucleic acid-cetyltrimethylammonium lipid complex layer, Appl. Phys. Lett., 85, 1627, (2004)

17. J A Hagen, Enhanced luminous efficiency and brightness using DNA electron blocking layers in bio-organic light emitting diodes, PhD thesis, University of Cincinnati, (2006)

18. J A Hagen, W Li, A J Steckl, J G Grote, Enhanced emission efficiency in organic light-emitting diodes using deoxyribonucleic acid complex as an electron blocking layer, Appl. Phys. Lett., 88, 171109, (2006)

19. J A Hagen, J G Grote, W X Li, A J Steckl, D E Diggs, J S Zetts, R L Nelson, F K Hopkins, Organic light emitting diode with a DNA biopolymer electron blocking layer, Organic Light Emitting Materials and Devices X, edited by Z H Kafafi, F So, Proc. of SPIE, 6333, 63330J, (2006)

20. K Nakamura, T Ishikawa, D Nishioka, T Ushikubo, N Kobayashi, Color-tunable multilayer organic light emitting diode composed of DNA complex and tris(8-hydroxyquinolinato)aluminum, Appl. Phys. Lett., 97, 193301, (2010)

21. Supplementary material, K Nakamura, T Ishikawa, D Nishioka, T Ushikubo, N Kobayashi, Color-tunable multilayer organic light emitting diode composed of DNA complex and tris(8-hydroxyquinolinato)aluminum, Appl. Phys. Lett., 97, 193301, (2010), doi: 10.1063/1.3512861

22. N Kobayashi, BiOLED with DNA/Conducting polymer complex as active layer, Nonlinear Optics and Quantum Optics, 43, 233, (2011)

23. I C Chen, Y W Chiu, L Fruk, Y C Hung, Enhanced light emission from blue organic light emitting devices with DNA biopolymer, Quantum Electronics Conference & Lasers and Electro-Optics (CLEO/IQEC/PACIFIC RIM), 2011, 28 August - 1 September 2011, Sydney, Australia, 182-164, (2011)

24. R Grykien, B Luszczynska, I Glowacki, J Ulanski, F Kajzar, R Zgarian, I Rau, A significant improvement of luminance vs current density efficiency of a BioLED, Opt. Mater., 36, 1027, (2014)

25. E F Gomez, V Venkatraman, J G Grote, A J Steckl, Exploring the potential of nucleic acid bases in organic light emitting diodes, Adv. Mater., 2014, 1, (2014)

26. E F Gomez, V Venkatraman, J G Grote, A J Steckl, DNA bases thymine and adenine in bio-organic light emitting diodes, Sci. Rep., 4, 7105, (2014)

27. Q Sun, G Subramanyam, L Dai, M Check, A Campbell, R Naik, J Grote, Y Wang, Highly efficient quantum-dot light-emitting diodes with DNACTMA as a combined hole-transporting and electron-blocking layer, ACS Nano., 3, 737, (2009)

28. Supplementary material, Q Sun, G Subramanyam, L Dai, M Check, A Campbell, R Naik, J Grote, Y Wang, Highly efficient quantum-dot light-emitting diodes with DNACTMA as a combined hole-transporting and electron-blocking layer, ACS Nano., 3, 737, (2009)

29. R B Gupta, S Nagpal, S Arora, P K Bhatnagar, P C Mathura, Ultraviolet electroluminescence from zinc oxide nanorods/deoxyribonucleic acid hybrid bio light-emitting diode, J. Nanophotonics, 5, 059505-1, (2011)

30. Y W Chiu, I C Chen, Y C Hung, Enhanced efficiency in biopolymer nanocomposite light-emitting devices, Organic Photonic Materials and Devices XV, edited by C E Tabor, F Kajzar, T Kaino, Y Koike, Proc. of SPIE, 8622, 862217, (2013)

31. Q Sun, D W Chang, L Dai, J Grote, R Naik, Multilayer white polymer light-emitting diodes with deoxyribonucleic acid-cetyltrimetylammonium complex as a hole-transporting/electron blocking layer, Appl. Phys. Lett., 92, 251108 (2008)

32. D Madhwal, S S Rait, A Verma, A Kumar, P K Bhatnagar, P C Mathur, M Onoda, Increased luminance of MEH–PPV and PFO based PLEDs by using salmon DNA as an electron blocking layer, JoL, 130, 331, (2010)

33. D Madhwal, I Singh, J Kumar, C S Bhatia, P K Bhatnagar, P C Mathur, Increasing the luminous efficiency of an MEH-PPV based PLED using salmon DNA and single walled carbon nanotube, JoL, 131, 1264, (2011)

34. P Zalar, D Kamkar, R Naik, F Ouchen, J G Grote, G C Bazan, T Q Nguyen, DNA electron injection interlayers for polymer light-emitting diodes, J. Am. Chem. Soc., 133, 11010, (2011)

35. M Leclerc, Polyfluorenes: Twenty Years of Progress, J. Polym. Sci. A Polym. Chem., 39, 2867, (2001)

36. S Thomas, Y Grohens, P Jyotishkumar, Characterization of polymer blends: miscibility, morphology and interfaces, John Wiley & Sons, 831-835, (2014)

37. M Voigt, J Chappell, T Rowson, A Cadby, M Geoghegan, R A L Jones, D G Lidzey, The interplay between the optical and electronic properties of light-emitting-diode applicable conjugated polymer blends and their phase-separated morphology, Org. Electron., 6, 35, (2005)

38. F Huang, H Wu, D Wang, W Yang, Y Cao, Novel electroluminescent conjugated polyelectrolytes based on polyfluorene, Chem. Mater., 16, 708, (2004)

39. H Wu, F Huang, Y Mo, W Yang, D Wang, J Peng, Y Cao, Efficient electron injection from a bilayer cathode consisting of aluminum and alcohol-/water-soluble conjugated polymers, Adv. Mater., 16, 1826, (2004)

40. B Xiao, H Wu, Y Cao, Solution-processed cathode interfacial layer materials for high-efficiency polymer solar cells, Mater., Today, 18, 385, (2015)

7

General Conclusions

Abstract

This chapter summarizes the major findings reported in this thesis by drawing attention to the applicability of DNA:PG dye-lipid complex as a nonlinear optical material and as a lasing medium. However, such system could not find relevance as a light emitting polymer/dye due to the high lowest unoccupied molecular orbital (LUMO) level of the DNA that restrict itself as a host material for light emitting dyes. By the use of DNA as an electron blocking layer, we fabricated all solution processable polymer LED with improved performance. We further propose possible future advancements in DNA Photonics.

We would like to conclude this thesis by reminding its essence – which is bringing 'green technology' to aid the future generation. Photonic and electronic industries strive to become more 'green' by using natural materials that are renewable, abundant and inexpensive. Biomaterials, that are biodegradable, biocompatible, and bioresorbable plays an important role in creating a sustainable future. Over the past decade, the biomaterial, deoxyribonucleic acid known as the 'molecule of life' has been investigated in various photonic applications. The unique optical and electronic properties such as low optical loss, visibly transparent, suitable refractive index, thermal stability, mechanical robustness, wide HOMO/LUMO energy gap, lower resistivity, effective charge transport, led DNA to be a promising optical material.

In this context, this thesis was aimed at developing DNA-based new photonic materials and investigations were carried out in nonlinear optics, lasing materials and organic light emitting diodes. The major findings of this thesis which have contributed to the scientific knowledge are summarized below.

- The nonlinear optical properties of PicoGreen dye have been studied using open aperture transmission Z-Scan technique and found to possess nonlinear absorption coefficient of 116 cm/GW. PicoGreen dye exhibited an optical limiting type behavior with a threshold value of 36.2 MW/cm^2.

- We have also investigated nonlinear optical properties of Triazatriangulenium salt, which possesses nonlinear absorption coefficient of 810 cm/GW. The salt exhibited saturable absorption behavior with an RSA valley at the focus.

- The nonlinear refractive index of PicoGreen and Triazatriangulenium dyes were calculated using closed aperture transmission Z-Scan technique. It was found to be of the order of 10^{-12} cm^2/W for both the dyes. Reviewing the literature, it could be learnt that the materials with a nonlinear refractive index as that of PicoGreen and Triazatriangulenium salt are highly desirable for all-optical switching applications.

- On intercalation of these dyes with deoxyribonucleic acid, the TPA coefficient was reduced. One interesting feature was that the PicoGreen dye that exhibited

optical limiting property started to behave like saturable absorber on increasing the concentration of DNA added to it.

- However, in the case of TATA salt, the saturable absorption effect was reduced. This effect was similar to the one reported by Nithyaja et al from our laboratory in Rhodamine 6G when the concentration of DNA was increased.

- Intercalation of PicoGreen dye with DNA showed enormous enhancement in fluorescence, which was amplified in a resonator cavity to observe amplified spontaneous emission.

- The PicoGreen-DNA lipid complex thin film exhibited an ASE threshold of 1.7 mJ/cm^2 when excited at 355 nm, which was lower than that for the common lasing dye, Rhodamine 6G.

- The exponential gain coefficient was found to be 5.2 cm^{-1} for the dye:DNA complex that exhibited a fluorescence quantum yield of 0.64.

- The photostability of PicoGreen dye in the presence of DNA was found to be at par with most organic dyes.

- The DNA as an electron blocking layer was investigated with polymer light emitting diodes using fluorene-based PFO:F8BT as an active material.

- The brightness of DNA based LED was enhanced by four-fold over devices without electron blocking layer. At a typical current density of 460 mA/cm^2 devices with DNA:CTMA layer exhibited an eight-fold increase in luminance performance.

- Similar work was performed using PFO as the active material with an increase in brightness by two-fold, using DNA:CTMA as electron blocking layer.

The science of DNA has opened up new avenues and novel ideas for developments of new optical materials for various applications. It is clear from the applications of DNA, that DNA research spans various scientific and engineering fields and is truly an interdisciplinary field. With DNA being developed in various photonic and optoelectronic applications, it is essential to understand the role of DNA and the

underlying mechanisms at the molecular level in these DNA-based hybrid materials. It is, therefore, necessary for physicists, chemists and biotechnologists to unify and collaborate to provide solutions and develop new technology exploiting the unique optical and electronic properties of this wonderful biomolecule. Finally, it would be best to quote the words of Steckl et al. to describe DNA as the 'molecule of light' that would soon become the 'silicon' of the next generation.

A

Author's published work

Paper I

Amplified spontaneous emission from PicoGreen dye intercalated in deoxyribonucleic acid lipid complex

C Pradeep, C P G Vallabhan, P Radhakrishnan and V P N Nampoori

Amplified spontaneous emission from PicoGreen dye intercalated in deoxyribonucleic acid lipid complex

C Pradeep[1], C P G Vallabhan[1], P Radhakrishnan[1] and V P N Nampoori[1,2]

[1] International School of Photonics, Cochin University of Science and Technology, Cochin 682022, Kerala, India
[2] Department of Optoelectronics, University of Kerala, Thiruvananthapuram 695037, Kerala, India

E-mail: chandran@cusat.ac.in

Abstract

DNA as a genetic biomolecule is more commonly referred to in life sciences, genetics, and microbiology. With the development of 'DNA photonics', it has shown tremendous applicability as an optical and photonic material. In this letter, we introduce a novel dye PicoGreen as a lasing medium in which DNA not only acts as a host matrix but also functions as a fluorescence enhancer. A dramatic increase in the fluorescence led us to the observation of optical amplification in dye doped DNA thin films. We also indicate the possible tunability of the output emission in the green–yellow region. With the obtained results, we have enough reasons to lead to the development of DNA-based bio-lasers.

Keywords: amplified spontaneous emission, PicoGreen, deoxyribonucleic acid, DNA : CTMA

(Some figures may appear in colour only in the online journal)

1. Introduction

With the discovery of the double helical structure of deoxyribonucleic acid in 1953 by James Watson and Francis Crick, DNA has been a center of attraction for researchers in biology, genetics, and medicine. Barely sixty years later, DNA remains in the limelight, attracting the awe of scientists and researchers in other fields as well.

With the advent of DNA photonics, DNA continues to stimulate interest among researchers in many fields, especially photonics, by finding applicability in the fluorescence enhancement of dyes, as a host matrix for lasing dyes, organic light emitting diodes, memory devices, as a template for self-assembling of nanostructures, and application in nonlinear optics. Recently various groups [1–9] have reviewed the application of DNA in various fields, namely organic electronics, photonics, optoelectronics, nanotechnology, nonlinear optics, organic catalysis, etc, clearly demanding intense research, whereby DNA could be exploited to its full potential. In the context of application of the biomolecule in lasing and light emission, DNA is used as a host matrix for a lasing

medium, which tends to enhance the fluorescence of lasing dyes and improve the fluorescence quantum yield. There are many reports of amplified spontaneous emission and lasing from various dyes doped in either pure DNA films [10] or in a DNA surfactant lipid complex [11–14]. Studies are performed in various geometries like liquid solution in a simple cuvette cavity, optical fiber by the gel-spinning method [15, 16], planar micro-cavity with surface relief grating [17, 18], dynamic distributed feedback (DFB) grating [19–21], or distributed Bragg reflectors (DBR) as resonators. DNA thin films could be easily prepared using simple techniques such as spin coating, drop casting, tape casting [22], and dip coating [23].

PicoGreen (PG) is a fluorescent dye used in biomedical research for DNA quantitation assays [24]. PG does not fluoresce in its free state, but on binding with double-stranded DNA, the fluorescence is enhanced by 1000-fold or more. This enhancement has been exploited in DNA quantitation in solution and gels, real-time PCR, cell chromosome staining, and other techniques [25]. Dragan *et al* [26] recently proposed the possible modes of binding to DNA and explained the change in quantum yield and excited state lifetime. In their paper it was detailed
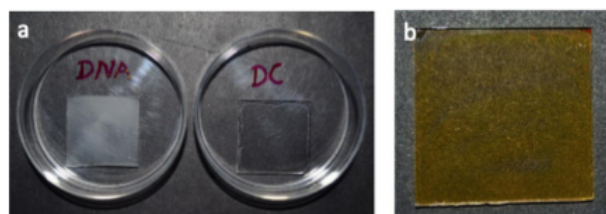
Figure 1. Photograph of the (a) comparison of undoped DNA (left) and undoped DNA : CTMA (right) film, (b) prepared DNA : CTMA : PG thin film.
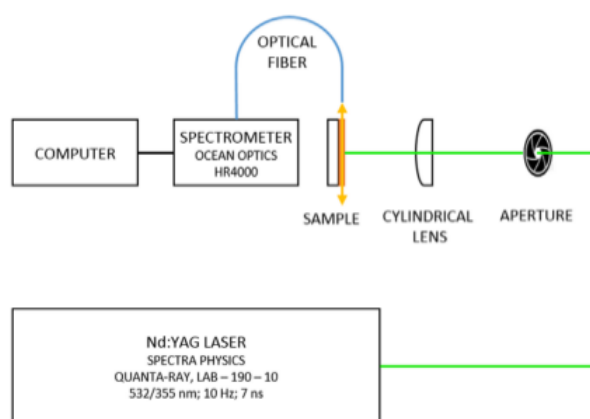
Figure 2. Experimental setup for the measurement of ASE.

that the negligible fluorescence from the pristine dye was due to a dynamic quenching process and subsequent dequenching by intercalation with DNA molecules has improved the fluorescence quantum yield and excited state lifetime dramatically. This enormous enhancement in fluorescence made us interested in taking up the amplified spontaneous emission studies, which could lead us to the development of DNA-based lasers.

2. Materials and methods

The DNA extracted from salmon testes and PG dye was purchased from Sigma Aldrich, USA and Invitrogen, USA respectively. DNA : CTMA lipid complex was prepared in butanol at a concentration of $20 \, \text{mg ml}^{-1}$ [27]. The molecular structure, absorption spectrum, and fluorescence enhancement of PG in the presence of DNA were already presented in our earlier work [28, 29]. PG is available in liquid form with DMSO as a solvent. The PG solution was doped in the DNA : CTMA lipid complex in a volume ratio 1 : 2. The mixture was then drop casted on a glass plate and annealed at 40 °C in vacuum for 2 h. The annealing in vacuum was necessary to evaporate DMSO at lower temperature and thus not degrade the DNA. Additionally, we also prepared bilayer thin films by drop casting PG solution over a pristine DNA : CTMA film and

pure DNA film, which were soluble in water. DNA : CTMA films were optically more transparent than pure DNA films, see figure 1(a). This was similar to the immersion technique used by Suzuki *et al* [23] for increasing the doping concentration of the dye. However, this technique did not yield a good and uniform thin film. The thin film prepared by an earlier method, as shown in figure 1(b), was used for further studies. The absorption and fluorescence spectra were measured using a Jasco V-570 spectrophotometer and a Varian Cary Eclipse fluorimeter.

For the ASE measurements, the typical setup [10] is shown in figure 2. The samples were excited using second and third harmonic frequencies from a Nd:YAG laser (Quanta-Ray, Lab-190-10) with a pulse duration of 7 ns and a repetition rate of 10 Hz. The beam was made into a stripe geometry 10 mm in length and 1 mm in width using an aperture and a cylindrical lens. The output emission was collected perpendicular to the excitation beam using a fiber and recorded with a spectrometer of resolution 0.27 nm (Ocean Optics HR4000).

3. Results and discussion

The thickness of the DNA : CTMA : PG film was estimated to be 0.35 μm. The normalized absorption and normalized
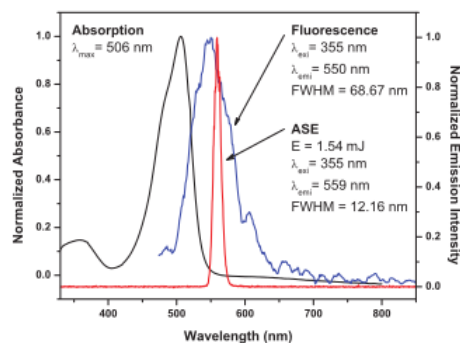
Figure 3. Normalized absorption, fluorescence, and amplified spontaneous emission from PG doped in the DNA : CTMA lipid complex.

fluorescence spectra along with ASE of the DNA : CTMA : PG film are presented in figure 3. The absorption range of the thin film is from 450 nm to 550 nm with its peak at 506 nm. The fluorescence peak and ASE peak were observed at 550 nm and 559 nm, respectively, while the full width half maximum (FWHM) of the latter was reduced by 57 nm.

According to Samuel *et al* [30], we confirm the observance of ASE and lasing action in the gain medium consisting of DNA : CTMA : PG thin film on a glass substrate by spectral narrowing, distinct threshold in linewidth and output intensity, and the output beam.

Figure 4(a) shows the dependence of FWHM and output ASE intensity as a function of input energy using a laser pump beam of 532 nm. We could observe spectral narrowing with a decrease in the linewidth of the emission spectrum from 69 nm to 13 nm. A clear threshold in the output power was observed at an input energy density of 3 mJ cm^{-2}. Figure 4(b) depicts the similar characteristics while using a 355 nm pump beam. Here we observe the threshold at 1.7 mJ cm^{-2}, beyond which the linewidth reduces to 5.7 nm. However, the spectral characteristics of the emission while exciting at 532 and 355 nm were different.

Figure 5(a) shows the ASE spectra from the thin films when excited at a wavelength of 532 nm (8.6 mJ) and 355 nm (3.2 mJ). We could observe modulation structures from a resolution-limited spectrometer ranging from 562 to 579 nm under green excitation and from 555 to 563 nm under UV excitation. These features may be due to the random lasing or surface roughness of the film. Figure 5(b) shows the spectral structures obtained from DNA : CTMA : PG thin film when excited at 532 nm at 12.35 mJ. With suitable pumping wavelength and cavity design, it could be possible to tune lasing wavelength from 555 to 579 nm.

The exponential gain coefficient was calculated by the Shank method by providing a block and measuring the emission intensity for an excitation stripe length of 1 cm and 0.5 cm. The calculated gain coefficient using the formula given below was, $\gamma = 4.7$ cm^{-1} (at 532 nm) and 5.2 cm^{-1} (at 335 nm).
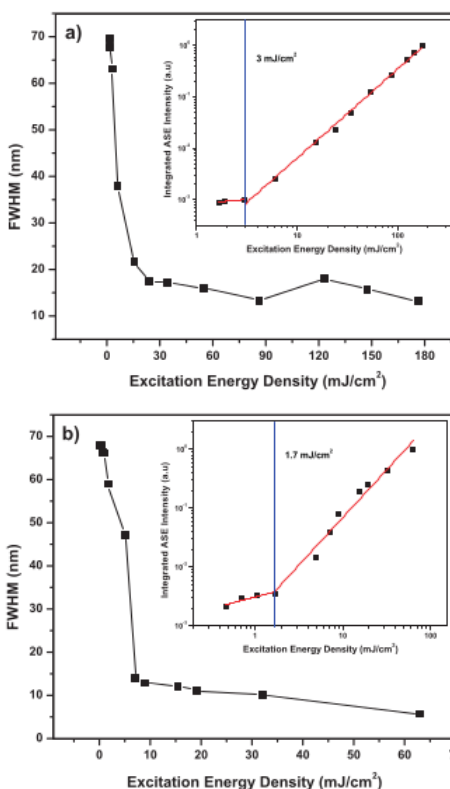

Figure 4. Dependence of FWHM and output lasing intensity (inset) on input excitation energy at a wavelength of (a) 532 nm and (b) 355 nm.

$$\gamma = \frac{2}{L} \ln \left(\frac{I_L}{I_{L/2}} - 1 \right).$$

Another important factor is the photodegradation of PG, which will determine its practical applicability as a lasing medium. The experimental results of the photodegradation property using laser excitation are shown in figure 6. While using a pump beam of 532 nm pulses at 1.6 mJ and measuring the output spectrum every 15 s, we estimated that the output intensity was reduced to 50% of its initial value after 215 excitation pulses. With the available literature we conclude that this value is typical for an organic dye. We show the photograph of the observed output beam on a white paper when excited at 355 nm in figure 7. The appearance of green light is due to the fluorescence from the white screen.

4. Conclusion

In summary, we investigated a new dye for lasing when embedded in deoxyribonucleic acid, which not only acts as a host
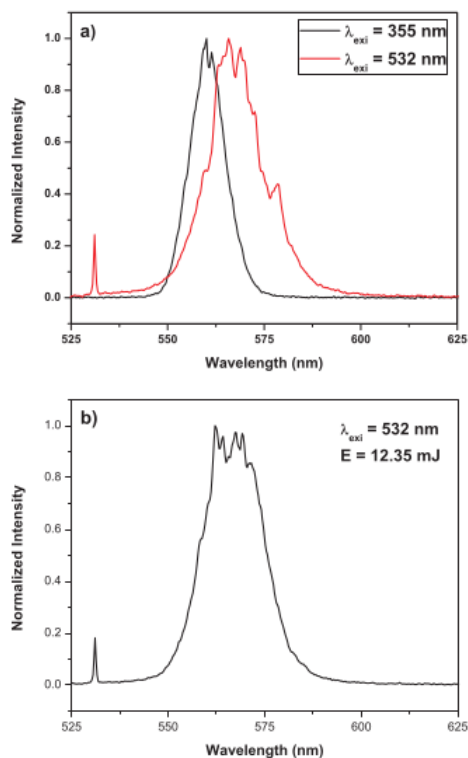
Figure 5. (a) ASE spectra from DNA:CTMA:PG thin film excited with second (8.6 mJ) and third (3.2 mJ) harmonic frequency from a Nd:YAG laser. (b) Spectral features obtained from thin film when excited with 532 nm at 12.35 mJ.
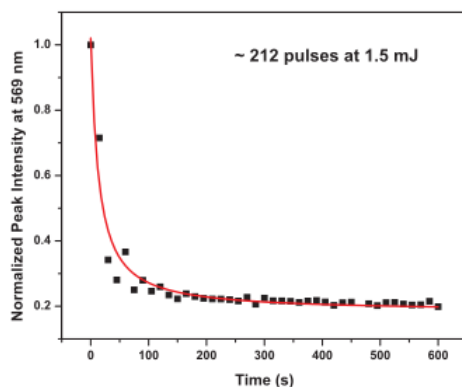
Figure 6. Dependence of ASE intensity of PG dye doped in DNA lipid complex thin film over time using a 10 Hz, 532 laser.

matrix for the dye but also as a fluorescence enhancer through the dynamic dequenching process. We have therefore fabricated
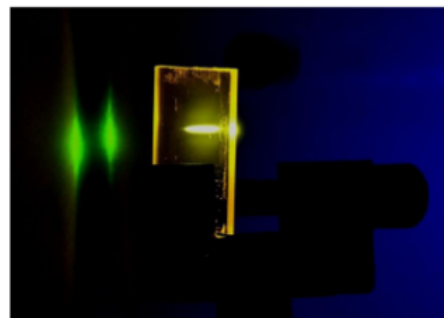
Figure 7. Photograph of yellow lasing (seen as green) from the two faces of the film when excited at 355 nm.

a modified DNA lipid complex intercalated with PG dye thin film and observed amplified spontaneous emission at 568 nm and 560 nm while exciting at the second and third harmonic frequency, respectively, from a Nd:YAG laser. We also observed modes ranging from 555 to 579 nm and also propose probable tunable emission by utilizing a proper cavity structure and excitation wavelength. We estimated an ASE threshold at ~2–3 mJ cm^{-2} with a spectral narrowing from 69 nm to 5.7 nm. The film 0.35 μm thick could sustain approximately 215 pulses of 1.5 mJ, 532 nm laser radiation before the emission could degrade to 50% of the initial intensity. Though we find an exponential gain coefficient of ~5.0 cm^{-1} with our samples, which is in par with most of the organic dyes, it is necessary to find the optimum doping concentration of dye with the intercalating DNA. Here, we see that the DNA not only acts as a host material but also plays an important role in the luminescence of the dye molecules, which could lead to the development of DNA-based lasers.

Acknowledgments

References

[1] Hung Y C, Bauer D M, Ahmed I and Fruk L 2014 *Methods* **67** 105–15
[2] Yang D, Campolongo M J, Tran T N N, Ruiz R C H, Kahn J S and Luo D 2010 *WIREs Nanomed. Nanobiotechnol.* **2** 648–69
[3] Singh T B, Sariciftci N S and Grote J G 2010 *Adv. Polym. Sci.* **223** 73–112

DNA PHOTONICS

[4] Grote J G *et al* 2005 *Mol. Cryst. Liq. Cryst.* **426** 3–17
[5] Steckl A J 2007 *Nat. Photon.* **1** 3–5
[6] Rau I, Grote J G, Kajzar F and Pawlicka A 2012 *C. R. Phys.* **13** 853–64
[7] Vladu M I 2014 *Chem. Soc. Rev.* **43** 588–610
[8] Kwon Y W, Lee C H, Choi D H and Jin J I 2009 *J. Mater. Chem.* **19** 1353–80
[9] Vladu M I, Sariciftci N S and Bauer S 2011 *J. Mater. Chem.* **21** 1350–61
[10] Rau I, Szukalski A, Sznitko L, Miniewicz A, Bartkiewicz S, Kajzar F, Sahraoui B and Mysliwiec J 2012 *Appl. Phys. Lett.* **101** 171113
[11] Mysliwiec J, Sznitko L, Miniewicz A, Kajzar F and Sahraoui B 2009 *J. Phys. D: Appl. Phys.* **42** 085101
[12] Honda M, Nakai N, Fukuda M and Kawabe Y 2007 *Proc. SPIE* **6646** 664609
[13] Kawabe Y, Wang L, Horinouchi S and Ogata N 2000 *Adv. Mater.* **12** 1281–3
[14] Hung Y-C, Su C-H and Huang H-W 2012 *J. Appl. Phys.* **111** 113107
[15] Ozaki M, Kagami Y, Wada M, Ogata N, Mito K, Ishikawa T and Horinouchi S 2005 *Proc. SPIE* **5635** 194
[16] Wang L, Ishihara K, Izumi H, Wada M, Zhang G, Ishikawa T, Watanabe A, Horinouchi S and Ogata N 2002 *Proc. SPIE* **4905** 143
[17] Mysliwiec J, Sznitko L, Sobolewska A, Baetkiewicz S and Miniewicz A 2010 *Appl. Phys. Lett.* **96** 141106
[18] Sznitko L, Mysliwiec J, Karpinski P, Palewska K, Parafiniuk K, Bartkiewicz S, Rau I, Kajzar F and Miniewicz A 2011 *Appl. Phys. Lett.* **99** 031107
[19] Chida T and Kawabe Y 2014 *Opt. Mater.* **36** 778–81
[20] Yu Z, Li W, Hagen J A, Zhou Y, Klotzkin D, Grote J G and Steckl A J 2007 *Appl. Opt.* **46** 1507–13
[21] Chida T and Kawabe Y 2012 *Nonlinear Opt. Quantum Opt.* **45** 85–91
[22] Kawabe Y, Wang L, Nakamura T and Ogata N 2002 *Appl. Phys. Lett.* **81** 1372
[23] Suzuki T and Kawabe Y 2014 *Opt. Mater. Express* **4** 1411–9
[24] Singer V L, Jones L J, Yue S T and Haugland R P 1997 *Anal. Biochem.* **249** 228–38
[25] Ahn S J, Costa J and Emanuel J R 1996 *Nucleic Acids Res.* **24** 2623–5
[26] Dragan A I, Finet J R C, Bishop E S, Strouse R J, Schenerman M A and Geddes C D 2010 *Biophys. J.* **99** 3010–9
[27] Heckman E M, Hagen J A, Yaney P P, Grote J G and Hopkins F K 2005 *Appl. Phys. Lett.* **87** 211115
[28] Pradeep C, Mathew S, Nithyaja B, Radhakrishnan P and Nampoori V P N 2014 *Appl. Phys. A* **115** 291–5
[29] Pradeep C, Mathew S, Nithyaja B, Radhakrishnan P and Nampoori V P N 2013 *Appl. Phys. B* **111** 611–7
[30] Samuel I D W, Namdas E B and Turnbull G A 2009 *Nat. Photon.* **3** 546–9

Paper II

Enhanced brightness from all solution processable biopolymer LED

C Pradeep, M A G Namboothiry, C P G Vallabhan, P Radhakrishnan and V P N Nampoori

Proceedings of SPIE, Volume 9557, 95570O, (2015)

Enhanced brightness from all solution processable biopolymer LED

C Pradeep[1,*], M A G Namboothiry[2], C P G Vallabhan[1], P Radhakrishnan[1], V P N Nampoori[1,3]

[1]International School of Photonics, Cochin University of Science and Technology, Cochin 682022, Kerala, India;
[2]School of Physics, Indian Institute of Science Education and Research, Thiruvananthapuram 695016, Kerala, India;
[3]Department of Optoelectronics, University of Kerala, Thiruvananthapuram 695037, Kerala, India

ABSTRACT

Biopolymer light emitting diodes were fabricated by using all solution processable polymers incorporating biomaterials such as deoxyribonucleic acid lipid complex as an electron blocking layer. Light emission is from a blend of fluorene based copolymers. The devices with electron blocking layer exhibited higher brightness and luminous efficiency. The increased luminance of the multilayer polymer LED is attributed to the contribution from DNA:CTMA as electron blocking layer and PFN, a derivative of polyfluorene, as electron injection layer. Our results show four fold increase in luminance values when DNA is used as electron blocking layer.

Keywords: biopolymer LED, deoxyribonucleic acid, DNA:CTMA, electron blocking layer, light emitting polymers, PFO:F8BT

1. INTRODUCTION

Since the discovery of light emission from polymers over two decades ago, especially conjugated polymers have paved the way for simpler technology viz. solution casting method to make light emitting devices. However in the past few years, biopolymers such as DNA has gained tremendous interest among researchers trying to develop BioLED. Deoxyribonucleic acid from salmon sperm has been exploited as biodegradable polymeric material for photonic and electronic applications. Recently the "molecule of life" had made way into the field of photonics, semiconductors and display technology. Many devices such as optical waveguides, bio-organic light emitting devices, bio field effect transistors and bio sensors are at the research table with promising results. What the DNA could offer in LED application is multifold. Steckl et al[1] in his article elaborated how DNA, through the emerging field of 'DNA Photonics', could be exploited as a biodegradable polymeric material for photonics and optoelectronics applications. Apart from being biodegradable, abundant, inexpensive and renewable resource, they hold unique optical and electrical properties. Being optically transparent in the visible region, electrically conductive, tunable resistivity from 10^{15} to 10^9 Ω-cm by varying its molecular weight, suitable refractive index and dielectric constant, all leading towards a promising material for optical devices. Additionally, the HOMO (5.6 eV) and LUMO (0.9 eV) levels support hole transportation and also effectively block electrons enabling it to be used as an electron blocking layer (EBL) in LED which has resulted in increased brightness and luminous efficiency.

DNA entered the photonics field as a host material for lumophore – thereby avoiding agglomeration of molecules and enhancing photoluminescence. Kobayashi et al[2] was the first to incorporate DNA doped with Ru(bpy)$_3^{2+}$ in light emitting diodes using dip coating technique in the form of water soluble DNA polyaniline complex. Koyama et al later introduced organic solvent soluble DNA lipid complex in light emitting devices[3]. They hosted DNA lipid complex as a matrix for dye molecules such as ethidium bromide and fluorescein and claimed that DNA could be a good hole transporting layer. Though they were not clear about the role of DNA in light emission, they opened a whole new interest. After a careful

---
[*]corresponding author: C Pradeep (chandran@cusat.ac.in); phone +91 0484 2575845; fax +91 0484 2576714; photonics.cusat.edu

scrutiny of the HOMO and LUMO levels of DNA, Hirata et al in 2004[4] confirmed the electrical conduction in LEDs and followed from J. Hagen et al[5] and Sun et al[6] complimented the electron blocking ability of DNA in OLED (organic light emitting diodes) and QDLED (quantum-dot light emitting diodes) respectively. Kobayashi et al[7,8] came up with a voltage controlled color tunable OLED based on DNA. The green to red tunability was contributed by green emitting Tris(8-hydroxyquinolinato)aluminium (Alq$_3$) and subsequent shift in the recombination site to red emitting Tris(bipyridine)ruthenium(II) (Ru(bpy)$_3$$^{2+}$). Madhwal et al[9,10] supported the enhanced luminance and luminous efficiency by incorporating DNA in PLEDs (polymer light emitting diodes). Instead of hexadecyltrimethylammonium (CTMA) as lipid, Chen et al[11] demonstrated BioLED with benzyltrimethylammonium chloride (BTMAC) as surfactant to DNA and achieved efficient OLED at lower driving voltages. Recently, Grykien et al[12] claimed 40% improvement in luminous efficiency by fabricating DNA as EBL in phosphorescent Ir(ppy)$_3$ based OLED.

Motivated by the potential of DNA as an interesting material in the field of light emitting diodes, much research was directed to designing and developing BioLED and a solution to increase the efficiency and brightness. This paper presents the effect of thickness of electron blocking DNA layer in polymer LEDs. We demonstrated an efficient bio-LED using all solution processable polymer layers except for the cathode. Here we used a blend of green emitting poly(9,9-dioctylfluorene-*alt*-benzothiadiazole) (F8BT) and blue emitting poly(9,9-di-n-octylfluorenyl-2,7-diyl) (PFO) as a light emitting polymer.

2. EXPERIMENTAL

2.1 Materials and Methods

Marine derived DNA (extracted from salmon testes, saDNA), CTAB [hexadecyltrimethylammonium bromide], F8 (PFO) [Poly(9,9-di-n-octylfluorenyl-2,7-diyl)], F8BT [Poly(9,9-dioctylfluorene-*alt*-benzothiadiazole)], PFN [poly [(9,9-bis(3'-(N,N-dimethylamino)propyl)-2,7-fluorene)-alt-2,7-(9,9–dioctylfluorene)], PEDOT:PSS [Poly(3,4-ethylenedioxythiophene)-poly(styrenesulfonate)] and Aluminum used in this study were supplied by Sigma Aldrich, USA. The ITO glass plates were supplied by Delta Technologies, Limited, USA. The molecular structure of DNA and other polymers are shown in Figure 1.

The DNA:CTMA lipid complex was prepared as described elsewhere[13]. DNA (4g/L) and CTAB (4g/L) aqueous solution was prepared using Milli-Q water. For reducing the molecular weight of DNA, the DNA aqueous solution was sonicated in ice bath for 50 cycles, with each containing 10 sec sonication - at 50% of the output power and 50% duty cycle - and 20 sec rest period. The molecular weight of the sonicated sample was measured by gel electrophoresis method and was estimated to be less than 500 bp (see Figure 2). The CTAB solution was added to DNA solution drop by drop while stirring and was additionally stirred for 2 more hours. The DNA:CTMA precipitated was filtered using 0.45 μm nylon membrane and dried in vacuum at 40°C overnight. The lipid complex was dissolved in butanol at the desired concentration.

2.2 Device fabrication

The devices were fabricated by following the procedure detailed below. The ITO coated glass plates of sheet resistance 8-12 Ω/sq were cleaned under ultrasonication in a series of solvents, viz. laboratory detergent, DI water, acetone, iso-propanol, ethanol, each for 15 minutes. Further, the plates were blown with nitrogen gas, dried in vacuum oven and treated with UV/O$_3$ prior to coating.

The device structure and its energy level diagram are presented in Figure 3. A control device (Device A) was also fabricated without DNA:CTMA layer to compare the effect of DNA layer with the following structure ITO/PEDOT:PSS/PFO:F8BT/PFN/LiF/Al. PEDOT:PSS was filtered using a pore size of 0.45μm PVDF filter and used without any dilution. It was spun at 5000 rpm for 30 s to yield a thickness of 80 nm. Annealing at 150 °C for 5 min ensured evaporation of any excess solvent. To study the effect of DNA as EBL, DNA:CTMA layer was introduced between the active layer and the hole transporting PEDOT:PSS. Device B and C were structured by incorporating DNA:CTMA of concentration 1 mg/ml and spun at 5000 and 10000 rpm respectively. In devices D and E, DNA:CTMA of concentration 0.7 mg/ml was used and spun at 5000 and 10000 rpm respectively. The thickness of DNA:CTMA layer in devices B, C, D and E were 29 nm, 27 nm, 17 nm and 17.5 nm. The light emitting copolymer was prepared by dissolving PFO and F8BT separately in toluene at a concentration of 15mg/ml and mixed in a volume ratio if 19:1. 55 nm thick layer was obtained by spinning the blend solution at 8000 rpm for 20 s and annealing at 80°C for 10 min. An electron injection, PFN layer was prepared by mixing it in methanol at 2 mg/ml along with an addition of few drops of acetic acid and spinning it at

2000 rpm. All the polymers were filtered uing 0.2 μm PTFE syringe filter to ensure smooth and uniform films. Finally Aluminum (100 nm) as cathode was coated using thermal evaporation with lithium fluoride (2 nm) as buffer layer. The mask used here provided an active area of 9 mm^2. The devices were then encapsulated using a commercially available epoxy in nitrogen atmosphere and cured under UV irradiation for 30 minutes. The devices were characterized in air immediately thereafter.
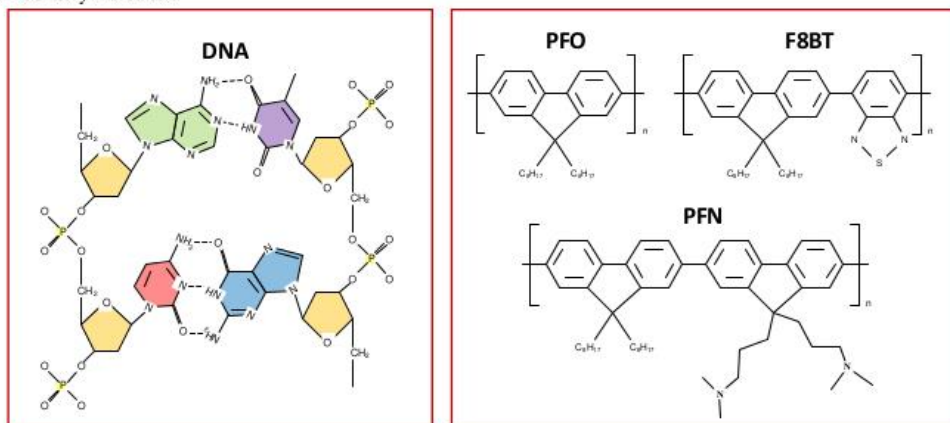

Figure 1: Molecular structure DNA, PFO, F8BT and PFN.
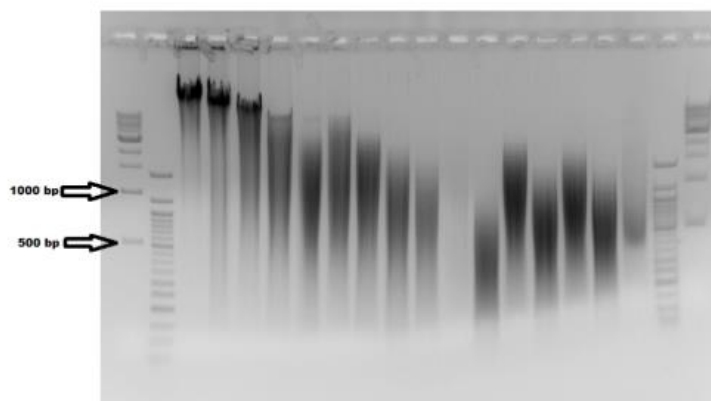
Figure 2: Gel phase electrophoresis - reduction of molecular weight of DNA by sonication

2.3 Measurements and Characterization

The mechanical shearing of DNA was realized using a probe type Branson 250 analog ultrasonic processor. The luminance and current density versus voltage characteristics were simultaneously recorded using (Keithley 2400) SMU and photocurrent was recorded using a calibrated photodiode (Thor Labs, PDA 36A-EC) connected to (Keithley 2000) digital multimeter with the help of LabView program The electroluminescence spectra was observed using Ocean Optics (HR4000) spectrophotometer. The thickness of thin polymer films were measured by optical reflectance system using ThetaMetrisis (FR-pOrtable). All measurements were carried out in air at room temperature.
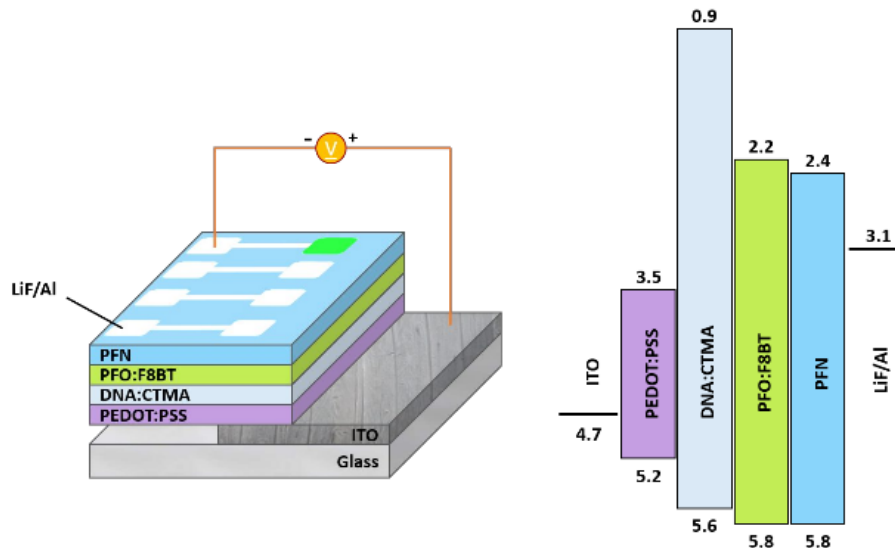
Figure 3: Device structure (left) and energy level diagram (right) of the fabricated BioLED

3. RESULTS AND DISCUSSIONS

All the materials used in this device structure except for the electrodes are polymers. Here, the transparent ITO is used as anode with a work function of 4.7 eV while PEDOT:PSS, a well know polymer, is used to transport holes effectively due to its matching HOMO level. The biopolymer, DNA:CTMA is used as an electron blocking layer to control the flow of electrons from cathode directly to anode and help the recombination sites localized in the active layer (PFO:F8BT). The active layer is a blend of two polymers, a blue emitting PFO and green emitting F8BT. The emission is by fluorescence decay due to the absorption of photons emitted by the recombination of holes and electrons in the π and π^* band of the polymer. PFN is an aminoalkyl substituted polyfluorene co-polymer employed as cathode interfacial layer[14,15] which helps to avoid the use of low work function metals such as Ca or Ba, that are susceptible to moisture and oxygen. Though the presence of PFN in the device reduced the brightness, the efficiency was much improved. A thin layer of Lithium Fluoride (LiF) was coated prior to the deposition of Aluminum without breaking the vacuum to alter the work function of Aluminum from 4.7 eV to 3.1 eV. We have also confirmed that combined contribution of PFN and LiF increased the efficiency compared to a device with either PFN or LiF.

The L-j-V (Luminance – Current density - Voltage) characteristic of PFO:F8BT based device with and without DNA layer (Device A and E) is shown in Fig 2a and 2b respectively. The turn-on voltage for Device A was at 6 V and for all other DNA based devices it was at 10 V. This is due to the additional DNA:CTMA layer that increased the overall resistance of the device.

A comparison of current density-bias voltage of devices A to E are shown in figure 3a which dictates the increased resistance in EBL based devices. While comparing the luminous performances of the devices in figure 3b, it could be observed that devices with thin EBL layer (17.5 nm) achieved higher luminance over devices with thick EBL layer (28.5 nm); which in turn was higher than device with no EBL layer. It was observed that the luminance from PFO:F8BT based devices with DNA were enhanced by more than 4 times over the devices without DNA complex layer.
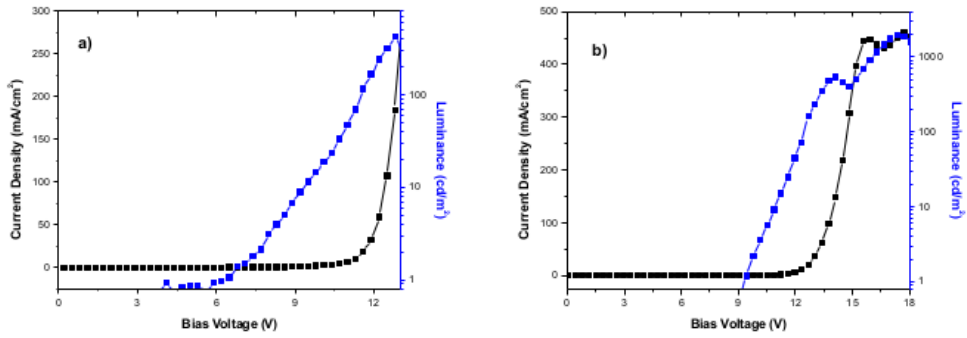
Figure 2: Luminance Current Voltage characteristic of a) Control LED (Device A) and b) BioLED (Device E)
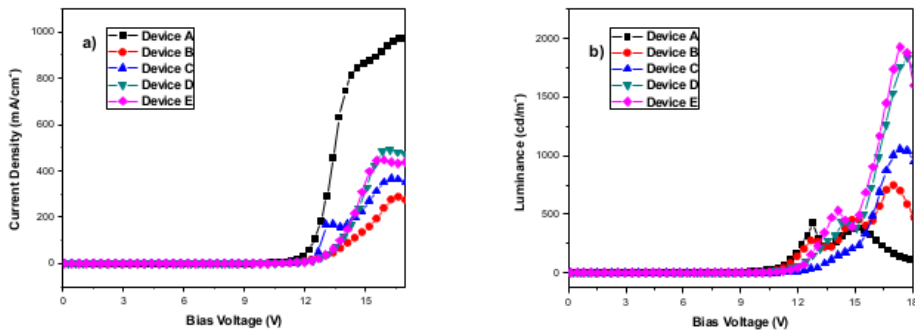

Figure 3: Comparison of a) Current density – Voltage characteristic and b) Luminance – Voltage characteristic of all the devices
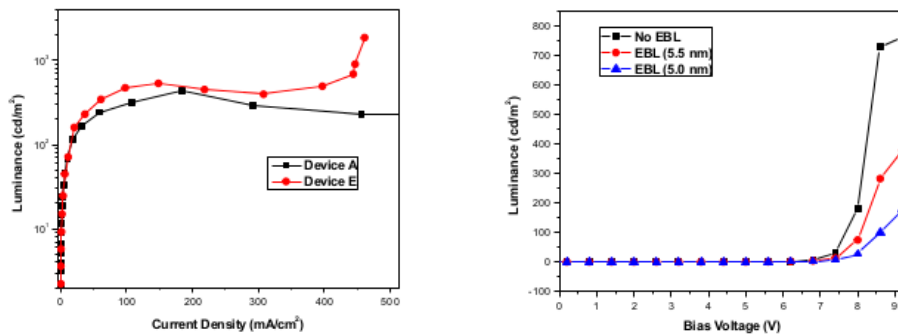

Figure 4: (a) Comparison of Luminance – Current density for Control LED (Device A) and BioLED (Device E) (b) Comparison of Luminance for devices with thin electron blocking layer

Figure 4a shows the luminous performance of Device A and Device E as a function of current density. It could be noted that at a current density of 180 mA/cm^2 the devices without EBL produce maximum luminance, which is enhanced by introducing the EBL. At a current density of 460 mA/cm^2 the device with EBL shows an 8 times increase in luminance over the device without EBL. In a separate set of experiments, DNA complex layer was reduced to ~5 nm by varying the concentration of the lipid complex extracted from the same batch used in earlier experiments. However, such devices showed no improvement in luminance (see Fig. 4b). It may be concluded that other factors apart from thickness such as the molecular weight and mobility of charges plays an important role. The normalized electroluminescent spectra of the device is shown in figure 5, depicting a dominant wavelength at 534 nm. Figure 8 shows the photograph of the green emission from the Device E.
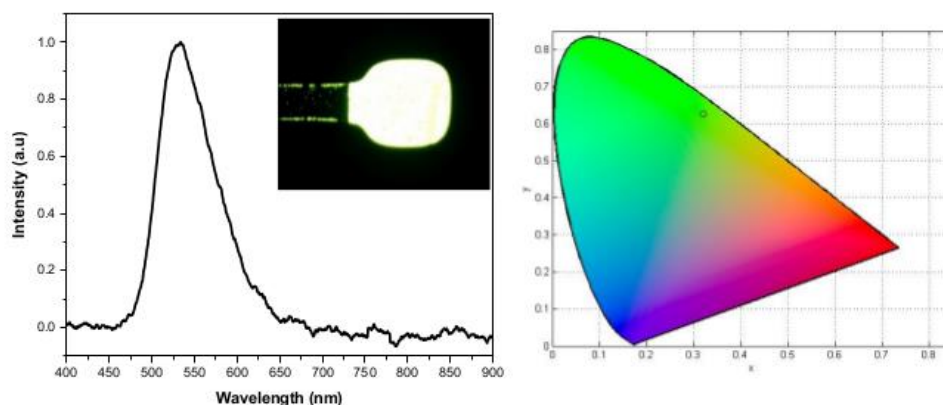

Figure 5: Electroluminescence spectra (left) and 1931 CIE color chromaticity plot (right) of BioLED. Inset on the left figure shows the actual photograph of emission from LED at 17 V.

4. CONCLUSION

We have reported a four fold increase in brightness of a polymer LED by introducing PFN as the electron injection layer and DNA:CTMA as electron blocking layer on either side of the polyfluorene active layer. It has been observed that the variation in thickness of DNA layer even at small values is very crucial. While the thickness is much lower (~5 nm), there was no improvement in luminance.

ACKNOWLEDGMENTS

REFERENCES

[1] A. J. Steckl, H. Spaeth, H. You, E. Gomez and J.Grote, "DNA as an optical material", Opt. Photonics News, 22, 35, (2011).

[2] N. Kobayashi, S. Uemura, K. Kusabuka, T. Nakahira and H. Takahashi, "An organic red-emitting diode with a water-soulble DNA-polyaniline complex containing Ru(bpy)$_3^{2+}$", J. Mater. Chem. 11, 1766, (2001).

[3] T. Koyama, Y. Kawabe and N. Ogata, "Electroluminescence as a probe for electrical and optical properties of deoxyribonucleic acid", Proc. SPIE 4464, Organic Light-Emitting Materials and Devices V, 248, (2002).

[4] K. Hirata, T. Oyamada, T. Imai, H. Sasabe and C. Adachi, "Electroluminescence as a probe for elucidating electrical conductivity in a deoxyribonucleic acid-centyltrimetnylammonium lipid complex layer", Appl. Phys. Lett. 85, 1627, (2004).

[5] J. Hagen, W. Li, A. Steckl, J. Grote and K. Hopkins, "Enhanced emission efficiency in organic light-emitting diodes using deoxyribonucleic acid complex as an electron blocking layer", Appl. Phys. Lett. 88, 171109, (2006).

[6] Q. Sun, G. Subramanyam, L. Dai, M. Check, A. Campbell, R. Naik, J. Grote and Y. Wang, "Highly efficient quantum-dot light-emitting diodes with DNA-CTMA as a combined hole-transporting and electron-blocking layer", ACS Nano, 3, 737-743, (2009).

[7] K. Nakamura, T. Ishikawa, D. Nishioka, T. Ushikubo and N. Kobayashi, "Color-tunable multilaye organic light emitting diode composed of DNA complex and tris(8-hydroxyquinolinato)aluminum", Appl. Phys. Lett. 97, 193301, (2010).

[8] N. Kobayashi, "BioLED with DNA/Conducting Polymer Complex as Active Layer", Nonl. Opt. Quant.Opt. 42, 233-251, (2011).

[9] D. Madhwal, S. S. Rait, A. Verma, A. Kumar, P. K. Bhatnagar, P. C. Mathur and M. Onoda, "Increased luminance of MEH-PPV and PFO based PLEDs by using salmon DNA as an electron blocking layer", J. Lumin, 130, 331-333, (2010).

[10] D. Madhwal, I. Singh, J. Kumar, C. S. Bhatia, P. K. Bhatnagar and P. C. Mathur, "Increasing the luminance efficiency of an MEH-PPV based PLED using salmon DNA and single walled carbon nanotube", J. Lumin, 131, 1264-1266, (2011).

[11] I-C. Chen, Y-W. Chiu and Y-C. Hung, "Efficient biopolymer blue organic light-emitting devices with low driving voltage", Jpn. J. Appl. Phys. 51, 031601, (2012).

[12] R. Grykien, B. Luszczynska, I. Glowacki, J. Ulanski, F. Kajzar, R. Zgarian and I. Rau, "A significant improvement of luminance vs current density efficiency of a BioLED", Opt. Mat., 36, 1027-1033, (2014).

[13] E. M. Heckman, J. A. Hagen, P. P. Yaney, J. G. Grote and F. K. Hopkins, "Processing techniques for deoxyribonucleic acid: Biopolymer for photonics applications", Appl. Phys. Lett. 87, 211115, (2005).

[14] H. Wu, F. Huang, Y. Mo, W. Yang, D. Wang, J. Peng and Y. Cao, "Efficient Electron Injection from a Bilayer Cathode Consisting of Aluminum and Alcohol-/Water-Soluble Conjugated Polymers", Adv Mater., 16, 1826-1830, (2004).

[15] D. An, J. Zou, H. Wu, J. Peng, W. Yang and Y. Cao, "White emission polymer light-emitting devices with efficient electron injection from alcohol/water-soluble polymer/Al bilayer cathode", Org. Electron., 10, 299-304, (2009).

Paper III

Effect of marine derived deoxyribonucleic acid on nonlinear optical properties of PicoGreen dye

C Pradeep, S Mathew, B Nithyaja, P Radhakrishnan and V P N Nampoori

Effect of marine derived deoxyribonucleic acid on nonlinear optical properties of PicoGreen dye

C. Pradeep · S. Mathew · B. Nithyaja ·
P. Radhakrishnan · V. P. N. Nampoori

Abstract We have investigated the effect of DNA on nonlinear absorption of PicoGreen dye using single beam open aperture Z-scan technique in nanosecond regime. We observed reverse saturable absorption at 532 nm for Pico-Green without DNA. In the presence of DNA, the sample begins to behave like saturable absorbers and this effect increased as the concentration of DNA was increased. The dye-intercalated DNA showed SA characteristics near the focus but exhibited RSA characteristics at the focus. Theoretical analysis has been performed using a two-photon absorption model based on nonlinear absorption coefficient and saturation intensity. Such tailoring of optical nonlinear absorption in PicoGreen makes it a potential candidate for photonic application.

1 Introduction

Deoxyribonucleic acid (DNA), a highly nonlinear bio-organic polymer, has made way into the field of photonics, semiconductors and display technology [1]. Many devices such as optical waveguides [2], bio-organic light emitting devices [3–7], bio field emitting transistors [8–12], bio sensors [13], and lasing medium [14–16] provide promising results. DNA entered into photonic industry to determine its base pair sequence using fluorophores that could be easily intercalated into its base stacks [17]. It was also found that the fluorescence emission of various dyes is enhanced many

C. Pradeep (✉) · S. Mathew · B. Nithyaja · P. Radhakrishnan
· V. P. N. Nampoori
International School of Photonics, Cochin University of Science and Technology, Cochin 682022, India
e-mail: pradeepchandran_123@yahoo.co.in;
pradeep@photonics.cusat.edu

fold on doping with DNA [18]. Of various dyes used, most of them including certain metal nanoparticles showed fluorescence enhancement on intercalation with DNA [19], which was primarily due to the disassociation of dye molecules. This property of DNA was exploited to serve as a photonic material in various optoelectronic devices. There has been numerous investigations on various fluorophore-doped DNA and reported its amplified spontaneous emission and lasing action [20–22]. Thus, the biopolymer with its renowned double helical structure has emerged to develop a new field 'DNA Photonics' [23–26], transforming itself into an exciting photonic material.

Nonlinear optical properties of dye-incorporated DNA system are useful in developing devices based on optical limiting, two-photon absorption, etc. Here we introduce Picogreen (PG) dye as a nonlinear optical material that could be exploited in optical limiting applications, two-photon microscopy and photonic devices. The molecular structure and chemical formula of PG dye have been referred elsewhere [27]. PG is used as a standard stain for quantification of double stranded DNA (dsDNA), single stranded DNA (ssDNA) and ribonucleic acid (RNA) [28]. To understand the detailed aspects of DNA biomolecule interaction with the dye, investigation on nonlinear optical properties of dye-doped DNA is carried out. The nonlinear properties of the dye were studied using single beam Z-scan technique developed by Sheik Bahae et al. This technique is a well established tool for the determination of nonlinear refraction and absorption and has been widely used in material characterization. It has been reported that two-photon absorption (TPA) is possible in DNA at 532 nm corresponding to twice the wavelength of the main absorption peak (260 nm) [29–31]. The properties of DNA and PG having optical limiting behavior and the enhancement of fluorescence of the dye on binding with the

biomolecule invited interest in studying the interaction between the two in the context of nonlinear optical response.

2 Experimental

PG and marine-derived DNA (DNA from salmon testes, saDNA) was made available from Invitrogen, USA and Sigma Aldrich, USA, respectively. Commercially available PG reagent is in liquid form with solvent being dimethyl sulfoxide (DMSO). DMSO was supplied by S. D. Fine Chem Limited, India. The saDNA is fibrous and is used as received without any further purification. Single distilled water was used to prepare aqueous solution of saDNA. Two concentrations of DNA aqueous solution were prepared viz. 2 and 20 g/L. The UV–visible absorption spectra are recorded using Jasco V-570 Spectrophotometer and the photoluminescence was measured using Varian Cary Eclipse Fluorimeter. The Z-scan setup used in this experiment is already discussed in our earlier work [32].

3 Results and discussion

The linear normalized absorption spectra and normalized photoluminescence of PG are shown in Fig. 1. Absorption peak of PG dye is prominent in the visible region around 500 nm along with two minor peaks in the UV region (not shown). The intrinsic fluorescence of free PG dye was negligible when excited at 500 nm. Upon binding with dsDNA the fluorescence enhanced many folds with its emission peak at 535 nm.

It has been shown from our previous work that DNA exhibited strong nonlinear absorption due to two-photon
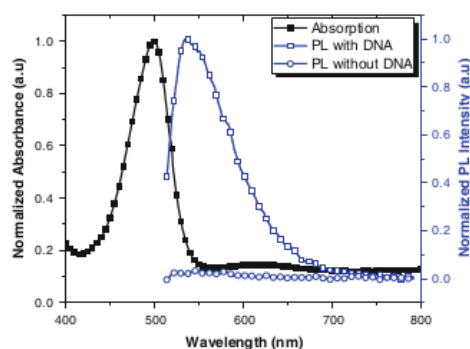

Fig. 1 Normalized absorption spectra and normalized fluorescence emission of PG dye with and without DNA

absorption [32]. To estimate the role of DNA on nonlinear property of the PG solution, we performed open aperture Z-scan on PG with and without DNA. In open aperture Z-scan technique, the sample is moved across a focused beam, where the transmittance is collected as a function of position of the sample (or on-axis input intensity). Figure 2a shows the plot related to open aperture Z-scan experiment of the dye and dye-intercalated DNA at an incident intensity of 0.10 GW/cm^2. In PG dye, without any intercalation with DNA, as the sample approaches the beam waist the transmittance decreased rapidly. This indicates reverse saturable absorption or optical limiting phenomena. When the dye was intercalated with DNA at a concentration of 2 g/L, there developed a hump in the transmittance curve very close to the beam waist. Interestingly, at a DNA concentration of 20 g/L the humps developed further and tends to flip the nonlinear absorption curve around the focus indicating the existence of saturable absorption. While at the focus the transmittance increased relative to the dye alone. In other words, the DNA:dye complex exhibits SA behavior around the focus and RSA behavior at the focus. This indicates the presence of more than one type of nonlinear optical processes taking place in the complex medium. Such multiple nonlinear absorption processes were reported by various groups in different materials [33–40]. Nithyaja et al. [32] had reported a flip of SA to RSA as DNA was doped in Rhodamine 6G. However, in this case, the flip was from RSA to SA, which was due to the effect of DNA. To determine the irradiance dependence of the nonlinear absorption coefficient, the measurements were performed at different laser energies. Figure 2b, c shows open aperture Z-scan experiments at an incident intensity of 0.23 and 0.32 GW/cm^2, respectively. Though the SA effect (the humps that flank the central RSA) increased with the concentration of DNA, it was less pronounced at higher irradiances.

To explain the nonlinear behavior we numerically fit the experimental data and are analyzed using the approach described by Sheik Bahae et al. [41]. The experimental data show both RSA and SA behavior and hence we define effective nonlinear absorption coefficient, $\alpha(I)$ instead of considering the TPA coefficient, β alone. The effective nonlinear absorption coefficient contains two terms, the first describing saturable absorption and the other representing the two-photon absorption. The effective nonlinear absorption coefficient is expressed as [35]

$$\alpha(I) = \left(\frac{\alpha_0}{1 + I/I_s} + \beta I \right) \quad (1)$$

where, α_0 is the unsaturated linear absorption coefficient at the excitation wavelength, I being the incident laser intensity and I_s the saturation intensity. The normalized transmittance of the open aperture Z-scan is given by the equation,
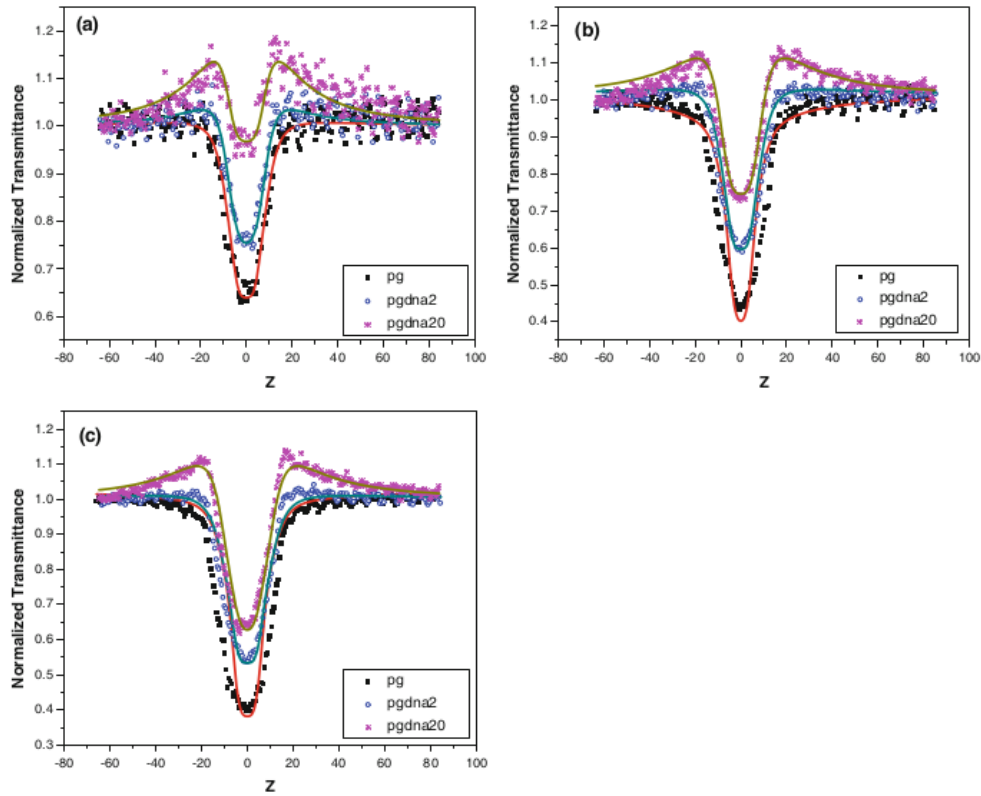
Fig. 2 Open aperture Z-scan curve of PG (pg) and dye intercalated DNA (pgdna2, 2 g/L and pgdna20, 20 g/L) at an incident intensity of **a** 0.10 GW/cm^2 **b** 0.23 GW/cm^2 and **c** 0.32 GW/cm^2. The *solid lines* denote the theoretical fit to the experimental data

$$T(z) = \sum_{m=0}^{\infty} \frac{\left(-\alpha I_0 L_{\text{eff}}/1 + \gamma^2\right)^m}{m+1} \qquad (2)$$

where, $L_{\text{eff}} = (1 - \exp(-\alpha l)/\alpha$, L_{eff} the effective interaction length, I_o is the irradiance at the focus, and l the sample length. $\gamma = (z/z_0)$, where z and z_0 are the longitudinal displacements of the sample from focus and the Rayleigh length, respectively. Theoretical fit of the experimental data was obtained using the Eqs. 1 and 2 from which I_s and β are calculated. The values of these parameters are presented in Table 1. We find that the theoretical simulation is in good agreement with the experimental data indicating the two-photon absorption model used here is quite reasonable.

In Fig. 3, the normalized transmittance is plotted against input intensity. This data were extracted from open aperture Z-scan curve of DNA (20 g/L) doped in dye at an

input intensity of 0.10 GW/cm^2 at the focus. The displacement of sample from the focus z in the Z-scan plot is converted to corresponding input fluence using Eq. 3. From this plot, it could be understood that at lower input intensities the transmittance increased, while above the critical value (37.5 MW/cm^2) the transmittance decreased. This effect could be exploited in dye-based optoelectronic switches.

$$I(z) = \frac{I_o}{1 + (z^2/z_o^2)} \qquad (3)$$

With the variation of transmitted intensity observed in DNA doped in dye, it is important to check the effect of DNA on DMSO, the solvent used in the dye. DNA solutions (15 g/L) were prepared by dissolving DNA in both distilled water and DMSO and were subjected to open aperture Z-scan at same input intensity. Figure 4 shows the

614   C. Pradeep et al.

Table 1 Key parameters related to the open aperture Z-scan plot of PG and dye intercalated DNA

| Sample	Input intensity, I_o (GW/cm^2)	TPA coefficient, β (m/GW)	Saturation intensity, I_s (MW/cm^2)
pg	0.10	1.1305	25.46
pgdna2		0.9827	27.74
pgdna20		0.5117	62.69
pg	0.23	0.5228	55.07
pgdna2		0.5296	51.48
pgdna20		0.5179	61.94
pg	0.32	0.4294	67.05
pgdna2		0.4029	67.67
pgdna20		0.4866	65.92

pg PicoGreen dye, *pgdna2* PicoGreen doped in 2 g/L DNA, *pgdna20* PicoGreen doped in 20 g/L DNA
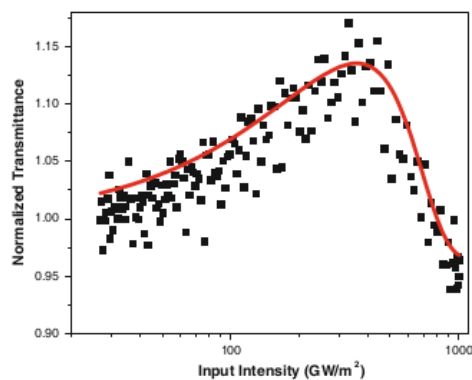
Fig. 3 Normalized transmittance of PG intercalated DNA at an incident intensity of 0.10 GW/cm^2 as a function of input intensity. The *solid line* denotes the theoretical fit

RSA behavior of DNA in both solvents. From the observations, it has been found that there was only a minuscule change in their nonlinear absorption. This might be due to a minor difference in the concentration of DNA.

4 Conclusion

In summary, the results depicted here show interesting features of saDNA and its effect on nonlinear absorption of PG dye. The dye alone showed optical limiting behavior when excited at 532 nm. On intercalating the dye with saDNA, we observe a saturable absorption behavior at low incident intensity (away from the focus) and reverse saturable absorption at high incident intensity (at the focus). Best theoretical fit was made and, saturable intensity and nonlinear absorption coefficients were estimated. Thus, it
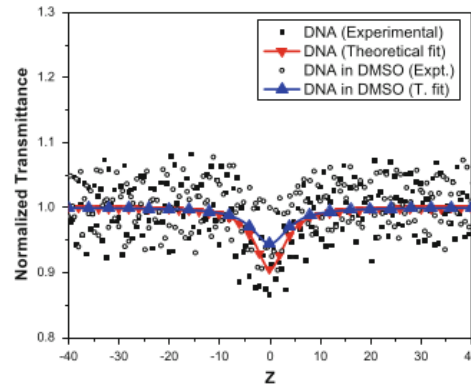
Fig. 4 Comparison of open aperture Z-scan of DNA in distilled water and DMSO solvent. The *solid line* denotes the theoretical fit

could be concluded that DNA plays an interesting role in tailoring the nonlinear absorption coefficient of PG dye. In comparison with our previous results concerning the effect of DNA in Rhodamine 6G [32], it could also be concluded that DNA can be used to switch the nonlinear behavior of intercalating dyes. However, more extensive research in various dyes could ascertain these conclusions. Such flexibility in controlling the optical nonlinear properties of dyes by saDNA could be exploited in developing various photonic devices.

References

1. A. Steckl, H. Spaeth, H. You, E. Gomez, J.G. Grote, in *Optics and Photonics News* (2011), p. 35–39
2. J. Yoshida, Y. Kawabe, N. Ogata, in *Proceedings of SPIE*, vol. 7765 (2010), p. 776506
3. E.F. Gomez, H.D. Spaeth, A.J. Steckl, J.G. Grote, in *Proceedings of SPIE*, vol. 8103 (2011), p. 81030A–1
4. G.M. Farinola, R. Ragni, Chem. Soc. Rev. **40**, 3467–3482 (2011)
5. T. Koyama, Y. Kawabe, N. Ogata, in *Proceedings of SPIE*, vol. 4464 (2002), p. 248
6. K. Hirata, T. Oyamada, T. Imai, H. Sasabe, C. Adachi, T. Koyama, Appl. Phys. Lett. **85**, 9 (2004)
7. J.A. Hagen, W.X. Li, J.G. Grote, A.J. Steckl, Appl. Phys. Lett. **88**, 171109 (2006)
8. F. Ouchen, P.P. Yaney, J.G. Grote, in *Proceedings of SPIE*, vol. 7403 (2009), p. 74030F–1
9. F. Ouchen, P.P. Yaney, C.M. Bartsch, E.M. Heckman, J.G. Grote, in *Proceedings of SPIE*, vol. 7765 (2010), p. 77650A–1

10. B. Singh, N.S. Sariciftci, J. Appl. Phys. **100**, 024514 (2006)
11. C. Yumusak, B. Singh, N.S. Sariciftci, J. Grote, J. Appl. Phys. **95**, 263304 (2009)
12. B. Singh, N.S. Sariciftci, in *Proceedings of OEC-06* (2006)
13. N. Ogata, in *Proceedings of SPIE*, vol. 8103 (2011) pp. 810302–1
14. J. Mysliwiec, L. Sznitko, A. Sobolewska, S. Bartkiewicz, A. Miniewicz, J. Appl. Phys. **96**, 141106 (2010)
15. T. Chida, Y. Kawabe, in *Proceedings of SPIE*, vol. 8103 (2011), p. 81030P
16. Y. Kawabe, L. Wang, T. Nakamura, N. Ogata, Appl. Phys. Lett. **81**(8), 1372 (2002)
17. I. Braslavsky, B. Hebert, E. Kartalov, S.R. Quake, Proc. Natl. Acad. Sci. **100**(7), 3960–3964 (2003)
18. V.L. Singer, L.J. Jones, S.T. Yue, R.P. Haugland, Anal. Biochem. **249**, 228–238 (1997)
19. B. Nithyaja, H. Misha, V.P.N. Nampoori, in *Proceedings of SPIE*, vol. 8173 (2011), p. 81731K
20. Y. Kawabe, L. Wang, S. Horinouchi, N. Ogata, Adv. Mater. **12**, 1281 (2000)
21. Z. Yu, W. Li, J.A. Hagen, Y. Zhou, D. Klotzkin, J.G. Grote, A.J. Steckl, Appl. Opt. **46**, 1507 (2007)
22. G.S. He, Q. Zheng, P.N. Prasad, J. Grote, F.K. Hopkins, Opt. Lett. **31**(3), 359 (2006)
23. J.G. Grote, D.E. Diggs, R.L. Nelson, J.S. Zetts, F.K. Hopkins, N. Ogata, J.A. Hagen, E. Heckman, P.P. Yaney, M.O. Stone, L.R. Dalton, Mol. Cryst. Liq. Cryst. **426**(1), 3–17 (2005)
24. F.D. Lewis, Pure Appl. Chem. **78**(12), 2287–2295 (2006)
25. J. Grote, De Y. Zang, F. Ouchen, G. Subramanyam, P. Yaney, C. Bartsch, E. Heckman, R. Naik, in *Proceedings of SPIE*, vol. 7765 (2010), p. 776502
26. N. Ogata, K. Yamaoka, J. Yoshida, in *Proceedings of SPIE*, vol. 7765 (2010), p. 776508
27. H. Zipper, H. Brunner, J. Bernhagen, F. Vitzthum, Nucleic Acids Res. **32**(12), e103 (2004)
28. G. Cosa, K.S. Focsaneanu, J.R.N. McLean, J.P. McNamee, J.C. Scaiano, Photochem. Photobiol. **73**, 585–599 (2001)
29. J.G. Grote, E.M. Heckman, D.E. Diggs, Proc. SPIE **5934**, 593406 (2005)
30. G. Zhang, H. Takahashi, L. Wang, J. Yoshida, S. Kobayathi, S. Horinouchi, N. Ogata, in *Proceedings of SPIE*, vol. 4905 (2002), p. 375
31. A. Miniewicz, A. Kochalska, J. Mysliwiec, A. Samoc, M. Samoc, J.G. Grote, Appl. Phys. Lett. **91**, 041118 (2007)
32. B. Nithyaja, H. Misha, P. Radhakrishnan, V.P.N. Nampoori, J. Appl. Phys. **109**, 023110 (2011)
33. S.V. Rao, N.K.M.N. Srinivas, D.N. Rao, Chem. Phys. Lett. **361**, 439–445 (2002)
34. N.K.M.N. Srinivas, S.V. Rao, D.N. Rao, J. Opt. Soc. Am. B. **20**, 2470 (2003)
35. Y.C. Gao, X.R. Zhang, Y.L. Li, H.F. Liu, Y.X. Wang, Q. Chang, W.Y. Jiao, Y.L. Song, Opt. Commun. **251**, 429 (2005)
36. Z.B. Liu, Y. Wang, X.L. Zhang, Y.F. Xu, Y.S. Chen, J.G. Tian, Appl. Phys. Lett. **94**, 021902 (2009)
37. R.R. Rojo, L. Stranges, A.K. Kar, M.A.M. Rojas, W.H. Watson, Opt. Commun. **203**, 385 (2002)
38. J. He, W. Ji, G.H. Ma, S.H. Tang, H.I. Elim, W.X. Sun, J. Appl. Phys. **95**, 6381 (2004)
39. T. Cassano, R. Tommasi, A.P. Meacham, M.D. Ward, J. Chem. Phys. **122**, 154507 (2005)
40. B. Karthikeyan, M. Anija, C.S.S. Sandeep, T.M.M. Nadeer, R. Philip, Optics Commun. **281**, 2933–2937 (2008)
41. M.S. Bahae, A.A. Said, T.-H. Wei, D.J. Hagan, E.W. Van Stryland, IEEE J. Quantum Electron. **26**, 760 (1990)

Paper IV

Studies of nonlinear optical properties of PicoGreen dye using Z-scan technique

C Pradeep, S Mathew, B Nithyaja, P Radhakrishnan and V P N Nampoori

Studies of nonlinear optical properties of PicoGreen dye using Z-scan technique

**C. Pradeep · S. Mathew · B. Nithyaja ·
P. Radhakrishnan · V.P.N. Nampoori**

Abstract In this paper we study the nonlinear optical properties of PicoGreen dye. The investigations involve the single-beam Z-scan technique and measurements were carried out at different incident intensities. Both open and closed aperture Z-scan techniques were performed at 532 nm and it was found that the dye exhibited a reverse saturable absorption with significant nonlinear absorption coefficient and intensity-dependent negative nonlinear refraction coefficient, indicating self-defocusing phenomena. The third-order nonlinear susceptibility and optical limiting threshold were also measured.

1 Introduction

There has been an extensive need for nonlinear optical materials that can be used with low-intensity lasers due to their potential application in optical switches and devices [1, 2]. Large nonlinear optical susceptibility resulting from the nonlinear response of organic molecules has attracted much attention. Many reports have been published for the case of single crystals of organic molecules [3, 4], organic molecules in liquid solutions [5, 6] and organic and biological materials doped in various solids [7, 8]. Nonlinear optical phenomena can be due to electronic, thermal (non-electronic) or anisotropic orientational processes. The electronic nonlinearity arises from electronic structural change due to distortion of electronic clouds or distribution of electrons to different levels. The response time is of the order

of femtoseconds. The thermal nonlinearity occurs as a result of generation of phonons on absorption of light. The orientational nonlinearity is due to birefringence when off resonance and dichroism on resonance. There are various techniques to ascertain the underlying phenomena of optical nonlinearity and often two or more experiments are required to confirm the same. The single-beam Z-scan technique, developed by Sheik-Bahae et al. [9, 10], is a well-established tool for determining the nonlinear properties and is widely used in material characterization since it can provide not only the magnitudes of the real and imaginary parts of nonlinear susceptibility, but also the sign of the real part. In this method, the intensity-dependent transmission is computed, which can rapidly measure both nonlinear refraction and nonlinear absorption.

We report here the optical nonlinear measurements of PicoGreen (PG) dye [11, 12]. PG is an asymmetrical cyanine dye used as a nucleic acid stain in molecular biology described by various manuals and protocols [13–15]. This expensive dye is commonly employed as quantitation reagent used to detect and quantify nucleic acid. This stain selectively binds to double-stranded DNA (dsDNA) and has a characteristic similar to that of SYBR Green I. This cyanine dye is a fluorochrome which has a low fluorescence as such. Its fluorescence enhances by over 1000 fold as it binds to dsDNA [16], with high quantum yield and molar extinction coefficient when binding to as little as 25 pg/ml dsDNA [17]. It can also stain single-stranded DNA (ssDNA) and RNA with relatively lower performance. PG (IUPAC: 2-[N-bis-(3-dimethylaminopropyl)-amino]-4-[2,3-dihydro-3-methyl-(benzo-1,3-thiazol-2-yl)-methylidene]-1-phenyl-quinolinium [18]) with its molecular formula $C_{34}H_{42}N_5S$ has an average mass of 552.794983 Da [19]. The molecular structure of the dye has been determined by Zipper et al. [18] and is shown in Fig. 1.

C. Pradeep (✉) · S. Mathew · B. Nithyaja · P. Radhakrishnan · V.P.N. Nampoori
International School of Photonics, Cochin University of Science and Technology, Cochin 682022, India
e-mail: pradeep@photonics.cusat.edu
Fax: +91-0484-2576714

Fig. 1 Molecular structure of PG dye

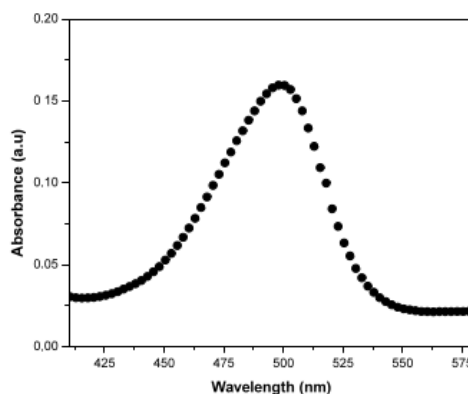**Fig. 2** Absorption spectrum of PG in the visible region
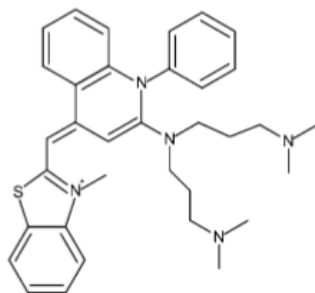
2 Experimental

PG was made available from Invitrogen, USA. Commercially available PG reagent is in liquid form with the solvent being dimethyl sulfoxide (DMSO). DMSO was supplied by S.D. Fine Chem Limited, India. The UV–visible absorption spectra are recorded using a Jasco V-570 spectrophotometer. The linear refractive index of the dye was measured using an Abbe refractometer.

PG was stored away from light as it is susceptible to photobleaching at prolonged exposure to room light. Hence, the dye was immediately subjected to investigation once removed from storage.

The Z-scan technique was used to measure optical nonlinearity employing a mode-locked Nd:YAG laser having 7 ns pulses at a repetition rate of 10 Hz giving a second harmonic at 532 nm. The sample is moved along the beam axis of light focused with a lens of focal length 20 cm. The radius of the beam waist w_0 is calculated to be 42 μm. The Rayleigh length, $z_0 = \pi w_0^2 / \lambda$, is estimated to be 10.7 mm, which is much greater than the thickness of the sample cuvette (1 mm), which is an essential prerequisite for Z-scan experiments. The transmitted beam energy, reference beam energy and their ratio are measured simultaneously by an energy ratio meter having two identical pyroelectric detector heads. The Z-scan system is calibrated using CS_2 as a standard.

3 Results and discussion

The linear absorption spectrum of PG is shown in Fig. 2. The absorption is prominent in the visible region at around 440 nm to 540 nm with its peak at 499 nm. The concentration of the reagent was calculated to an approximate value of 2.75×10^{-5} mol/L based on the molar extinction coefficient reported by Singer et al. as 70000 $cm^{-1} M^{-1}$ [16]. The solvent used by Singer et al. was phosphate buffer while that of our study is DMSO. However, the nonlinear properties of the dye solution will not be affected due to the change in the solvent. The original concentration was maintained during Z-scan experiments without diluting the dye. Figure 3 shows the open aperture Z-scan curve of the dye at 532 nm with an incident intensity of 0.1 GW/cm^2. An optical limiting type (reverse saturable absorption, RSA) behavior was observed with nonlinear absorption coefficient, β, at 1.1 m/GW. A decrease in nonlinear absorption coefficient with increased intensity of the incident laser was observed at this wavelength and the numbers are presented in Table 1.

When an aperture was introduced in the far field of the sample (closed aperture Z-scan), the resulting transmittance exhibited a self-defocusing effect with an asymmetrical peak–valley curve as shown in Fig. 4. The suppressed peak and enhanced valley were due to the fact that the closed aperture measurement is sensitive to both nonlinear absorption and nonlinear refraction. Some materials such as ZnSe and BaF_2 showed a similar asymmetrical curve as reported by Sheik-Bahae et al. [20]. Shahriari and Yunus have also reported similar Z-scan results in silver nanofluid [21, 22]. By dividing the closed aperture data by the open aperture data, the Z-scan curve due to nonlinear refraction alone could be obtained. Figure 5 shows the results of dividing the closed aperture data by the open aperture data at an incident intensity of 0.3 GW/cm^2.

In explaining the nonlinear behavior of the dye, we used two-photon-absorption (TPA) geometry and found the best fit for the experimental data. In a circularly symmetric laser beam incident on PG dye, the normalized transmittance detected in the far field in the closed aperture and open aperture Z-scan experiments is given by Eqs. (1) and (2) [11, 12].
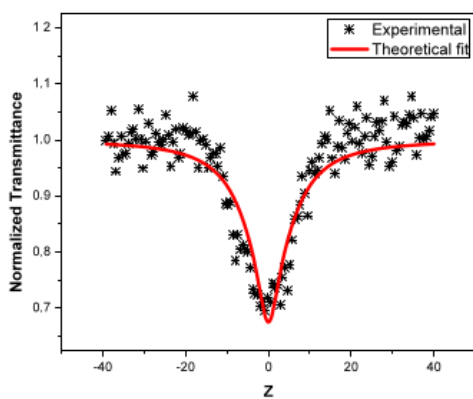
$$T(z) = 1 - \frac{4\Delta\phi\gamma}{(1+\gamma^2)(9+\gamma^2)}, \tag{1}$$

Studies of nonlinear optical properties of PicoGreen dye using Z-scan technique   293

Table 1 Key parameters related to nonlinear optical properties of PicoGreen dye
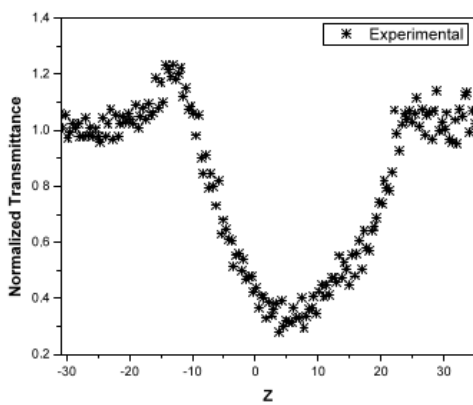
Intensity, I_0 (GW/cm²)	Nonlinear absorption coefficient, β (m/GW)	Optical limiting threshold, Th_{OL} (MW/cm²)	Nonlinear refractive index, n_2 (esu) $\times 10^{-10}$	Third-order susceptibility, $|\chi^{(3)}|$ (esu) $\times 10^{-11}$
0.1	1.1	36.2	-5.7	9.3
0.2	0.7	63.0	-3.2	5.2
0.3	0.5	77.6	-1.9	3.2

Fig. 3 Open aperture Z-scan of PG at an incident intensity of 0.1 GW/cm²
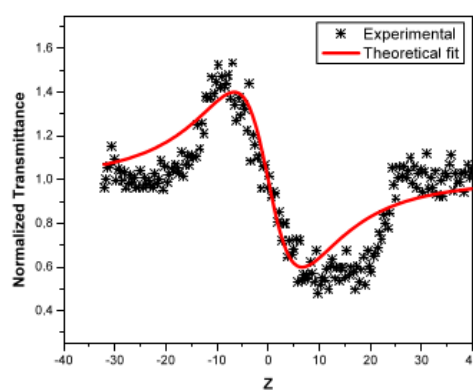
Fig. 5 Results of division of closed aperture by open aperture data at an incident intensity of 0.3 GW/cm²

the longitudinal displacement of the sample from focus and the Rayleigh length, respectively.

$$T(z) = \sum_{m=0}^{\infty} \frac{(-q_{(z,0)}/(1+\gamma^2))^m}{(m+1)^{3/2}}, \tag{2}$$

where $q_{(z,0)} = \beta I_0(t) L_{\text{eff}}$. Theoretical fit of the experimental data was obtained using Eqs. (1) and (2). The nonlinear absorption coefficient, β, was calculated using the above equations. The nonlinear refractive index was calculated as $n_2 = c n_0 \Delta\varphi_0 / 40\pi k I_0(t) L_{\text{eff}}$. The linear refractive index, n_0, of the PG dye was measured using a refractometer and was found to be 1.46. It is observed that the peak–valley of the closed aperture Z-scan satisfies the condition $\Delta z = 1.7z_0$, thus confirming the presence of third-order optical nonlinearity. The real and imaginary parts of the third-order nonlinear susceptibility $\chi^{(3)}$ of the cyanine dye were calculated from the values of n_2 and β using Eqs. (3) and (4).
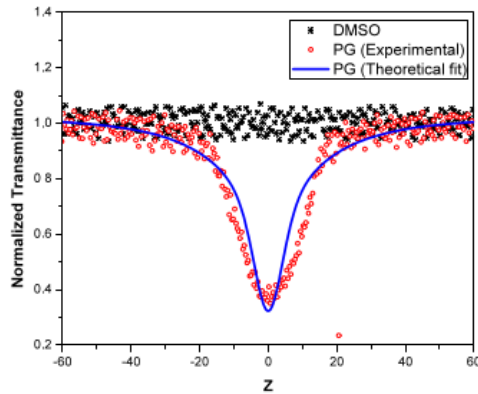
$$\text{Re}\,\chi^{(3)} = \frac{n_0 n_2}{3\pi} \text{ (esu)}, \tag{3}$$

$$\text{Im}\,\chi^{(3)} = \frac{n_0^2 c^2 \beta}{240\pi^2 \omega} \text{ (esu)}. \tag{4}$$

Fig. 4 Closed aperture Z-scan of PG at an incident intensity of 0.3 GW/cm²

where $\Delta\phi = 2\pi(n_2 I_0(t) L_{\text{eff}}/\lambda)$ with $\gamma = (z/z_0)$ and $L_{\text{eff}} = (1 - \exp(-\alpha l))/\alpha$, $\Delta\phi$ being the phase distortion at the focus, I_0 the incident laser power at the focus, L_{eff} the effective interaction length and l the sample length. z and z_0 are

**Fig. 6** Open aperture Z-scan of DMSO solvent and PG dye solution

Fig. 7 Optical limiting response of PG dye

The nonlinear susceptibility $\chi^{(3)}$ was computed using the relation $[(\mathrm{Re}\,\chi^{(3)})^2 + (\mathrm{Im}\,\chi^{(3)})^2]^{1/2}$. The calculated values of nonlinear optical parameters are depicted in Table 1.

Some cyanine dyes such as PC (1,1′-diethyl-3,3,3′,3′-tetramethyl-indolepentylmethinecyanine iodine) and various polymethine cyanine dyes which possess considerable nonlinear absorption coefficient, nonlinear refractive index and third-order susceptibility have been reported. Research is targeted towards exposing new materials with higher nonlinear refractive index due to the possibility of applications as optical limiters based on the Kerr effect. We present here a material (PG) that possesses a nonlinear absorption coefficient that is two orders of magnitude higher than the polymethine dyes [23] and nonlinear refractive index and third-order nonlinear susceptibility of approximately two orders of magnitude higher than the PC solution [24].

To confirm the cause of optical limiting type behavior of the PG solution, open aperture Z-scan was performed on both solvent alone and the dye solution. As shown in Fig. 6, no obvious nonlinear absorption was found for DMSO solvent while PG solution showed strong nonlinear absorption with its TPA coefficient, β, taking the value 0.4 m/GW at an incident laser intensity of 0.35 GW/cm^2. Hence, optical limiting is only due to the dye.

One of the important exploits of RSA behavior in materials is its application as an optical limiter. In principle, an optical limiter is opaque to high input intensities while transmitting low light intensities. An important term in optical limiting (OL) measurement is the limiting threshold. An ideal optical limiting material should have low limiting threshold. Here we have used open aperture data to extract the limiting threshold by expressing the abscissa in terms of
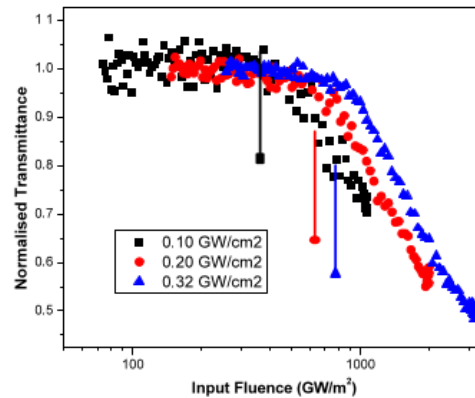
the input fluence using Eq. (5).

$$I(z) = \frac{I_0}{1 + (z^2/z_0^2)}. \tag{5}$$

Figure 7 shows the OL response of PG dye at different incident intensities; the limiting threshold was observed at 36.2 MW/cm^2 at an incident intensity of 0.1 GW/cm^2. As the incident intensity was increased, the limiting threshold also increased. The continuous line with a head in the figure indicates the approximate threshold value (Th$_{\mathrm{OL}}$), which is determined graphically as the intersection between the linear and nonlinear parts of the OL curve. The OL threshold at various intensities is presented in Table 1.

4 Conclusion

In summary, our Z-scan experiments revealed interesting features of optical nonlinear properties of PG dye. Using the 532 nm line of a Nd:YAG laser, the cyanine dye exhibited an optical limiting characteristic and the closed aperture experiments depicted a self-defocusing effect. The dye exhibited a significant TPA coefficient, β, and intensity-dependent third-order nonlinear refraction, n_2, and third-order susceptibility, $\chi^{(3)}$. These attractive properties of PG could be exploited in developing it as an optical limiter and as various photonic and optoelectronic devices.

References

1. M.A. Kramer, W.R. Tompkin, R.W. Boyd, Phys. Rev. A **34**, 2026 (1986)
2. F.E. Hernandez, A.O. Marcano, Y. Alvarado, A. Biondi, H. Maillotte, Opt. Commun. **152**, 77 (1998)
3. G.M. Carter, M.K. Thakar, Y.J. Chen, J.V. Hryniewez, Appl. Phys. Lett. **47**, 457 (1985)
4. Ch. Bosshard, K. Sutter, R. Gunter, J. Opt. Soc. Am. B **6**, 721 (1989)
5. G.S. He, G.S. Xu, P.N. Prasad, B.A. Reinhardt, J.C. Bhatt, A.G. Dillard, Opt. Lett. **20**, 435 (1995)
6. J.L. Bredas, C. Adant, P. Tackx, A. Persoons, Chem. Rev. **94**, 243 (1994)
7. T.A. Shankoff, Appl. Opt. **8**, 2282 (1969)
8. S.C. Yang, Q.M. Qian, L.P. Zhang, P.H. Qiu, Z.J. Wang, Opt. Lett. **16**, 548 (1991)
9. M. Sheik-Bahae, A.A. Said, E.W. Van Stryland, Opt. Lett. **14**, 955 (1989)
10. M. Sheik-Bahae, A.A. Said, T. Wei, D.J. Hagan, E.W. Van Stryland, IEEE J. Quantum Electron. **QE26**, 760 (1990)
11. C. Pradeep, S. Mathew, B. Nithyaja, P. Radhakrishnan, V.P.N. Nampoori, in *Int. Conf. Fiber Optics and Photonics*, IIT Madras, Chennai, December, 2012, TPo.38
12. C. Pradeep, S. Mathew, B. Nithyaja, P. Radhakrishnan, V.P.N. Nampoori. Appl. Phys. B. doi:10.1007/s00340-013-5380-y
13. Quant-iT PicoGreen dsDNA Reagent and Kits, manuals, Invitrogen
14. PicoGreen Assay for dsDNA, Protocol ND-300, Thermo Scientific
15. C. Labarca, K. Paigen, Anal. Biochem. **102**, 344 (1980)
16. V.L. Singer, L.J. Jones, S.T. Yue, R.P. Haugland, Anal. Biochem. **249**, 228 (1997)
17. G. Cosa, K.S. Focsaneanu, J.R.N. Mclean, J.P. McNamee, J.C. Scaiano, Photochem. Photobiol. **73**, 585 (2001)
18. H. Zipper, H. Brunner, J. Bernhagen, F. Vitzthum, Nucleic Acids Res. **32**, 12 e103 (2004)
19. ChemSpider CSID: 17230578
20. E.W. Van Stryland, M. Sheik-Bahae, A.A. Said, D.J. Hagan, Prog. Cryst. Growth Charact. **27**, 279 (1993)
21. E. Shahriari, W.M.M. Yunus, Am. J. Eng. Appl. Sci. **3**, 98 (2010)
22. E. Shahriari, W.M.M. Yunus, Digest J. Nanomater. Biostruct. **5**, 939 (2010)
23. R.A. Ganeev, R.I. Tugushev, A.A. Ishchenko, N.A. Derevyanko, A.I. Ryasnyansky, T. Usmanov, Appl. Phys. B **76**, 683 (2003)
24. H. Kang, Y. Yuan, Z. Sun, Z. Wang, Chin. Opt. Lett. **5**(7), 428 (2007)

CURRICULAM VITAE

Pradeep Chandran C

email: chandran@cusat.ac.in

skype: pradeep.chandran.c

profile: RexearchGate | ORCID | LinkedIn

Pradeep Chandran was born to Mr. Chandran Krishnan and Mrs. Mandakini Kesavan on 23rd October, 1984 at Chennai, Tamil Nadu in India. He was tutored at ICF Silver Jubilee Matriculation Higher Secondary School and completed his schooling in 2002. He received his bachelors in Electrical and Electronics Engineering from Sri Venkateswara College of Engineering and Technology, Thiruvallur in 2006 and subsequently qualified Graduate Aptitude Test in Engineering the following year. He took his masters in Laser and Electro Optical Engineering from College of Engineering, Guindy, a constituent college of Anna University Chennai in 2009.

He joined International School of Photonics in 2010, as a junior research fellow of CSIR (Council of Scientific and Industrial Research, India) project and pursued his doctoral studies since then. He is herewith submitting his PhD thesis entitled 'Studies on deoxyribonucleic acid based photonic materials and their applications' in December 2015.

പ്രദീപ്